***AB-INITIO* STUDY OF ELECTRONIC AND MECHANICAL STRUCTURE PROPERTIES OF THE SUPERCONDUCTING IRON PNICTIDE $EuFe_2As_2$**

OMBOGA KERUBO NAOMY

B.ED SCIENCE (KISII UNIVERSITY)

A THESIS SUBMITTED TO THE BOARD OF POST-GRADUATE STUDIES IN PARTIAL FULLFILLMENT OF THE REQUIREMENTS OF THE DEGREE OF MASTER OF SCIENCE IN PHYSICS IN THE SCHOOL OF PURE AND APPLIED SCIENCES, DEPARTMENT OF PHYSICS, KISII UNIVERSITY

2023

DECLARATION

DECLARATION BY THE CANDIDATE

This research thesis is my original work prepared with no other than the indicated sources and support and has not been presented elsewhere for a degree or any other award.

Name……………………………………………….. **Admission Number**……………………..

Signature…………………. ………………   Date……………………………………..

DECLARATION BY THE SUPERVISORS

We have reviewed the research thesis and recommend it to be accepted in partial fulfillment of the requirement for award of the degree of Master of Science in Physics.

Dr. Calford Otieno

Department of Physics

Kisii University

Sign: ………………………………….. **Date**: …………………………………….

Dr. Phillip O. Nyawere

Department of Biological and Physical Sciences

Kabarak University

Sign: ………………………………….. **Date**: …………………………………….

PLAGIARISM DECLARATION

Definition of plagiarism

It is academic dishonesty which involves; taking and using the thoughts, writings, and inventionsof another person as one's own.

DECLARATION BY STUDENT

i. I declare that I have read and understood Kisii University Postgraduate Examination Rules and Regulations, and other documents concerning academic dishonesty.
ii. I do understand that ignorance of these rules and regulations is not an excuse for a violation of the said rules.
iii. If I have any questions or doubts, I realize that it is my responsibility to keep seeking an answer until I understand.
iv. I understand I must do my own work.
v. I also understand that if I commit any act of academic dishonesty like plagiarism, my thesis/project can be assigned a fail grade ("F")
vi. I further understand that I may be suspended or expelled from the University for Academic Dishonesty.

Name______________________________ Signature

Reg.No__________________________ Date__________________________

DECLARATION BY SUPERVISOR (S)

i. We declare that this thesis has been submitted to plagiarism detection service.
ii. The thesis/project contains less than 20% of plagiarized work.
iii. We hereby give consent for marking.

1. Name___________________________ Signature

   Affiliation__________________________ Date

2. Name___________________________ Signature

   Affiliation_____________________________ Date

DECLARATION OF NUMBER OF WORDS FOR MASTERS THESIS

This form should be signed by the candidate and the candidate's supervisor (s) and returned to Director of Postgraduate Studies at the same time as you copies of your thesis/project.

Please note at Kisii University Masters and PhD thesis shall comprise a piece of scholarly writing of more than 20,000 words for the Master's degree and 50 000 words for the PhD degree. In both cases this length includes references, but excludes the bibliography and any appendices.

Where a candidate wishes to exceed or reduce the word limit for a thesis specified in the regulations, the candidate must enquire with the Director of Postgraduate about the procedures to be followed. Any such enquiries must be made at least 2 months before the submission of the thesis.

Please note in cases where students exceed/reduce the prescribed word limit set out, Director of Postgraduate may refer the thesis for resubmission requiring it to be shortened or lengthened.

Name of Candidate: …………………………………….. ADM NO……………………….

Faculty…………………………………………………. Department………………………

Thesis Title:

……………………………………………………………………………………………………
……………………………………………………………………………………………………
……………………………………………………………………………………………………

I confirm that the word length of:

1) The thesis, including footnotes, is 39287 2) the bibliography is 1874

and, if applicable, 3) the appendices are 1298

I also declare the electronic version is identical to the final, hard bound copy of the thesis and corresponds with those on which the examiners based their recommendation for the award of the degree.

Signed: ……………………………………….. Date:……………………….

(Candidate)

I confirm that the thesis submitted by the above-named candidate complies with the relevant word length specified in the School of Postgraduate and Commission of University Education regulations for the Masters and PhD Degrees.

Signed: .... Email………….……………. Tel………………….. Date:……………

(Supervisor 1)

Signed: .... Email…………………….. Tel………………….. Date:……………

(Supervisor 2)

COPYRIGHT

All rights are reserved. No part of this thesis/project or information herein may be reproduced, stored in a retrieval system or transmitted in any form or by any means electronic, mechanical, photocopying, recording or otherwise, without the prior written permission of the author or Kisii University on that behalf.

© 2023, Omboga Kerubo Naomy

DEDICATION

This work is dedicated to my family and close friends for their tireless efforts and spiritual, financial and emotional support up to this level. God bless you all.

ACKNOWLEDGEMENT

First, great thanks to God Almighty for life, opportunity, health, resources and everything. This far the Lord has brought us! For without God we are not, everything is meaningless and useless. I am very grateful for God being patient with me, and for leading me on. As the wise man says, put God first in everything you do, and he will surely show you the right path. I cannot forget to thank Kisii University, for providing me with the chance to undertake my studies there, right from the undergraduate level. Great thanks to the School of Pure and Applied Sciences under the leadership of Dr. Obogi Robert for the chance to undertake my studies in your department. For the support offered by the Physics department I am also thankful.

Thanks to Dr. Otieno Calford for reading through my work, correcting the errors and advising me on the right path to follow always, also, for the supportive software provided to me at no cost. I am also grateful for the mentorship he freely gave me and for being a valuable coach and someone I could always look up to. Heartfelt thanks to my other supervisor Dr. Phillip Nyawere for the constant push to see that this research gets completed in time. Furthermore, thank you for reading through my work ad suggesting key changes and corrections to be made. Also for following up on my progress at all time to ensure I completed the study on time. God bless you. Thanks to Dr. Ketui Daniel for providing valuable software to me and also for the valuable advice on various concepts. Your contribution is highly appreciated.

My great appreciation goes to Mr. Agora Jared for introducing me to Quantum ESPRESSO and the Linux operating system. I remember how green I was when I was starting out but he was patient with me, and taught me a lot of things. Phigrey Jomo has also been instrumental in guiding and helping me the whole of his time. I also thank my colleagues whom we started this journey with: Richard Maranga, Lydia Mairura and Amos Ogera for the valuable and useful discussions and brain storming towards a better research, and for the life skills you people taught and imparted in me. I am forever grateful.

Great appreciation goes to Dr. George Manyali of the Kaimosi Friends University College for the tireless effort and guiding directive in the correct path of computation. The long hours of night video calling and working are highly appreciated sir. James Sifuna and Elicah for providing tips here and there on Density Functional Theory (DFT) and Quantum Espresso(QE). I cannot go without mentioning my spiritual father and advisor Pastor Stephen Ongige of the Jogoo District. I thank you for constantly praying for me, praying with me and encouraging me to move on in this journey. Stay blessed.

I would also like to thank the International Centre for Theoretical Physics(ICTP), Italy, for providing resources for travel and accommodation to Kigali, Rwanda for DFT workshops and seminars. This exposed me to a number of great scientists and expanded my scope of thinking. In particular I would love to thank Oshakuede of Nigeria for introducing me to the materials cloud site, a site that proved quite useful in the generation of input files for quantum simulations. Christelle Ekossa, little woman from Cameroon. I am glad I met you. You proved to be such an inspiration to me and I highly value the informing conversations we had. Linnet Allan, Dr. Victor Odari, and my Tanzanian friends Joachim Chengula and Amos Makoye are not forgotten. You made my stay in a faraway land much more bearable and comfortable.

I appreciate Dr. Holiness Nose of Technical University of Kenya for supportive measures and for interactive sessions with colleagues from various universities in the DFT computation field. Great appreciation to my mother Teresa, father Michael, brothers Bernard, Japheth and Dennis, sisters in law Dorcas and Nancy and my nieces Blessing, Bilha, Eliana and little Evanna for their encouragement and prayers throughout this period. I also would love to thank and

appreciate me, for believing in my potential, for never giving up, and for working tirelessly to see this dream come true. The failings and falling only made me stronger and more resilient. The list is quite long but I would love to wrap it up here. To all those who made a contribution in any way to this journey I am very much thankful and may the Almighty God shower all of you with numerous blessings.

ABSTRACT

Europium Diiron Diarsenide is one of the iron pnictide materials that exhibit superconductivity at high critical temperature. As a superconducting material it can be used in the manufacture of Magnetic Resonance Imaging (MRI) machines, design of cables that can be used to transmit electricity without energy losses hence lowering energy transmission costs. Although superconductivity has proven to be such a useful phenomenon, there is limited information available on the mechanical and electronic structure properties of Europium Diiron Diarsenide and most of the few available data is experimental, therefore constraining the use of this material in industry. Therefore, it is from this context that this research sought to investigate these properties, to provide complimentary information on the few available experimental data, so as to improve on the understanding of the materials properties and enhance its applicability in industry as a superconducting material. The aim of this study is to employ theoretical methods through the Density Functional Theory to investigate computationally the mechanical and electronic structure properties, the effect of pressure on these properties and on superconductivity sso as, in combination with the available experimental data, to be able to enhance its applicability in industry. The open source software Quantum Espresso which employs the plane wave and pseudo potentials of the ground state has been used in this study. A study on the mechanical structure property as obtained in the study indicates that the material is ductile and also anisotropic. The material is also mechanically stable. Electronic structure properties showed that the compound was a metal. The study of the effect of pressure on the Fermi energy also showed that the Fermi energy increases as the pressure increases. The Debye temperature also revealed that the compound has a high thermal conductivity. The phonon dispersion study revealed distinct acoustic modes and optical modes.

TABLE OF CONTENTS

CHAPTER THREE

CHAPTER FOUR

CHAPTER FIVE

LIST OF TABLES

Page

LIST OF FIGURES

Page

LIST OF APPENDICES

LIST OF ABBREVIATION

DFT	Density Functional Theory
PW	Plane Wave
ESPRESSO	opEn-Source Package for Research in Electronic Structure, Simulation, and Optimization
LDA	Local Density Approximation
LSDA	Local Spin Density Approximation
$EuFe_2As_2$	Europium Diiron Diarsenide
QE	Quantum ESPRESSO
E_{cut}	Plane wave cutoff energy
eV	Electron volt unit
H	Hamiltonian
Fig	Figure
SDW	Spin Density Wave
SC	Superconductor
B	Bulk modulus
G	Shear modulus
E	Young's modulus

CMP	Condensed Matter Physics.
BME	Birch Munaghan Equation
GGA	Generalized Gradient Approximation
MRI	Magnetic Resonance Imaging
MBSE	Many-body Schrödinger Equation
SE	Schrödinger Equation
CHPC	Center for High Performance Computing
BCS	Bardeen, Cooper and Schrieffer
FeAs	Iron Arsenide
MP	Materials Project
MC	Materials Cloud
HF	Hartree Fock
K-S	Kohn-Sham
H-K	Hohenberg-Kohn
V_H	Hartree potential
Z	Atomic number
A	Atomic mass
Gpa	Giga Pascal
SCF	Self-Consistent Field
NSCF	Non Self Consistent Field

GRACE	Graphical Advanced Computing and Exploration of data
E_{XC}	Exchange and Correlation energy of interacting system
PBE	Perdew Burke Ernzerhof
PBEGGA	Perdew Burke Ernzerhof Generalized Gradient Approximation
K	Kelvin
V_{ext}	External potential
∇^{n}	Charge density variation
PDOS	Projected Density of States
BS	Band Structure
n(r)	Electron charge density
∇	Gradient operator/ Laplacian operator
PP	Pseudo Potential
PWSCF	Plane Wave Self Consistent Field
ICTP	International Center for Theoretical Physics
DFPT	Density Functional Perturbation Theory
LAPW	Linearized Augmented Plane Waves
FeSC	Iron based superconductors.

CHAPTER ONE

INTRODUCTION

1.1 Background of the study

There has been increasing interest over the recent past and in the present amongst the science community especially Physicists over the phenomena of superconductivity due to its present and projected advantagesand uses. H. Kamerlingh Onnes in 1911was the first to discover the concept of superconductivity, whichwas later illustrated by Bardeen, Cooper and Schrieffer in 1957 (Si, Yu, & Abrahams, 2016). Superconductivity refers to the total vanishing of electrical resistance to direct current in a material. Resistivity tends to zero while conductivity tends to infinity.

The iron Pnictides in particular have attracted special attention because they are relatively easier to synthesize and they exhibit superconductivity under conditions such as doping or application of external pressure (Miclea *et al*., 2009). Superconductivity in the iron pnictide family was first discovered in 2008 (Si *et al*., 2016).

Superconductivity arises when pairs of electrons which have opposite momentum move uniformly and transmit electricity without energy loss. Most power plants burn coal and fossil fuels to produce electricity (Ang & Su, 2016), which releases harmful toxics to the environment. Minimized energy losses due to use of superconducting cables decreases the quantity of electricity that power stations have to produce, hence reducing the quantity of fossil fuels that are burned everyday which benefits the environment by reducing the amount of toxic fumes released by power plants. Energy losses in form of heat are eradicated through the use of superconductors. High temperature superconductivity has been observed in iron Pnictides (Norman, 2008), $EuFe_2As_2$ being one of them.

Superconductors have other projected uses due to their advantages mentioned above and some of the projected areas of uses are: First, the Rapid Single Flux Quantum integrated circuit receiver that helps to achieve gigahertz frequencies. These high frequencies cannot be easily achieved by the current semiconductors that are used in cell phones due to energy loses so as to make the phones more efficient and reliable (Chen, Rylyakov, Patel, Lukens, & Likharev, 1999). This kind of integrated circuit can be achieved through use of superconducting materials. Secondly, in transport, magnetic trains (Ng, 1995) can be advanced since they are super quick as a result of the huge magnetic fields generated by a superconductor.

Superconducting magnets are already in use in areas such as in hospitals where Magnetic Resonance Imaging machine (MRI) (Green, 2001), which is used in patient diagnosis without performing unnecessary surgery. The Magnetic Resonance Imaging machine produces much better results than the x-ray technique, hence one important use of superconductors today. Magnetic Resonance Imaging machine can be improved as a result of development of cheaper superconducting materials, hence improved access to better health care. The Magnetic Resonance Imaging machine is used to perform 'knife less' surgery and diagnosis on patients suffering from various ailments. Currently, the Magnetic Resonance Imaging machine uses liquid helium for its superconducting properties which is quite expensive. Liquid Helium also undergoes easy evaporation causing losses. Superconductors have resistance being equal to zero and conduction is infinite. The use of superconducting grids to transmit electricity from one place to another would eliminate power loses and minimize extra costs being incurred as a result of resistance experienced in the cables used in transmission grids. The superconducting current is self-sustaining and persists on a conductor for a very long time. Some other areas where superconducting materials are applied include in microwave sensors that employ infrared and in refrigeration where liquid helium is used although having the disadvantage of easy evaporation.

1.2 Superconductivity

Superconductivity is one of the most fascinating concepts of quantum mechanics. It refers to the state of no resistance below a given materials critical temperature. It can be achieved through doping or application of external pressure to a material. Below the critical temperature, the electrical resistivity of a material vanishes completely, therefore, electrons can move without energy dissipation. Actually, in the superconducting state, the resistance goes to zero (Bardeen, Cooper, & Schrieffer, 1957) and conduction to infinity. The onset of superconductivity in a material is as a result of interaction between conduction electrons and lattice vibration. Ginsburg and Landau considered the density of the material changing in space.

The Ginsburg Landau theory was restructured from the concept of London theory to include an effective wave function that can be normalized so that the local density can be obtained (Bardeen *et al*., 1957). The phenomenon of high temperature superconductivity has been among the most challenging work in the science community, most especially amongst condensed matter physicists (Li, Zhu, Chen, & Ting, 2012).

The BCS theory of superconductivity is extended to the Migdal-Eliashberg theory, which relates the critical temperature to atomic scale properties of materials, in particular, the electronic band structures, phonon dispersions, which properties can be calculated using the Density Functional Theory. The electronic structure of a compound varies with temperature. This is because temperature leads to phonon excitations. The population of phonon would couple with electronic states and renormalize the energy of the electron energy. The zero Kelvin is the ground state of condensed matter. Electron to electron coulomb interaction gives rise to superconductivity in iron Pnictides.

Generally, superconductors are classified basing on the following criterion: the operational theory, the critical temperature, the nature of the material and how they react to a magnetic field. Basing on how they react to a magnetic field, they can be grouped into type one and type two superconductors. Basing on the theory of operation, they can be classified as conventional or unconventional superconductors, and basing on their critical temperature, they can be classified as high temperature superconductors and low temperature superconductors. Also, basing on the makeup material, they can be classified as ceramics, chemical superconductors, organic superconductors and superconducting Pnictides.

Superconductivity is unique in that not all materials that are conductors can exhibit superconductivity. It is not even related to atomic weight and number or electro-negativity. In some rare cases, a superconducting material can be formed from a combination of non-superconducting elements. The BCS theory predicts a correlation between critical temperature, lattice vibration, and average atomic mass. This theory is as a result of the theorem that Cooper put forward, that, the ground state of an electron gas is unstable and there exists a tiny attraction between its particles against the forming of pairs of electrons. In the BCS theory, superconductivity is illustrated at temperatures that are near 0K. Here, the cooper pairs are created which then occupy states but have the same but opposite momentum and opposite spin, basing on the Pauli Exclusion Principle that no two electrons with the same spin can occupy the same state simultaneously. In a scenario where the angular momentum due to orbiting of particles is zero, cooper pairs are generated. Cooper pairs are usually made up of particles that undergo spin $\frac{1}{2}$.

Superconductivity can be classified as conventional superconductivity and unconventional superconductivity. In conventional superconductivity, phonons lead to the generation of pairs of electrons in a process of attraction. This type of superconductors conforms to the BCS theory. Conventional superconductors can be type one or type two. Unconventional superconductors do not align with the BCS theory. The iron Pnictides are generally classified under the unconventional super conductors (Si *et al*., 2016). High temperature superconductivity is an example of unconventional superconductivity and the critical temperature is in the range of 7K to 100K. The resistant behavior in metals falls considerably in very low temperatures. Reduction in resistance implies much improved electrical conductivity. Initially, there were various speculations amongst scientists as to what would take place in the electrical resistance if the temperature of a material was lowered to 0K. Some of the scientists such as William Kelvin suggested that if the temperature was set to much lower levels, the electrons moving in the conducting material would stop moving completely (as the temperature is lowered to approach zero Kelvin.). Other scientists such as Onnes suggested that the resistance of a very cold wire would disappear. This prompted Onnes to begin searching for answers to this phenomenon. He performed an experiment which included passing direct current through a pure mercury wire while lowering the temperature, at the same time he noted down the resistance as he lowered the temperature. When he lowered the temperature and reached a temperature of 4.2K, the resistance disappeared all of a sudden and the direct current was now flowing freely through the mercury. The 4.2K is the transition temperature for superconductivity and he called this phenomenon superconductivity, hence bringing an end to the various speculations as to what happens to resistance when temperature is decreased. Take for instance, in a conducting material such as copper, electrons in the outer energy level move from one atom to another, hence conducting electricity from one point to another. However, the behavior of electrons in superconductors is very much different; the electrons move in a much different way. The electrons do not collide or bump with anything as they move through the lattice; therefore they move freely, transmitting electricity at no resistance, as compared to normal conductors where the electrons collide with impurities in the lattice and fly off in different directions, which leads to energy loss as heat. In summary, a superconducting material can be termed as conventional if it can be described using the BCS theory and other theories derived from it, and it is unconventional if it cannot be illustrated by the BCS theory.

The London equations explain superconductivity in a simplified manner as the Ohm's equation explains conductivity. The London equations are as given in Eqs 1.1 and 1.2 below:

$$\frac{\partial j}{\partial t} = \frac{n_s e^2}{m} E \qquad \text{……………………………………………………………………………………………………….1.1}$$

$$\nabla \times j = -\frac{n_s e^2}{m} B \qquad \text{…………………………………………………………………………………………………….1.2}$$

Where, j is the superconducting current density, E is the electric field, B is the magnetic field, e is the charge of an electron, m is the mass of an electron, n_s is the density of the superconducting carriers.

The basic terms and phenomena in superconductivity include:

i. The Meissner Effect: Was put across by Walther Meissner and R. Ochsenfeld in 1933, who reported that superconductors have a special aspect of magnetism which includes the excluding of a magnetic field. The magnetic flux is excluded in a superconductor that has undergone cooling of up to below the temperature of transition in a magnetic field, and this concept is termed as the Meissner Effect. However, the Meissner Effect will take place when the field of magnetism is quite small. Superconductivity cannot exist in a large magnetic field. This is because the large field will enter into the material and expel superconductivity, therefore, superconductivity and magnetism cannot exist simultaneously in a material.

ii. Critical magnetic field: The critical magnetic field is closely related to the concept of critical temperature T_C, the temperature at which the resistance of a material to flow of electrons completely vanishes. Superconductivity will not exist in a material if there exist a magnetic field that is larger than the critical value of magnetism.

iii. The critical current density: this is the current density above which the superconducting state of a material disappears. The science community is still working hard to come up with a compound that can achieve superconductivity at room temperature, and this may be achieved by the use of the type two unconventional superconductors since they super conduct at fairly higher temperatures as compared to the conventional type one superconductors. Characteristics of materials are classified into two, and this classification depends on the ground state and the excited states. Some examples of ground state properties include the transition of crystals from one structure to another, the elastic constants, the density of charges, magnetic susceptibility and many others. Some examples of electronic excited state properties include: susceptibility of the Pauli spin, optical properties and many more. The ground state energy dictates the structure and small energy movements of the nuclei. Generally, materials are grouped depending on their electronic ground state since it dictates their nuclei bonding. In physics, there are basically two types of excitations, one type of excitation being through the removal or addition of an electron to the structure and the other excitation being by maintaining the count of electrons. Excitation can be regarded as a perturbation.

Superconductivity in the iron pnictide family of compounds was first discovered in 2008 (Si *et al., 2016*). From the above, one can now come into the conclusion that the study on superconductors is quite important to the science community and the world at large.

1.3 Statement of the Research Problem

In the recent past, there has been growing interest in the science community on the study of the superconductivity phenomena due to its various present advantages and projected future uses in industrial design of various machines. The iron pnictide family of compounds has shown high temperature superconductivity on doping or application of external pressure. Although superconductivity has proven to be such a useful phenomenon, there is limited information available on the mechanical and electronic structure properties of Europium Diiron Diarsenide and most of the few available data is experimental, therefore constraining the use of this material in industry. Therefore, it is from this context that this research seeks to investigate these properties, to provide complimentary information on the few available experimental data, so as to improve on the understanding of the materials properties and enhance its applicability in industry as a superconducting material.

1.4 Objectives

1.4.1 Main Objective

To apply *ab-initio* methods to investigate the electronic properties and mechanical structure of the iron pnictide compound $EuFe_2As_2$

1.4.2 Specific Objectives

i. To investigate computationally the mechanical structure properties including the Elastic constants, the Bulk modulus, Shear modulus, Young's modulus and the Poisson's ratio of the iron pnictide compound $EuFe_2As_2$.
ii. To analyze computationally the electronic structure properties of the iron pnictide compound $EuFe_2As_2$.
iii. To investigate the effect of external pressure on the mechanical and electronic structure properties of the iron pnictide compound $EuFe_2As_2$.
iv. To study the thermodynamic properties of Phonon Dispersion modes and Debye temperature of the iron pnictide compound $EuFe_2As_2$ in relation to superconductivity.

1.5 Justification for the Study

Europium diiron diarsenide ($EuFe_2As_2$) is a material that can be important for use in the design of superconducting cables for electricity transmission and the design of motors for ships and turbines. Design of microchips for cheap energy usage is projected to benefit from superconducting materials such as $EuFe_2As_2$. Although research on this material has been done experimentally, not much has been explored especially on the mechanical properties. Experimental results are available on the electronic structure properties (Adhikary *et al*., 2013) but mechanical properties have not yet been explored, hence motivating the study. Computational methods are here used because of low cost and reliability. Computational methods can also be tested in regimes of high pressure and temperature that may not be achieved experimentally. The main aim of this research is to investigate the mechanical and electronic structure properties of Europium diiron diarsenide in relationship to its experimental applicability so as to be able to come up with additional data about the material to enhance and direct its effective use in industry. Since there is limited theoretical data on the iron pnictide $EuFe_2As_2$, the results obtained here will help future theoretical studies on the material.

CHAPTER TWO

LITERATURE REVIEW

2.0 Related Studies on the Iron Pnictide Compounds, $\boldsymbol{A = (Ba, Ca, Eu, Sr)}$

By substitution of Europium with sodium or potassium superconductivity was obtained in the material. Also, when pressure was applied externally, or the material doped, superconductivity was achieved. There was a reduction of structural and magnetic phase transition temperature when the compound was doped or pressure applied externally to it, therefore superconductivity surfaces upon adequate suppression of the transition (Terashima *et al.*, 2009) .The iron pnictide compounds are also unique because their phase transition to superconductivity, magnetic and structural properties are closely connected and conceal the key to comprehending the basic properties of the material (Colonna, Profeta, Continenza, & Massidda, 2011). According to (W. O. Uhoya, Tsoi, Vohra, McGuire, & Sefat, 2011), $EuFe_2As_2$ experiences a phase transition from the tetragonal phase to orthorhombic phase at a pressure of 4.3GPa. This phase was maintained up to a pressure of 11GPa where it transits to a collapsed tetragonal phase, which was maintained up to a pressure of around 35GPa. The conductivity of iron Pnictides shows a highly anisotropic characteristic (Ivanovskii, 2009). Phase transition at low temperature is common in the iron Pnictide family of compounds. Experiments performed at high pressure revealed characteristics which link the electronic and structural properties to the superconducting properties of the compound. (Colonna *et al.*, 2011)

Superconductivity and ferromagnetism co-exist in Europium diiron diarsenide that has been doped with phosphorous (Terashima *et al.*, 2009). The iron spin density and the Europium (

Eu^{2+}) which orders anti-ferro magnetically makes Europium diiron diarsenide to be outstanding among the 122 iron Pnictide superconducting compounds. The FeAs layers in the compound of Europium diiron diarsenide are seen to be the source of the superconductivity (Miclea *et al.*, 2009).This compound is unique because of the additional magnetic moment of the localized Eu^{2+} given that other 122 compounds undergoes only the Spin Density Wave (SDW) transition. In the iron arsenide layer a square lattice is made by the ions of iron, while the ions or arsenic are situated overhead and underneath the middle of the above mentioned square.

Application of hydrostatic pressure on $EuFe_2As_2$ indicates that the SDW transition was continuously suppressed on pressure application. There is simultaneous occurrence of superconductivity, ferromagnetism and structural phase transition. Superconductivity is achieved on suppression of the magnetism. Application of chemical and physical pressure can be employed to change the properties of this material. Superconductivity transition temperature occurs at 30K at a pressure of 2.8 Giga Pascal (Ni *et al*., 2008).

Other studies in similar iron Pnictides have been done, though mostly experimental. Barium diiron diarsenide exhibits superconductivity on distorting the structure through application of pressure (Kimber *et al*., 2009). Superconductivity was achieved at a pressure of 5.5Gpa and temperature of 30.5K.The Iron Arsenide superconducting materials are resistant to disorder. Strontium diiron diarsenide also exhibits similar characteristics of superconductivity. Critical temperatures of up to 38 Kelvin have been previously discovered in the 122 family of iron Pnictides. The space group of $EuFe_2As_2$ transits from 14/mmm to Fmmm (Nandi *et al*., 2014).

Studies on Calcium diiron diarsenide have also revealed that it exhibits superconductivity on application of pressure and up to temperatures of 40K (W. Uhoya *et al*., 2010). Experimental results on Europium Diiron Diarsenide have also indicated that superconductivity occurs below temperatures of 33 Kelvin (Paulose, Jeevan, Geibel, & Hossain, 2009).

The tetragonal space group of $EuFe_2As_2$ is 14/mmm. On application of pressure increasingly on the material, the length of the a-axis increases while the length of the c-axis decreases hence compression on the material is anomalous (W. Uhoya *et al.*, 2010). The anomalous compression reaches its highest point at 8GPa and the lattice shows a normal trend as from 10GPa.The compound undergoes a phase transition at T_0 = 190K from the ambient tetragonal crystal structure to the orthorhombic phase (W. Uhoya *et al*., 2010).

The compound $EuFe_2As_2$ can be grown experimentally using self-flux methods. The experimental values of the lattice parameters are about a ~3.916 Angstrom, b=a, and c~ 12.052 Angstrom (W. Uhoya *et al*., 2010). The ratio of the axes *c/a* exhibits a quick decrease below pressure of 8GPa and a slow decrease above the mentioned pressure of 8GPa (W. Uhoya *et al*., 2010). This compound $EuFe_2As_2$ exists as a crystal at room temperature as the $ThCr_2Si_2$ structure (Tegel *et al.*, 2008). Doping of the iron arsenide superconductors subdues the spin density wave, which is linked to superconductivity (Tegel *et al*., 2008).

In the ground state, Pnictides show spin density wave. The main differentiating factor between Cuprates (which were initially the major materials under the study of superconductivity),is the behavior of the conducting electrons (Maiti, 2015). In iron Pnictides, the Fe 3d prevails over the electrons near the Fermi level. The p character is largely contained in the states near the Fermi level (Maiti, 2015). Upon subduing magnetism in iron Pnictides, there arises superconductivity. The magnetism is subdued by doping with a suitable element or by exerting pressure externally $EuFe_2As_2$ has unique characteristics .since the Eu^{2+} ions have 4f electrons and the combined spin of the electrons is $\frac{7}{2}$. The crystal structure of the Europium diiron diarsenide is as shown in Fig. 2.1:

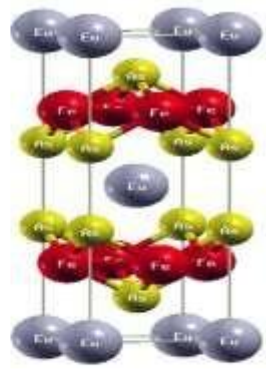

Fig. 2.1: The crystal structure of the Europium diiron diarsenide. (Mahesh & Reddy, 2018)

The Europium atom is at the center, while the iron and arsenic atoms occupy other parts of the crystal structure. This gives it a body centered crystal structure.

The general crystal structure of the AFe_2As_2 iron pnictide compounds is as given in Fig. 2.2:

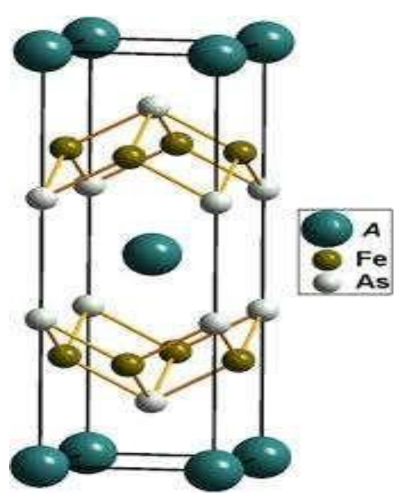

Fig. 2.2: The general crystal structure of the AFe_2As_2 iron pnictides. Source: (Alireza *etal.*, 2008)

The iron pnictides are usually body centered, as seen from Fig 2.2.

Calculating the band structure shows that Fe 3d orbitals brings about the states especially closeto the Fermi level of the iron pnictide (Li *et al*., 2012). Superconducting and ferromagnetic properties co-exist in the iron pnictide $EuFe_2As_2$ .To come up with superconductivity at a high temperature; there are two conditions that must be met: First, at the Fermi level, the Density of States should be large. Secondly, the pairing interaction should be strong since this can be connected to fluctuations in magnetism.(Li *et al.*, 2012) A crystal is a repetitive and periodic ordered state of matter. Also, a crystal can be defined as the regular and periodic arrangement of atoms in a material.

Iron Pnictide Superconductors have a high critical temperature of up to 56 Kelvin. The 122 iron Pnictide family has numerous similarities with the cuprate family, similarities which include the structure of the crystal that is layered , and, to achieve superconductivity, carrier doping is carried out (Katase *et al*., 2011). The difference is that iron Pnitides have the ability to exist in form of a metal or semi metal in the usual state, unlike the cuprates which are antiferromagnetic (Katase *et al*., 2011).

The superconductivity in iron pnictides is associated with the layered structure. The layer of iron pnictide enhances the current that is superconducting (Deng *et al*., 2009). Iron pnictide sand chalcogenides, Cooper pairs in superconductors that are iron based do not have any angular momentum and they are unconventional because they have different phases on different bands (Deng *et al*., 2009). Iron Pnictides are also unique because they have a differentiated degree of correlation which is known as the differentiation of orbitals. This normal state that is correlated is the main source of superconductivity (Deng *et al*., 2009). The iron based superconductors also experience a phase transition on application of pressure from the tetragonal crystal structure to the orthorhombic crystal structure. Furthermore, the number of electron and hole carriers is the same in the iron based superconductors (Deng *et al*., 2009) . Compounds based on copper have been previously known to be the only ones with a high critical temperature of superconductivity, higher than 40 Kelvin (Si, Yu, & Abrahams, 2016). An interaction between electrons pairs generates superconductivity in iron based superconductors (Si *et al*., 2016). They also have a wide range of electronic structures (Si et al., 2016).

Superconductivity can be achieved through doping, pressure application and also chemical substitution (Deng et al., 2009). Iron pnictides below a temperature of 150 Kelvin are metals (Yin, Haule, & Kotliar, 2011). When magnetism arises, the electronic structure is highly impacted, also, the optical conductivity increases. This is as a result of the Spin Density Wave (SDW) being much more analytical than the Para magnetism state (Yin *et al*., 2011). The paramagnetic state is solid like at a low temperature. Polarization of spin is large at points where the energy is high, while, polarization of orbitals is large at points in which the energy is low (Yin *et al*., 2011). There is no Mott transition in iron pnictides (Qazilbash *et al*., 2009). In the iron-pnictogen layers is where conduction of elecrons takes place. In the iron pnictide family, LaFePO (iron phosphide superconductor) is among the compounds which have high conductivity in the normal state (Qazilbash *et al*., 2009).

CHAPTER THREE

METHODOLOGY

3.1 Introduction to Density Functional Theory (DFT)

Density Functional Theory (DFT) provides a useful means for computation of the quantum state of particles. The density of a material usually determines the properties of a material. The ground state energy and hence wave function is a functional of the density. The electron density is the expectation or mean of the wave function. The electron density only relies on the variable coordinates x, y and z. Density Functional Theory is a useful technique for the study of materials since it solves directly approximate versions of the Schrödinger equation. The electron density determines the external potential, which in turn determines the wave function. It should be noted that no two different external potentials can have a similar density, That is to say, two different external potentials lead to two different electron densities. The Density Functional Theory is a mathematical theorem and it is exact. The Density Functional Theory attempts to solve the problem of the many body wave functions that arises due to the numerous degrees of freedom as a result of the many electrons and nuclei involved. Material modeling from first principles uses various theoretical and computational techniques which are based on Density Functional Theory or have a relationship with Density Functional Theory. The Density Functional Theory was an idea initially put forward by Thomas and Fermi in 1927, shortly after the introduction of quantum mechanics. This theory was later on developed more by Hohenberg, Kohn and Sham in the mid- sixties, which also led to the introduction of the Local Density Approximation during this period. In Density Functional Theory functionals are used to determine the properties of many electron system and the functionals of electron density are mostly considered.

Density Functional Theory originates from the condensed matter Physics. One of the reasons as to why DFT is advantageous is because it provides a reasonable starting point for ground state energy. Apart from solid state physics, Density Functional Theory can also be used in other areas such as Molecular dynamics. There are several Density Functional Theory codes for simulation and they are able to calculate various properties of a material (Hasnip *et al*., 2014). Density Functional Theory focuses on the electron density in place of the many-body wave function. Electron density refers to the number of electrons per unit volume at a specific point. The electron density is given in Eqs 3.1 below:

$$(r) = \sum \left(\left(\phi_i \right) (r) \right)^2 \qquad \text{...} \qquad 3.1$$

Where ϕ_i are the Kohn Sham orbitals of electrons that do not interact (Giustino, 2014).
Note: Summing up the electron density over all the space will yield the total electron number, that is to say: $\int (r) = n$, where n is the total number of electrons. Determining the electron density of a given system, just like the wave function, can enable us to determine the properties of the system. Density Functional Theory works on the principle that the total energy is a unique functional of the density of the electrons (Hasnip *et al*., 2014). Density Functional Theory is a quantum mechanics modeling tool.Properties of crystal systems and structures can be obtained by the use of this theory. Over the years the science community has been adapting the use of Density Functional Theory due to its reliability, transferability, and enabled software sharing. Density Functional Theory is not variational and can describe correlation. The Density Functional Theory technique can be used to describe various materials and can be transferred to be used in the study of other classes of materials. The equations employed in theorems such as Kohn and Sham is simple and intuitive. It is easy to share the software: open source software with free download and use are available for the science community to access. Correct results are usually

obtained from the computation and when compared with experimental data there is usually a minimal difference between them, making Density Functional Theory reliable. In Density Functional Theory, an assumption is made that there are no electron to electron interactions. Density Functional Theory has enabled computation on materials with very many electrons(up to thousands), which was difficult to achieve with wave function based methods due as a result of numerous number of interactions between electrons and nuclei. This has made computation of large compounds possible (Sholl & Steckel, 2011).

Density Functional Theory is implemented by three means which are: the pseudo potentials, exchange correlation and the plane wave. The basis sets for QUANTUM ESPRESSO are the plane wave basis sets. Plane waves are the set of functions which are put together so as to describe a wave function .They systematically improve basis sets to full or desired level of consistency. When using the plane wave basis, convergence in a system increases with an increase in the number of plane waves (Fiolhais, Nogueira, & Marques, 2003). Some advantages of the Plane wave basis are: It is simple to use, it is orthonormal, it is independent of the atomic positions, it is unbiased and it is easy to control convergence when using them. Plane waves take the form seen in Eqs 3.2 below:

$$(x,t) = A_0 \cos(kx - \omega t + \varphi) \quad \text{......} \quad 3.2$$

where A_0– amplitude, k-wave number, ω-angular frequency, φ - phase shift of the wave.

x- point along the x-axis, and $A(x,t)$ –magnitude of disturbance or displacement of the wave.

Plane waves help in calculating the total energy of a system by using the periodicity of the lattice of a given crystal. However, it should be noted that, the higher the number of plane waves, the more difficult it becomes to calculate the total energy of a system (Fiolhais et al., 2003). Plane waves are exact Eigen states and are not biased to any specific atom (Togo & Tanaka, 2015). The advantages of plane wave basis sets include the following: they are not difficult to implement, that is to say, they are simple and easy to use. They also allow convergence to be achieved systematically, and are independent of the positions of the atoms. The disadvantages of the plane wave basis include: it requires very many plane waves to attain a high level of accuracy and it is difficult to achieve convergence for the orbitals that are tight. Pseudo potential is the effective potential which is used as an approximation for the simplified description of complex systems such as the Many Body Schrödinger Equation, MBSE. The valence electrons in an atom influence the properties of the material and are used to classify the material. The pseudo potential replaces the potential and the core electrons which barely determine the properties of the material. Pseudo wave functions take the place of true valence wave functions hence enabling the use of lesser number of plane waves since they are node less. This is because the electron wave functions near the nucleus oscillate rapidly as a result of interaction with the positively charged nucleus, therefore need to be replaced by plane waves of short wavelength which results into large cut-off energy, an issue addressed by the pseudo potential.

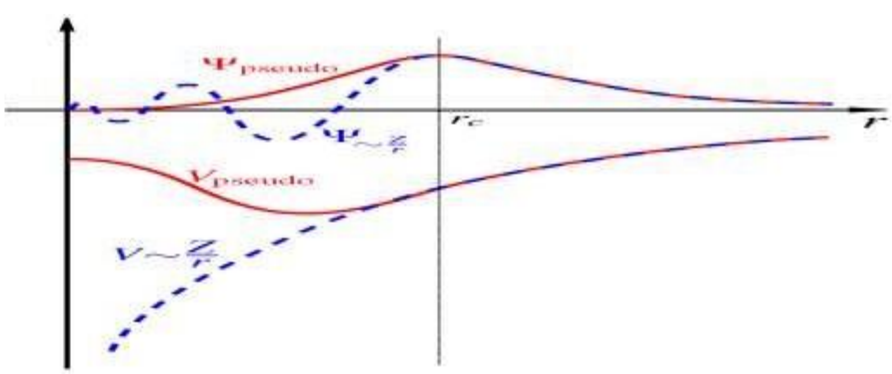

r_c-cut off atomic radius, V-potential, ψ-wave function

Fig. 3.1: General representation of pseudo potential. The real and pseudo wave function at a given cut-off atomic radius are in good agreement, (Togo & Tanaka, 2015) justifying the use of pseud potentials.

Therefore the pseudo potentials represent the real potentials of the system with a high level of accuracy at a certain cut off atomic radius.

Pseudo potentials cater for the core electrons, cover the strong potential of the core electrons and allow correct self-consistent field calculations (Hamann, Schlüter, & Chiang, 1979). As seen from the above diagram, the real and pseudo wave function at a given cut-off atomic radius are in good agreement, (Togo & Tanaka, 2015) justifying the use of pseudo potentials. The cut off radius is used to determine the quality of a given pseudo potential. Pseudo potentials with small cut off radius are realistic and strong, while those with a big cut off radius are unrealistic (Fiolhais *et al*., 2003).

A good pseudo potential should illustrate correctly the characteristics of valence electrons in numerous different chemical surrounding or it should be transferrable(Fiolhais *et al*., 2003) When using the pseudo potential approximation, the external potential is the sum of the individual pseudo potential of each atom that is present in the crystal.

The Projector Augmented Wave (PAW) Non Linear pseudo potentials were used in this research (Kresse & Joubert, 1999; Troullier & Martins, 1991). QUANTUM ESPRESSO supports the use of Projector Augmented Wave (PAW), Ultra Soft Pseudo Potentials (USSP), which are Norm Conserving (NC). Norm Conserving pseudo potentials are hard but they maintain the accuracy. Norm Conserving means that the integral of the square of the real all electron wave function should be equal to the integral of the square of the pseudo wave function. Norm Conservation improves on transferability. USSP tremendously decreases the cut off energy, especially for difficult elements. The Ultra Soft Pseudo Potentials can make the pseudo wave functions very soft and also select multiple references of energy. Projector Augmented Wave allows the user to reconstruct the wave function.

The factors one should consider in the selection of pseudo potentials include: the level of accuracy that can be achieved by using it, the transferability of the pseudo potential, relativistic and the semi core inclusions. Over the years, the Density Functional Theory methodology has become more popular in use amongst various scientists in the Physics and Chemistry fields; and lots of Density Functional Theory -based academic papers have been published. Apart from the numerous publications, there also exist several books printed to discuss the fundamentals of Density Functional Theory and related topics (Fiolhais *et al*., 2003), hence proving its increasing use as seen in the Fig. 3.2 below:

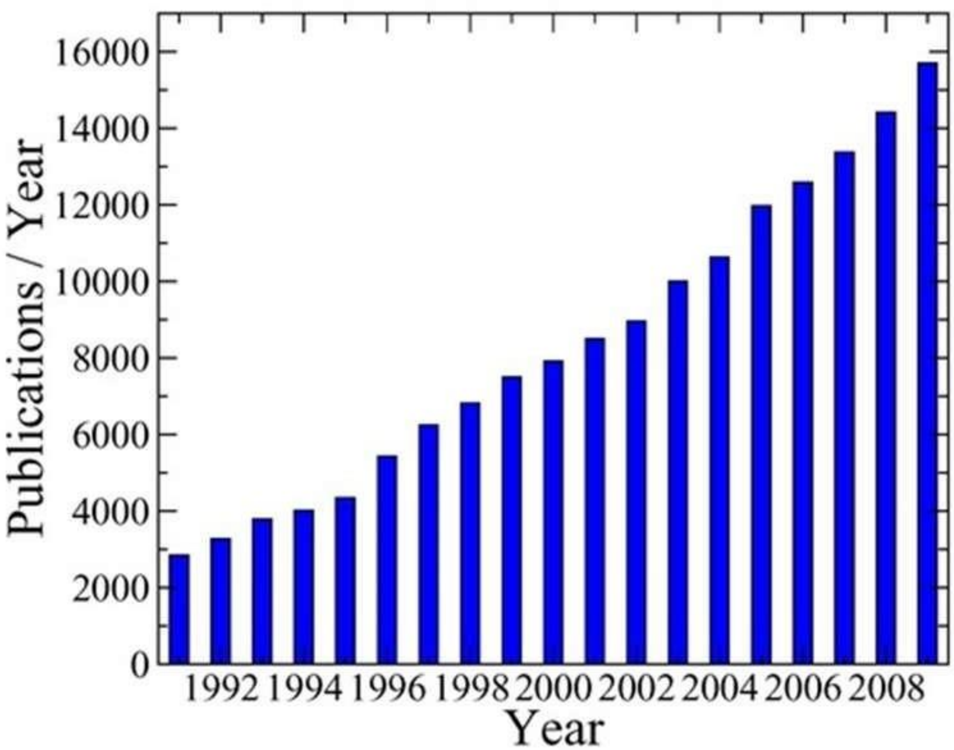

Fig. 3.2: DFT publications over the years up to 2009. The number of publications keeps increasing each year, implying that more scientists are employing this method to perform their research.

The use of DFT over the years has increased over the years as shown in the above figure, this is because it is much cheaper to use in research and provides results which are similar to those produced by experimentalists.

Density Functional Theory is based on two basic theorems which are:

i. Kohn and Hohenberg theorem
ii. Kohn and Sham theorem

The Kohn and Hohenberg theorem states that the energy of the ground state of a system is a unique functional of the density of the electron, which in turn relates the ground state energy to the wave function of the ground state (Giustino, 2014). The Kohn and Hohenberg theorem did not define exactly what the functional is, therefore, the Kohn and Sham theorem goes ahead to describe a useful characteristic of the functional: The density of the electron that makes the energy of the overall function minimum is the true density of the electron that corresponds to the solution of the Schrödinger equation; This means that, the electron density that takes the energy of the system to a minimum is the density that provides the solution to the Schrödinger equation, hence the electron density is a unique functional of the total energy of a given system. In the Kohn and Sham theorem, both the kinetic energy and density of electrons are known exactly from the orbitals (Togo & Tanaka, 2015). The Kohn and Sham equations are non-linear therefore they are solved through iterations to achieve self-consistency.

Kohn and Sham came up with a set of valid equations, which, to solve them, the Hartree potential must be defined, and, to do so, the density of electrons should be known. To obtain the density of electrons, the single-electron wave functions should be known; also to obtain the wave functions, the Kohn Sham equations should be solved. This appears like we are moving in a circle!

To solve the above problem, an iterative technique is used whereby:

i. The starting density of electron on trial is defined (A trial electron density selected.)
ii. The Kohn Sham equations are solved using the above trial electron density.
iii. The electron density is calculated as obtained from the Kohn-Sham single particle wave functions.
iv. The computed density of electron is compared with the density of electrons employed in solving the Kohn-Sham equations. If the above densities are similar, then this is the density of electrons in the ground state, if they are not similar, the trial density of electron should be changed and the procedure repeated from step two.

The iterative technique here leads to a self-consistent solution of the Kohn-Sham equations.

But, to obtain a solution of the Kohn-Sham equation, the exchange correlation functional should be defined, which is a bit complicated to define. However, in the uniform electron gas, this functional has been obtained exactly and it gives a means of using K-S equations.

3.2 The Many-Body Schrödinger equation

Matter consists of electrons and nuclei, hence understanding the properties of materials entail a proper comprehension of the characteristics and behavior of nuclei and electrons. Quantum mechanics is therefore of the most important branches of Physics, since it deals with the study of the characteristics of sub-atomic particles (Fiolhais *et al.*, 2003). Nuclei and electrons interact with each other and there exist two fundamental interactions: one, electrostatic interaction and two, Coulomb interaction. Electrons, especially the valence electrons move at velocities which are much lower as compared to the speed of light and therefore they are non-relativistic (Fiolhais *et al*., 2003). In quantum mechanics, the nature of atoms, their electrons and nuclei particles is illustrated in details. Understanding the electron and the electronic structure opens up a path to comprehending many more useful properties of materials; hence electrons are of importance in quantum mechanics. Quantization of energy is also studied, the Schrödinger equation forming a basis for these solutions. The Schrödinger equation , $H\psi = E\psi$, where H is the Hamiltonian and E is the energy, is one of the most important equations in quantum mechanics, since its solution yields the ground state energy and ground state wave function which contain useful information about any given crystal structure. The Hamiltonian term consists of both the kinetic and potential energy terms of the electrons and nuclei present in the material. The Schrödinger equation can be time dependent or time independent. In Condensed Matter Physics, the major concern is to obtain a solution to the non-relativistic time independent Schrödinger equation (Togo & Tanaka, 2015).

The Schrödinger equation can also be re-written as in Eqs 3.3 below:

$H = T_e + T_n + V_{ee} + V_{en} + V_{nn}$ ……………………………………… …………………...............3.3

Where, T_e and T_n are the kinetic energies of the electrons and nuclei respectively, V_{ee} describes the electron-electron interaction V_{en} describes the electron-nucleus interaction and V_{nn} describes the nucleus-nucleus interaction.

Solutions to the Schrödinger equation for simple atoms like the hydrogen atom can be obtained since it has a single electron. However, when the electrons increase in number, the Schrödinger equation becomes more complex and a bit complicated to obtain the exact solution, and it's now referred to as the Many-Body Schrödinger Equation. By solving the Many Body Schrödinger Equation**,** we obtain the ground state wave function hence the ground state energy. The wave function contains important information about the state of particles therefore we can obtain the properties of a material from it. The time independent many body Schrödinger equation is mainly considered in Density Functional Theory. Eqs 3.4 is the time-independent Many Body Schrödinger equation:

$$-\sum_{j}^{N}\frac{\hbar^2}{2m_j}\nabla_j^2-\sum_{i}^{n}\frac{\hbar^2}{2m_i}\nabla_i^2+\sum_{j}^{N}\sum_{p>j}^{N}\frac{Z_jZ_p}{R_j-R_p}-\sum_{i=1}^{n}\sum_{j=1}^{N}\frac{z_je}{r_i-e_j}+\sum_{i=1}^{N}\sum_{q>1}^{n}\frac{e^2}{r_i-r_q})\,\psi(r_1,r_2\,...\,r_n)=$$

$$E\psi(r_1,r_2\,...\,r_N)\text{……………….}3.4$$

The first term on the left hand side of the above equation is the kinetic energy of the nuclei, the second term kinetic energy of electrons, the third and fourth terms are potentials due to nuclei-nuclei interaction and nuclei to electron interaction respectively. The fifth term is the potential due to electron-electron interaction. In summary, the left hand side represents the Hamiltonian of the system. Due to many electrons and nuclei in the system, it's difficult to get exactly the solution to the system. Though difficult, there are valid approximations that are employed in solving the equation above. To solve the above equation, the scientific community came up with valid approximations. The approximations are as discussed below:

3.3 The Born Oppenheimer Approximation

The electron motion and the nuclei motion in molecules can be made into separate mathematical problems. This approximation focuses on the fact that the nucleus is much more heavier compared to the electron. Therefore, in terms of motion, the nucleus moves at a very slow speed compared to the electron hence it can be considered to be stationary or fixed. This therefore implies that the kinetic energy term of the nucleus in the many-body Schrödinger equation vanishes. This is the Born Oppenheimer approximation. On this approximation, The Many Body Schrodinger Equation is asshown below in Eq 3.5

$$-\sum_i^n \frac{\hbar^2}{2m_i}\nabla_i^2 - \sum_{i=1}^n \sum_{j=1}^N \frac{Z_j e}{r_i - r_j} + \sum_{i=1}^n \sum_{q>1}^n \frac{e^2}{r_i - r_q} + \sum_j^N \sum_{p>j}^N \frac{z_j z_p}{R_j - R_p}) \, \psi(r_1, r_2 \dots r_n) =$$

$$E\psi(r_1, r_2 \dots r_n) \ldots\ldots 3.5$$

The Born Oppenheimer Approximation is considered to be an adiabatic approximation (Pisana *et al*., 2007) because there exist no coupling between various electronic surfaces.

3.4 Thomas-Fermi Approximations

This approximation was developed by Thomas and Fermi. To obtain the total energy of a system, the potential energy and kinetic energy are summed as in Eq. 3.6 and below. The kineticenergy of electrons is obtained through the partial varying electron density η(r).

$$E = T + U_{e-z} + U_{e-e} \quad \ldots\ldots\ldots\ldots\ldots\ldots\ldots\ldots\ldots\ldots\ldots\ldots\ldots\ldots 3.6$$

3.5 Hohenberg-Kohn Approximation

The electron density contains important details about the particle, and the ground state energy is a functional of the density of the electron. The external potential is a functional of the electron density. The theorems address the energy function that Thomas and Fermi were not aware about in their previous discovery.

The theorems are as follows; The external potential ( ), and hence the total energy is a unique functional of the electron density $[(r)]$, and, a universal function for energy $[E(\eta(r))]$ can be defined in terms of density as in Eq 3.7 :

$$E(\eta(r)) = \int n(r) v_{ext}\, dr + F(\eta(r)) \quad \ldots\ldots\ldots\ldots\ldots\ldots\ldots\ldots\ldots\ldots\ldots\ldots 3.7$$

Therefore, according to the theorems, studying the electron density in the DFT can enable one to obtain the energy of a system hence the compound's properties can also be determined.

3.6 Kohn-Sham formulation

A fictitious non-interacting system is constructed such that its density is the same as that of the interacting electrons. The solutions of the Kohn–Sham are single electron wave functions that depend on only three spatial variables. The Kohn-Sham is taken to be exact because it gives a ground state density as that of the actual system. The exact ground state density can be written as the ground state density of a fictitious system of non-interacting particles, expressed as follows in Eq. 3.8:

$$E\eta(r) = E_k[\eta(r)] + E_{e-e}[\eta(r)] + U_{ei}\eta(r) + E_{xc}\eta(r) \quad \ldots\ldots 3.8$$

Where: $E_k[\eta(r)]$-Kinetic energy of the electrons, $E_{e-e}[\eta(r)]$- Electron-electron energy $U_{e-i}[n(r)]$- Electron-ion interaction potential and $E_{XC}(\eta(r)$ - Exchange correlation energy resulting from Pauli Exclusion Principle (Kohn, 1999)

To solve the Kohn Sham equations, self-consistency must be achieved in the iterative process. The equations are said to be 'simple', because the computational effort required to solve them is much less as compared to the one required to solve the Hartree Fock (Fiolhais *et al*., 2003). Being easy therefore does not imply that they are not difficult or fast to write. Computer codes have been written to solve the Kohn Sham equations for any given system. It should be noted that the Kohn Sham potential depends on the electron density (Fiolhais *et al*., 2003).

The Kohn Sham technique is the most extensively used technique of calculating the electronic structure in Condensed matter Physics (Fiolhais *et al*., 2003). The KS method gives the total energy of a system exactly, and leaves the exchange correlation energy to be estimated. This is quite trivial because of the following reasons: First, the total energy of a system takes a huge portion while the exchange correlation energy is just a small portion. Secondly, the total energy dictates the shell structure density oscillations and Friedel types. Lastly, the exchange correlation energy is more suitable for the local and half local estimation (Fiolhais *et al*., 2003).

3.7 Hartree-Fock (HF) method

DFT and wave function methods are strongly connected. HF is one of the wave function techniques related to the electron density in its working. This approximation method determines the wave function and energy of a given system in a stationary state. The many-electron problem is reduced to single electron problem and hence the single electron problem is solved to obtain the solution for the many electron problems. In this approximation, N-electrons wave function ψ is expressed as a single determinant of N-single particle wave function (x_i).

Where (x_i) is the product of (r_i) spatial orbital function and (s) electron spin functionexpressed in Eq. 3.9 below:

$$\psi_i x_i = \varphi_i(r_i)\sigma_s \quad \text{3.9}$$

The Hartree- Fock method did not take into account the energy of correlation, which is now the energy accounted for through approximations in Density Functional Theory as the exchange correlation energy through the use of Local Density Approximation and Generalized Gradient Approximation.

The Hartree-Fock method caters for the Pauli Exclusion Principle by writing the wave function as a Slater determinant of single electron wave function and is applicable to the non-degenerate ground states. Non-degenerate in this case means a state with different energy and quantum states. If any two electrons are in the same position at the same time, their determinant goes to zero. However, the Slater determinant above actually exists to cater for this by the using of Pauli Exclusion Principle which states that no two or more electrons can exist in the same quantum state at the same time. There exist two main limitations of Hatree-Fock approximation which includes; one, the nature of the function is not known and secondly, the necessary conditions to be met for a function $n(r)$ to be seen as the most accurate ground state solution are not well characterized. Other approximations such as the LDA+U are also present, the choice of the correlation function depending on the type of material you are working on and what exactly you need to achieve.

3.8 Exchange Correlation

The exchange correlation energy contains all the quantum effects in a given system and is given as in Eq. 3.10 below:

$$E_{xc} = E_c + E_x \qquad \text{3.10}$$

Where, E_X is the exchange energy between similar spin electrons and E_C is the correlation energy between electrons with different spin. The Exchange correlation also refers to the difference between the real kinetic energy and the Kohn Sham kinetic energy. The exchange correlation energy E_{XC} is usually a small fraction of the total energy of a given atom or system, but it greatly dictates the chemical bonding and other useful aspects such as the energy of atomization; therefore correct approximation of this term is essential in the DFT scheme (Fiolhais *et al*., 2003).

The exchange correlation functional is independent of external potential and is universal. In cases where the density of charges is slowly changing/ where the charge density is variable, GGA is much better than LDA although not for all systems (Togo & Tanaka, 2015). To obtain the exchange correlation energy, the Local Density Approximation and Generalized Gradient Approximation, Meta Generalized Gradient Approximation, and Hybrid functionals can be used. But, before addressing the exchange correlation functionals, it is important to hint about the uniform electron gas due to its various advantages to the generation of functionals as will be mentioned below:

The uniform electron gas.

The uniform electron gas is also known as the Jellium. It postulates that the electron density is constant over all space. Near the surfaces of materials, the electron density varies in an oscillatory way (Lang, 1969; Lang & Kohn, 1971, 1973). The most simplified systems play an important role in science. For instance, the study of the hydrogen atom is very important in quantum and atomic Physics, and the uniform electron gas is quite important in solid state Physics and Density Functional Theory. Since the electron density is constant over all space in the uniform electron gas, it implies that the number of electrons is infinite. In the Density Functional Theory scheme, the uniform electron gas is applied in the construction of the Local Density Approximation, which is the ‘mother’ of all the other approximations of exchange correlation energy. Using the quantum Monte Carlo computations of the uniform electron gas, correct values of the density of correlation energy have been acquired for numerous values of electron density, and these values have been employed in the construction of the half empirical correlation function (Ceperley & Alder, 1980; Perdew, McMullen, & Zunger, 1981).

3.8.1 The Local Density Approximation

This is one of the easiest approximations and all the other approximations are based on it. It has given reliable predictions of the frequency of vibration, stability of phases and moduli of numerous compounds hence its use in some cases. The Local Density Approximation uses the density of the electrons to determine the exchange correlation energy (Becke, 1988) and is expressed in Eq. 3.11

below:

$$E_{xc}(\rho) = \rho(r)\varepsilon_{xc}\rho(r)dr \quad \text{……3.11}$$

The Local Density Approximation over binds, that is it over compresses the system, therefore when one uses it they obtain results that are of lower figure when compared to experimental values.

The Local Density Approximation is quite economical computationally in the estimation of the exchange correlation energy but however, it overestimates the binding energy, hence the use of the Generalized Gradient Approximation (Neyman, Pacchioni, & Rösch, 1996).

3.8.2 The Generalized Gradient Approximation

The Generalized Gradient Approximation originates from the Local Density Approximation and uses the spatial variation of the electrons to determine the exchange correlation energy and it is expressed in Eq 3.12:

$$E_{xc}^{G}GA[\eta(r)] = \int drf\eta(r), \nabla\eta(r) \quad \text{……..3.12}$$

The Generalized Gradient Approximation uses both the density of electron and gradient of the electron density. The Generalized Gradient Approximation is a Perdew, Burke and Ernzerhof (PBE) functional.

It is advisable that when you are working with the GGA, use a pseudo potential that has been generated by the Generalized Gradient Approximation, that is to say, the pseudo potential and the functional should be the same (Fiolhais *et al*., 2003). The Generalized Gradient Approximation functional is size consistent (Fiolhais *et al*., 2003). Note: for two separate sub systems of energies E_1 and E_2, and densities $n(r_1)$ and $n(r_2)$, the total energy E of the system is the sum of the two individual energies, that is to say, $E= E_1 + E_2$ and the density of the system is the sum of the two individual densities i.e., $n(r)= n(r_1)+ n(r_2)$ (Fiolhais *et al*., 2003). Approximations that satisfy the above condition are said to be size consistent. The Generalized Gradient Approximation, unlike the LDA, under binds, that is, when one uses it, the results obtained are of a higher figure when compared to experimental figures. For example, when comparing the Generalized Gradient Approximation optimized values of the lattice parameters with experimental lattice parameter values, the Generalized Gradient Approximation values are seen to be a bit higher than experimental values, simply because the Generalized Gradient Approximation under binds. The Generalized Gradient Approximation generates bigger bond lengths, the LDA does an underestimation of the equilibrium lattice parameter and the Generalized Gradient Approximation over estimates the equilibrium lattice parameter (Fiolhais *et al*., 2003). One of the most famous Generalized Gradient Approximation is the PBE and BLYP. In this study, the PBE (Perdew, Burke and Ernzerhof) functional of the Generalized Gradient Approximation was used because of the nature of the compound. The Generalized Gradient Approximation may look as the grand solution for the exchange correlation energy, though this is not the case. The density of the core in an atom is quite important since it dictates the overall density of the material except for the very light atoms.

This therefore implies that in large gradients, the Generalized Gradient Approximation gives a better description of the density of the core. The functional one chooses depends on what the individual intends to achieve.

The Generalized Gradient Approximation cannot work for non-single Slater determinants and when the non-interacting energies are nearly degenerate. It also does not capture a diffusing long range tail in a system that is extended (Fiolhais *et al*., 2003). The Generalized Gradient Approximation has the disadvantage of under estimating the band gap when its results are compared to results from experiments. In summary, the Generalized Gradient Approximation is a better exchange correlation approximation for numerous systems than the LDA and gives a one to three percent range of error. It also gives a correction of the over binding element of the Local Density Approximation.

In this research the open source software Quantum Espresso which is a full *ab- initio* package for performing the electronic structure properties, energy, and mechanical property calculations was used. Take for instance the concept of the Jacob's ladder. At the bottom is the LDA, then the GGA above it and other hybrid functionals as you go up. The ladder leads us to the 'heaven' of chemical accuracy, therefore implying that the Generalized Gradient Approximation is more advanced than the LDA, though more painful and more expensive to work with in terms of computation resources and time. The Generalized Gradient Approximation corrects the Local Density Approximation to obtain results that are much more similar to experimental findings (Fiolhais *et al*., 2003).

The constant 'a' can be obtained through a theoretical estimation as a~1/4 for the case of molecules (Fiolhais *et al*., 2003). Hybrid functionals are considered to be the most correct functionals of the density that are used in quantum computations.

The Jacob's ladder (Fiolhais *etal*., 2003) of approximation of the functionals of density stretches from the 'Hartree world' to the 'heaven' of chemical accuracy (Janesko, 2013). The ladder has got five steps as explained below, starting from the bottom (Janesko, 2013).

i. Local spin density approximation (LSDA), is the 'parent' of the other approximations. It uses the spin up density of electrons and spin down density of electrons as its ingredients.

ii. The Generalized Gradient Approximation (GGA), it includes the gradient of the electron density in its operations.

iii. The Meta Generalized Gradient Approximation, it includes the derivatives of the gradient of electron density

iv. The hyper Generalized Gradient Approximation, it includes the exact exchange energy density. The hybrid functionals are actually classified under the hyper GGA.

v. Exx with partial exact correlation (Fiolhais *et al*., 2003)

Inbuilt in Quantum Espresso is the Plane-Wave Self-Consistent Field (PWSCF) code which is employed to do the calculation of the total energy in a system. PWSCF employs norm conserving Pseudo Potential (PP) and Ultra-Soft Pseudo Potential (USPP). Norm conserving pseudo potentials enable elimination of core electrons from *ab*- initio calculations, which makes the computation quicker. USSP solve the problem of strongly fluctuating pseudo potentials near the nucleus, hence making the study of elements in the row and transition elements easier to study. However, this leads to loss of details on the wave functions of the electrons in the nuclei vicinity, an issue overcome with the use of Projector Augmented Wave (PAW) method. Quantum Espresso is also inbuilt in the supercomputer at the CHPC South Africa where the calculations were done. One can run self- consistent calculations in QE to obtain the total energy of the system, the Fermi energy and much more valuable theoretically computed data. Self-consistent calculations are performed and once convergence is achieved, more calculations such as the Density of States, mechanical properties and band structure are done on the system. The flow diagram for the total energy calculation in the Density Functional Theory is as shown in Fig. 3.3. Upon the initial guess on our system, it indicated convergence hence other calculations followed after.

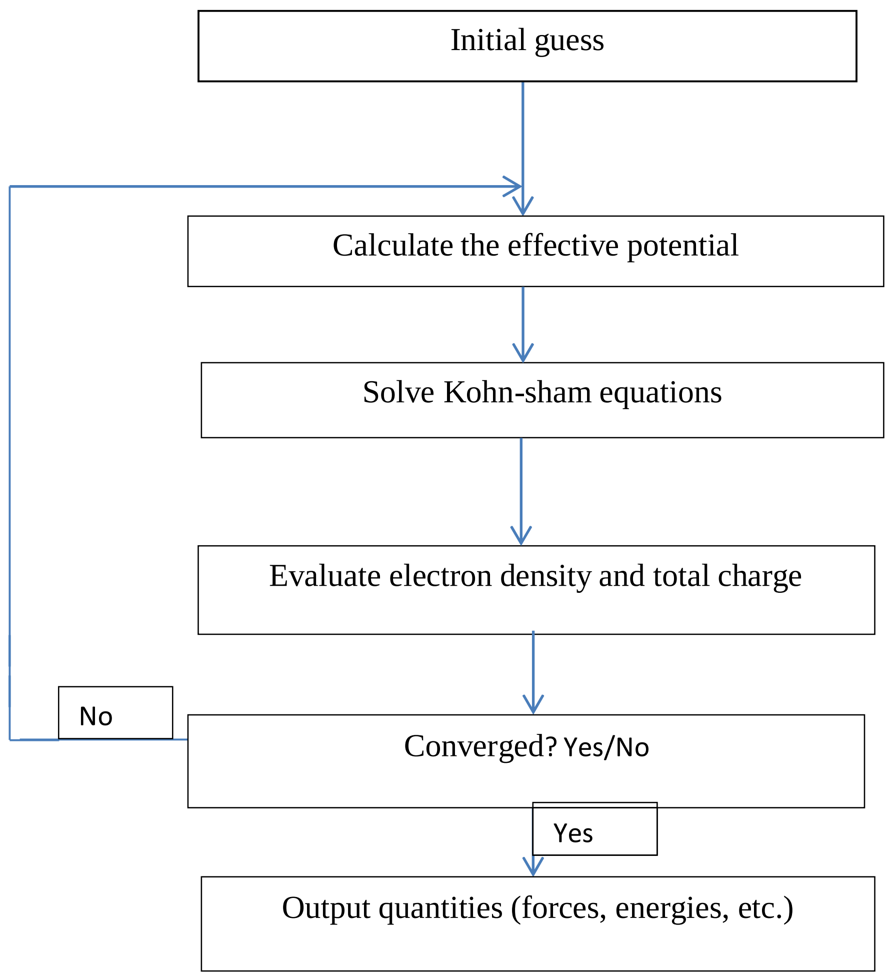

Fig. 3.3: The Density Functional Theory flow chart as adapted from (Hao, Moran, Liu, & Olson, 2003).

After the electron density and total energy have been evaluated, if convergence is achieved, calculation proceeds to provide output quantities such as forces and energies, if convergence is not achieved, the initial guess is reset and the steps repeated until the system converges.

The above procedures are followed systematically, if the system converges after a given limit of iterations then we proceed to further calculations, if the system does not converge, the process is repeated to achieve convergence. Convergence is a state in which the system has the lowest energy, hence at this point it is considered to be at its most stable state. It is achieved through the system performing several iterations on the compound, to attain the lowest energy of the system. This prevents unnecessary errors in the results obtained in the study. There is a great correlation between the critical temperature of a compound and the electronic band structure; hence, studying the electronic structure properties of the compound will generate useful data, since at a given critical temperature; there will be an onset of superconductivity in the material (Adhikary *et al*., 2013). The study of Density of States (DOS) and Partial Density of State (PDOS) will also provide additional valuable information on the electronic structure of the compound. The band structure diagram can reveal the states and energy levels available for occupation. The two dimensional diagram of the band structure can greatly assist in classifying a compound as a metal, semi-metal or insulator. It can also help to determine whether a material has a direct or indirect bad gap, basing on the position of the maximum band line in the valence band and minimum position of band line in the conduction band. Also, studying theoretically the mechanical properties of the material and establishing the Young’s modulus, shear modulus, bulk modulus and Poisson’s ratio and application of varying pressure on the material will help us establish and analyze how the material responds to mechanical stresses, and come up with a critical temperature at which indicates the onset of superconductivity of the material. For instance, studying the Poisson’s ratio of the compound as one of the mechanical properties will help us determine whether the compound is ductile or brittle, using the Frantserich (Frantsevich, Voronov, & Bokuta, 1983) technique. For a Poisson ratio less than 0.26 the material is brittle and for that greater than 0.26 the material is ductile.

The two main theorems on which DFT is based are applicable only to the ground state; this proves to be a limitation in the study of excited states. Though predictions of the excited states may be made from the ground state, they may not be very accurate. Also, in the case of weak vander Waal forces, DFT computations may provide results that are incorrect (Sholl & Steckel, 2011). Finally, when dealing with a system that has a large number of atoms, such as hundreds or thousands of atoms, it becomes computationally expensive in terms of time and resources required to perform computation (Sholl & Steckel, 2011). In summary, the basic model of solid state consists of Plane Waves, Pseudo Potentials and the Kohn Sham equations (Fiolhais *et al*., 2003).

Crystal Structure

A crystal structure is composed of a Bravais lattice and a basis. A Bravais lattice is a set of pointswhich are ordered in such a way that they look exactly alike when one views them from whatever position. Bravais lattice is the most sophisticated variety of lattice, in which case, a lattice refers to an array of points in which a similar pattern is repeated; such that if one viewed the points from any direction, they would look exactly the same therefore it would be difficult to differentiate them. Since lattices are formed through repetition of small units, structures can therefore be studied through studying just a small unit or region instead of the whole structure. The small unit or region is known as a primitive cell.

The inverse of the volume of the primitive cell gives the density of the material. The study of the structure of a crystal is quite important since in-depth computation of mechanical and electronic structure properties relies on knowledge of the positions of the individual atoms. Lattice can either be monoatomic lattices which are made up of atoms of one element or diatomic lattices. Compounds consist of two or more elements therefore cannot be classified as Bravais lattices, but as lattices with a basis. Lattices can be categorized depending on their symmetries and for the seven crystal systems; there are 14 Bravais lattices Crystal structures that are also made up of a unit cell.

The Bulk modulus is obtained using the Eqs 3.14, 3.15 and 3.16 below

$$B_v = \frac{2C_{11} + 2C_{12} + C_{33} + 4C_{13}}{9} \quad \text{……………………………………………………………….3.14}$$

$$B_R = \frac{C^2}{M} \quad \text{…………………………………………………………………………………3.15}$$

$$C^2 = (C_{11} + C_{12})_{33} - 2C_{13}^2$$

$$M = C_{11} + C_{12} + 2C_{33} + 4C_{13}$$

$$B = \frac{B_V B_R}{2} \quad \text{………………………………………………………………………………3.16}$$

The Shear modulus is obtained using Eqs 3.17 , 3.18 and 3.19 below:

$$G_v = \frac{M + 3C_{11} - 3C_{12} + 12C_{44} + 6C_{66}}{30} \quad \text{…………………………………………………………………3.17}$$

$$G_R = \frac{15}{\frac{18B_V}{C^2} + \frac{6}{C_{11} - C_{12}} + \frac{6}{C_{44}} + \frac{3}{C_{66}}} \quad \text{…………………………………………………………………………..3.18}$$

$$G = \frac{G_V + G_R}{2} \quad \text{……………………………………………………………………………..3.19}$$

The Young's modulus E and Poisson's ratio V were obtained respectively using the Eqs 3.20 and 3.21:

$$E = \frac{9GB}{3B + G} \quad \text{…………………………………………………………………………………3.20}$$

$$V = \frac{3B - 2G}{2(3B + G)} \quad \text{…………………………………………………………………………...3.21}$$

The word phonon originates from the Greek language and it means sound, since phonons generate sound. The idea of phonons was introduced by a physicist from Soviet, known as Igor Tamm. The study of phonons assists in understanding properties of materials such as thermal and electrical conductivity. It helps us to quantize the energy of vibration. A phonon refers to a kind of lattice vibration in a crystal, where the particles vibrate at the same single frequency (Simon, 2013). Phonons quantize the energy of vibration. From the phonon dispersion calculation, one can be able to calculate the critical temperature of the material in question. A dispersion relation refers to the relationship between the frequency of vibration and the wave vector and this relationship is given as in Eq 3.22 below:

$$\omega = v(k) \qquad \text{3.22}$$

Where, k - wave vector, - frequency of vibration and v - velocity of sound. (Simon, 2013) (Yu & Cardona, 1996). Phonons are assumed to have momentum (Meyers & Myers, 1997). Past studies have predicted that phonons may have some mass, and since they exhibit some movement, they therefore have momentum (Nicolis & Penco, 2018). There are two branches in phonon dispersion relation: the acoustic mode which is the lower mode and the optical mode, which is the upper mode (Misra, 2011). The acoustic mode refers to the in phase vibration mode while the optical mode refers to the out of phase vibration. The optical phonons get their name from the fact that they get excitedby the radiation of infra-red in crystals that are ionic (Mahan, 2011). There are two types of phonon calculation methods: the frozen phonon method and the Density Functional Perturbation Theory as implemented in PWSCF using ph.x. QE uses the DFPT to do the phonon calculation. DFPT is fast and reliable but has got some limitations such as it does not work for hybrid functionals.

The finite differences method cannot calculate the dielectric tensor or effective charges. The frozen phonons are computed for atoms at known positions. It is the computation of total energy as a function of the position where the atoms are located. For the case of Density Functional Theory phonons, big super cells are required and it takes a lot of time to do the calculation. However, this method can accurately do the calculation of the matrix of the force constant through displacement of the atoms.

The frozen phonon method is much faster and cheap in terms of computation as compared to the linear response technique that uses the Density Functional Perturbation Theory to perform calculation of the forces. This method however has the following setbacks: big super cells are required to correctly do the calculation of the matrix of the force constant. Also, the displacement of a single atom in the unit cell generates forces not only on all the atoms in the unit cell but also on the repeated image of atoms. Valence electrons, unlike the core electrons, are quite useful in the formation of bonds. The valence electrons are the ones that undergo ionization and are the electrons that conduct electricity in materials since they are not strongly attracted to the nucleus as the core electrons. As a result of this, the frozen core approximation method does away with the nucleus and core electrons and works with the valence electrons since they are the most active. This results to reduced number of wave functions.

Other advantages of frozen core approximation method include: there is a reduction in the number of plane waves required, therefore the computation is a lot quicker, and the researcher can work with many more electrons. The effect of relativity is removed from the system since this problem is brought about by the core electrons. The pseudo potentials produce a very little percentage of errors in their working**.**

CHAPTER FOUR

RESULTS AND DISCUSSION

4.1 Optimization

In this section, we report the various results obtained from the theoretical computation. The open source computer code Quantum Espresso, which incorporates the Density Functional Theory (DFT), Pseudo Potentials (PP) and the Plane Wave (PW) was used to perform calculations from first principles. Projector-Augmented Wave (PAW) Pseudo Potentials were used in these calculations. There are three types of atoms in the crystal, namely: Europium, Iron and Arsenide. The number of atoms in unit cell considered in these calculations is five; one Europium, two iron, and two arsenic atoms. Optimization of the k-points, lattice parameters and cut-off kinetic energy were carried out and the system was run to convergence. Optimization details and graphs are reported in details. The first step of the computation was to make an input file for the calculations. In our study, we used the Plane Wave method to investigate the electronic and mechanical structure properties of the compound from first principles, using the open source computer code Quantum-Espresso (Giannozzi *et al*., 2009). Self -Consistent Calculations were run to obtain the total and Fermi energy of the system, which are useful parameters in describing the electronic structure properties of the compound (West, Sun, & Zhang, 2012).The input files were designed such that the mechanical properties including the Bulk, Shear and Young moduli, and Poisson ratio were obtained. Quantum Espresso supports the use of Projector-Augmented Wave (PAW), Ultra Soft Pseudo Potentials (USPP), which are Norm Conserving. Norm Conserving Pseudo Potentials are well normalized, a feature useful for an accurate description of bonding in the compound (Hamann, 1989; Hamann *et al*., 1979).

PAW Non Linear Correction Pseudo Potentials were used in these calculations (Dalgarno, Bottcher, & Victor, 1970; Garrity, Bennett, Rabe, & Vanderbilt, 2014; Troullier & Martins, 1991). Before running the Self-Consistent Calculations, the Variable Cell relax (VC-relax)calculation was performed to obtain relaxed atomic positions and then optimization of cell dimensions, K-points, and the kinetic energy cut off(which was set at 45 Ry) was also done so as to obtain a relaxed crystal structure, to ensure that the ground state crystal structure is obtained and that the results are free from stress (Lund, Orendt, Pagola, Ferraro, & Facelli, 2013; Wales & Scheraga, 1999; Yang *et al*., 2009). The initial k-point sampling was done using 2π/a where a is the lattice parameter (W. Uhoya *et al*., 2010). Optimization of the k-points yielded the converged K-points, convergence ensuring a stress and strain free system. Sampling on the Brillouin zone was done using the Monkhost scheme and the mesh used was 8x8x6. Exchange correlation was computed by employing the Generalized Gradient Approximation as put forward by Perdew, Burke and Ernzerhof. Plane wave basis were used as a basis set for optimization of the lattice parameters, k-points and cut off kinetic energy so as to obtain converged total energy. Calculations were performed in the quenched paramagnetic state, implying that the polarization of the spin is not permitted on the Fe ions in the computation (Li *et al*., 2012). The Density Functional Theory which focuses on the electron density to study the properties of a many electron body system was employed. Experimental cell dimensions were used in the input file before optimization. Before optimization was carried out, the variable cell relax calculation was done to obtain relaxed atomic positions, which were then used to perform optimization on the compound. The optimization curves for the iron pnictide $EuFe_2As_2$ are as shown in Fig. 4.1:

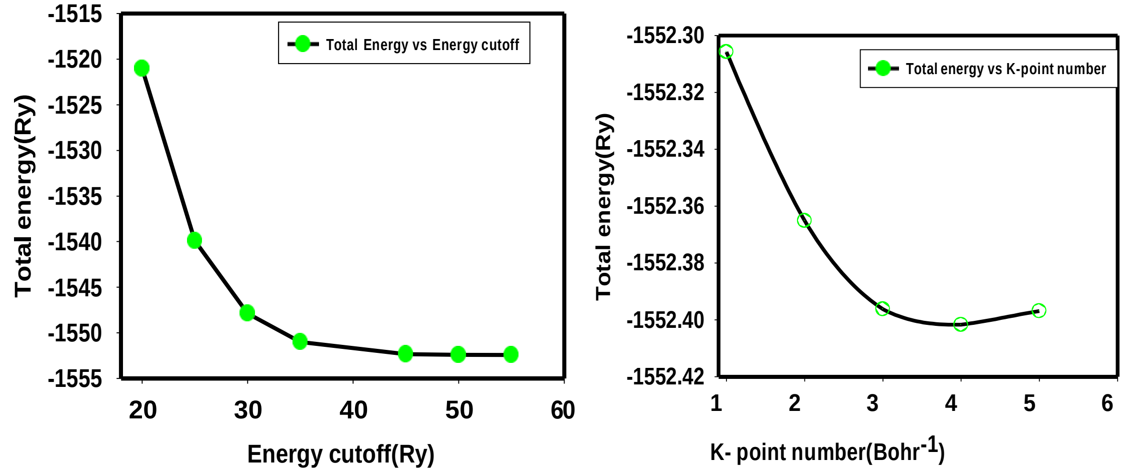

Fig. 4.1(a) **Fig 4.1(b)**

Fig. 4.1: Optimization curves for the kinetic energy cutoff (Fig4.1(a)) and k-points(Fig 4.1(b)). Both parameters exhibit convergence at ~ 45 Ry and ~4 Bohr respectively. K- Point sampling done using $\frac{2\pi}{a}$, *a* being the lattice parameter.. Theconverged k-point values are in good agreement with the experimental values (W. Uhoya *et al*., 2010)

So as to obtain accurate results, one must select the values above the obtained cut-off energy. However, cut-off energies that are very high are not good because they increase the cost of computation yet the results obtained from the computation are not of improved accuracy. Therefore, the energy should be as low as possible. Plane waves are a basis set: a set of functions that you join to describe a wave function. The more the plane waves, the better the description of the wave function therefore the cut off energy tells us about the cut off on the number of plane waves that are to be used to represent a wave function. K-points describe the different energy levels in the compound. They are the sampling points in the region nearest to the origin, in the first Brillouin zone.

Optimization of cell dimensions was done and below in Fig. 4.2 *a* and *b* is the converged graphs for the lattice parameters.

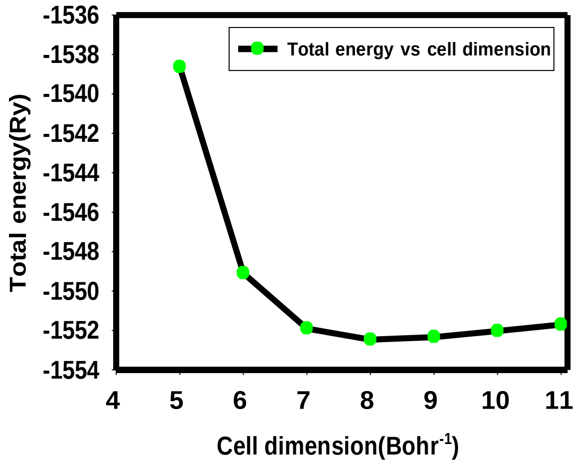

Fig 4.2a

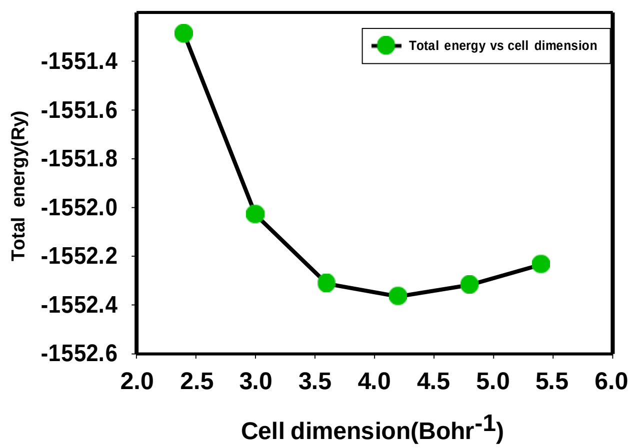

Fig 4.2b

Fig. 4.2: The optimization curves for cell dimensions; Fig 4.2a converges at approximately 8 Bohr while Fig 4.2b convergence at approximately 4.5 Bohr. These values correlate with the experimental values of 7.4 Bohr and 5 Bohr respectively (W. Uhoya *et al*.,2010).

After variable cell relax calculation (to obtain relaxed atomic positions of the crystal and optimization of cut-off energy and cell dimensions one and three, the crystal structure of the compound is as in figure 4.3:

4.2 Structural properties

The structure of a crystal dictates its mechanical properties and the electron structure dictates the optical and electrical properties (Fiolhais *et al*., 2003).

Fig. 4.3 is the crystal structure of $EuFe_2As_2$:

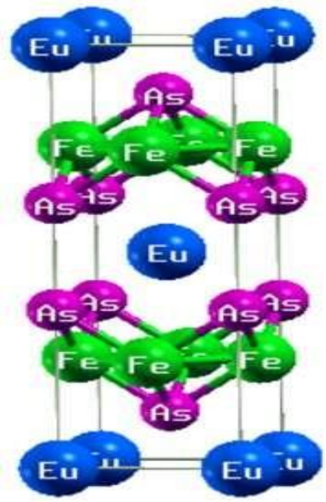

Fig. 4.3: The optimized crystal structure of $EuFe_2As_2$ as visualized using a Quantum Espresso package Xcrysden.

A body centered structure is portrayed as seen in Fig. 4.3 above. The Europium atom is locatedat the center, giving it the mentioned structure of Body Centered Tetragonal, with space group 14/mmm. We were more interested in the tetragonal crystal system since the compound we were researching on was of a tetragonal structure. For the case of tetragonal structures, the base of the compound is of a cubic shape, that is why the lattice parameter *a* is equal to lattice parameter *b* as seen in the above figure. The tetragonal system is made by stretching a cube's four sides into a rectangular shape.

The structural properties as obtained from computation and their comparison with experimental properties are as shown in the table 4.1.

Table 4.1

Comparison of the experimental and calculated structural values

Parameter	This work	Experimental	Reference
$a_0=b_0$ (ang)	3.991	3.989	(W. Uhoya *et al.*, 2010)
c_0 (ang)	10.846	10.738	(W. Uhoya *et al.*, 2010)

From table 4.1 above, it is realized that optimized and experimental lattice parameters are in good agreement, which shows that Density Functional Theory reliable (Ali, Rahman, & Rahaman, 2019). However, there is a slight deviation in the lattice parameters since optimized lattice parameters are temperature dependent and also due to the GGA rule.

4.3 Mechanical Properties

Mechanical properties such as elastic properties guide in understanding more about the nature of the force in the crystal. The elastic constants c_{ij} of the compound were computed at T=0K and P=0GPa. There exist six elastic constants in the body centered tetragonal structures (Ali et al., 2019), and they are as recorded in table two.

Table 4.2

The computed elastic constants of Europium Diiron Diarsenide at zero pressure

C_{ij}	Value (GPa)
C_{11}	531.61
C_{12}	284.81
C_{13}	253.34
C_{33}	505.73
C_{44}	141.31
C_{66}	225.69

Given the Born-Huang criteria (Piskunov, Heifets, Eglitis, & Borstel, 2004) shown below, a stable tetragonal structure should satisfy the criteria in Eqs 4.1, 4.2, 4.3, and 4.4:

- $C_{ii} > 0 (i = 1,3,4,6)$ ……………………………………………………………4.1
- $C_{11} + C_{33} - 2C_{13} > 0$ ……………………………………………………………4.2
- $2(C_{11} + C_{12}) + C_{33} + 4C_{13} > 0$ ……………………………………………………4.3
- $C_{11} - C_{12} > 0$ ……………………………………………………………………4.4

The values reported in the above table are all positive and satisfy all the above four criteria, hence proving that this tetragonal compound is stable. The above values of elastic constants have been reported for the first time and there are no experimental data to compare with. It is therefore left for experimental work to compute these values. The Bulk, Shear and Young's modulus are obtained using the Voigt-Reuss Hill Approximation method. Table 4.3 below shows the obtained Bulk, Shear and Young's modulus, and the Poisson's ratio

Table 4.3

Bulk, Shear and Young's moduli, and the Poisson's ratio of Europium diiron diarsenide at zero pressure.

Property	Voigt Approximation	Reuss Approximation	Voigt-Reuss-hill Average
Bulk modulus (B)	346.939Gpa	346.352Gpa	346.646GPa
Young modulus(E)	375.378Gpa	350.224Gpa	362.801GPa
Shear modulus(G)	142.224Gpa	131.518Gpa	136.871GPa
Poisson ratio(n)	0.31967	0.33147	0.3254

A large bulk modulus indicates that the material is relatively hard, but less hard than diamond whose bulk modulus is ~440Gpa. Pugh's ratio $-\frac{B}{G}$ (Pugh, 1954) indicates that:

$\frac{B}{G} > 1.75$ for ductile materials

$\frac{B}{G} < 1.75$ for brittle materials

Calculating the $\frac{B}{G}$ value from the above table gives a value of 2.53, implying that the compound under study is ductile.

Using the Frantserich method, ductile and brittle materials are classified on the basis of their Poisson's ratio. The value v~0.26, indicates the border of ductility and brittleness.

If v > 0.26, the material is ductile

If v<0.26, the material is brittle. Since v>0.26, as seen from the Table 4.3 above, this further proves that the compound is indeed ductile.

When the Poisson's ratio is in the range 0.25-0.5, implying that the forces present in the compound are central. The anisotropic character was also calculated using Eq 4.5 below.

$$A^{u} = \frac{5G^{v}}{G_{R}} + \frac{B_{V}}{B_{R}} - 6 \qquad \text{……4.5}$$

Where, if A^{U} =0, compound is totally isotropic

Also, considering the lattice parameters x, y and z, x is equal to y but they are both not equal to z, hence the compound is anisotropic. In this case, the material is anisotropic with anisotropic value of 0.408. The Bulk, Shear and Young's moduli values increased upon application of increasing pressure on the compound. For instance the Poisson's ratio, Bulk modulus, Shear modulus and Young's modulus at a pressure of 1GPa were 0.36100, 1196.9GPa, 326.6GPa and 889.0GPa respectively, showing a progressive increase up to 1GPa. Temperature and pressure are related by the equation of state, which is one of the most basic equations in condensed matter physics. At a particular temperature and pressure, the stable structure of the compound dictates other characteristics of the material. The energy at a temperature of zero is an important value in ab initio calculations. In theoretical studies, the volume of the system can be varied, and this is quite helpful because the results can be compared directly with experimental values. For a crystal structure to be considered stable at an unchanging pressure and temperature of zero, the enthalpy should be at its lowest. The Poisson's ratio was found to be ~0.32 at absolute zero temperature, our result compared well to a value of 0.302 for other families of Pnictides(Parvin & Naqib, 2019), the difference may be as a result of varying atoms present in the two compounds and a slight difference in the crystal structure. This value further confirmed that $EuFe_2As_2$ is a stable and metallic (Gercek, 2007; Park, 1987). Other Pnictides such as $SrFe_2As_2$ have a Poisson's ratio of ~0.48 upon application of pressure (Shein & Ivanovskii, 2008), which causes the lattice parameters to change. The Bulk modulus, Shear modulus, and Young's modulus were found to be ~346Gpa, ~136Gpa and ~362Gpa respectively, implying that the material is hard since the moduli are greater than 200GPa (Shein & Ivanovskii, 2008). The Voigt and Reuss values for the Bulk, Shear and Young moduli values are similar to each other hence they are averagely valid. However, there are scanty report on the structural properties (Ceder & Persson, 2010) of the iron Pnictide $EuFe_2As_2$. The study of elasticity dates back to Galileo and other 17^{th} century scientists. The fundamental physics of elastic constants was introduced in 1660 by Hooke (Rychlewski, 1984). Elastic constants are derivatives of free energy (Parrinello & Rahman, 1982) and they are highly linked to the thermodynamic characteristics of the system such as Debye temperature and specific heat. Elastic constants are important in the determination of phase, superconducting and structural transitions (Parrinello & Rahman, 1982). Solids that are amorphous contain isotropic elastic characteristics and crystals that are unit and have anisotropic elastic characteristics (Rychlewski, 1984) as proved above by the elastic constants of this iron pnictide. Solids that are isotropic can be elastically compressed and sheared. The coordination number is highly linked to the elastic properties of a given structure. There is decreased elasticityin group VI elements that are tetrahedral.

4.4 Electronic structure properties

In this section, we report on the calculations of the electronic structure properties which included the band structure calculation, Density of States and Partial Density of States. Europium Diiron Diarsenide in this case belongs to the 14/mmm space group, therefore the following high symmetry points in the Brillion zone were used Γ(0,0,0) ,*Z*(0,1/2,0) B(0,0,1/2), Y(1/2,0,0), C(1/2,1/2,0), D(0,1/2,1/2), A(-1/2,0,1/2), E(-1/2,1/2,1/2)**.** There is a band gap of 0.0eV, which is in agreement with other theoretical studies on the compound (Jain *et al*., 2013)

The density of states curve for the compound was obtained as shown in Fig. 4.4 below.

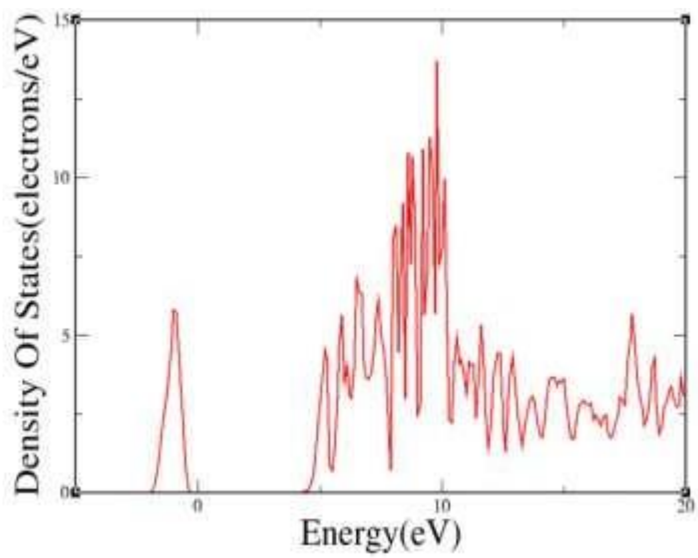

Fig. 4.4: The Density of States at zero pressure. There are two curves, separated by a superconducting gap of ~4.5eV, which is in close agreement with the results of other iron Pnictides such as $BaFe_2As_2$ (Ivanovskii, 2009) which yield coulomb parameters of ~4eV (Maier, Graser, Scalapino, & Hirschfeld, 2009); (Yang *et al*., 2009). It is within this gap that there exists the superconducting state of the compound (Ashcroft & Mermin, 2005).

The Density of State of this study is in good agreement with previous experimental studies on the material as done by (Nandi *et al*., 2014). Also, around the Fermi energy of the material, (8.5eV), the density of states is large hence proving that the material can exhibit superconductivity properties (Li *et al*., 2012). High Density of States at a given level of energy implies that there are numerous states available for occupation. The DOS above is continuous meaning this is not an isolated system. As seen in Fig. 4.4 above, there is a high Density of States around 10, given that the Fermi energy is also around this region. Usually, around the Fermi energy, there are many states available for occupation. Near the Fermi level, the states originate from the 3d Fe orbitals (Fiolhais *et al*., 2003). The Partial Density of States shows Europium and Iron atoms to be the major contributors to the projecting states. Other minor curves are left out in the illustration since their contribution to the Partial Density of States is minimal. The density of states of other Pnictides shows similar gaps (Parvin & Naqib, 2019).The Density Of States with the long and sharp peaks are between energies of ~ 7.8eV and ~10.2eV, and they represent the core electrons that have a minimal contribution to determining the properties of the electrons since they are considered to be chemically inert (Kahn, Baybutt, & Truhlar, 1976). The Density of States between the peaks is zero since states do not exist there as seen above in figure 4.4. A Kondo-like peak is as shown above, in agreement with results from similar iron Pnictides which show similar peaks (Yang *et al*., 2009). Similar pnictide such as $BaCa_2As_2$ also exhibits a sizeable gap far from the Gamma-X high symmetry line(Yi *et al*., 2009), similar to the one present in the band structure and Density of States. The band structure is as shown in Fig. 4.5:

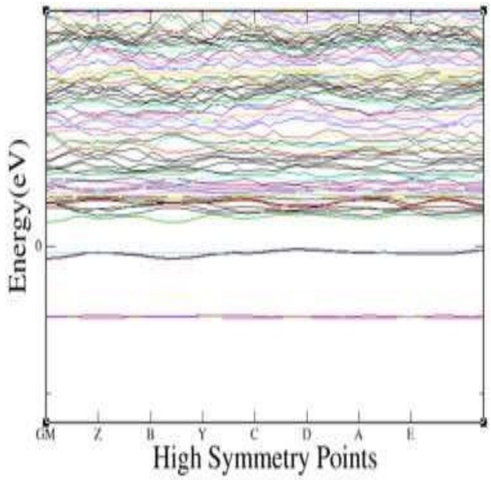

Fig 4.5(a)

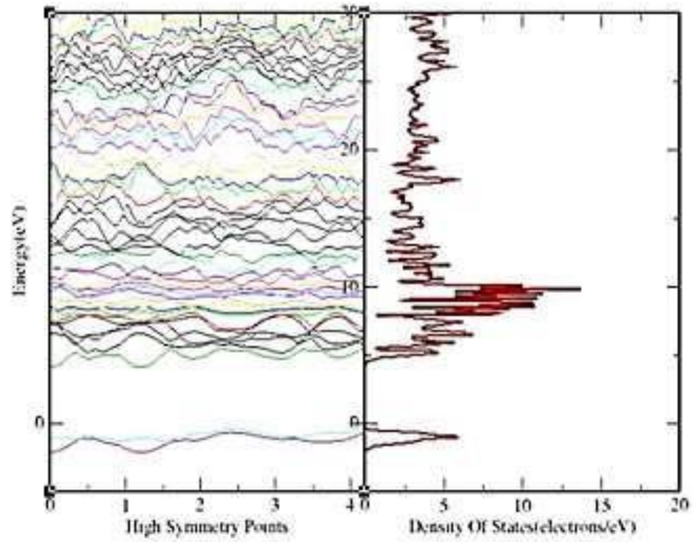

Fig 4.5(b)

Fig. 4.5: The band structure of Europium diiron diarsenide at zero pressure(fig 4.5(a)), and the combination of band structure and density of states(fig 4.5(b)): The high symmetry points include GM, Z, B, Y, C, D, A, E.

From Fig. 4.5 there exists no band gap in the material as seen from the graph above, similar to previous results from studies on the pnictide (Ceder & Persson, 2010), hence the material is a conductor. The Density of States and Band structure of the compound show very close similarity as seen above. The zero binding energy and Fermi level correspond, in agreement with previous studies on the material (Paramanik, Das, Prasad, & Hossain, 2013). There is no band gap so the compound is metallic, suggesting that it might be a superconductor, which is actually the proven fact from previous studies. The Fermi energy is above the highest occupied energy level, hence the compound is metallic. There also exists a clear distinction between the valence bands and conduction bands.

The Density of States and band structure were then calculated at various pressures, ranging from 0.2Gpa to 1Gpa. We plotted the results and the graphs are as seen in Fig. 4.6 below:

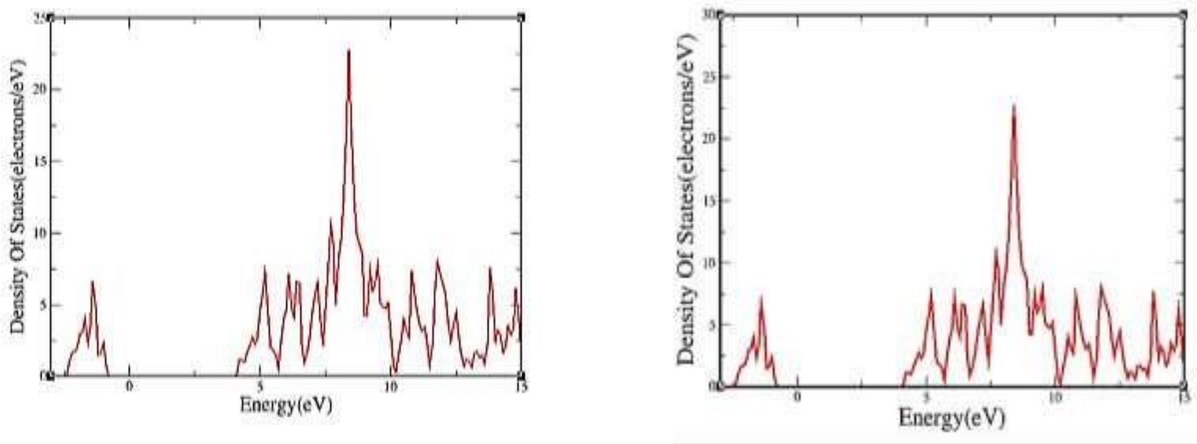

Fig. 4.6: The Density of States at 0.2Gpa and 1GPa

The range 0.2-1GPa was selected because past studies on the material indicate that the onset of superconductivity is from around 1-2.5GPa(Alireza *et al*., 2008; Miclea *et al*., 2009; Terashima *et al*., 2009; W. Uhoya *et al*., 2010), and the study sought to understand the properties of the material before it attained its superconducting state. The other range of 5GPa-35GPa was selected as a result of past experimental high pressure studies that went up to high pressures such as one reported by Uhoya (W. O. Uhoya *et al*., 2011). The band structure calculations show similar structure to that of the density of states. The Fermi energy versus pressure was also plotted at both low and high pressure. The low and high pressure plots are as shown in Fig. 4.7 below:

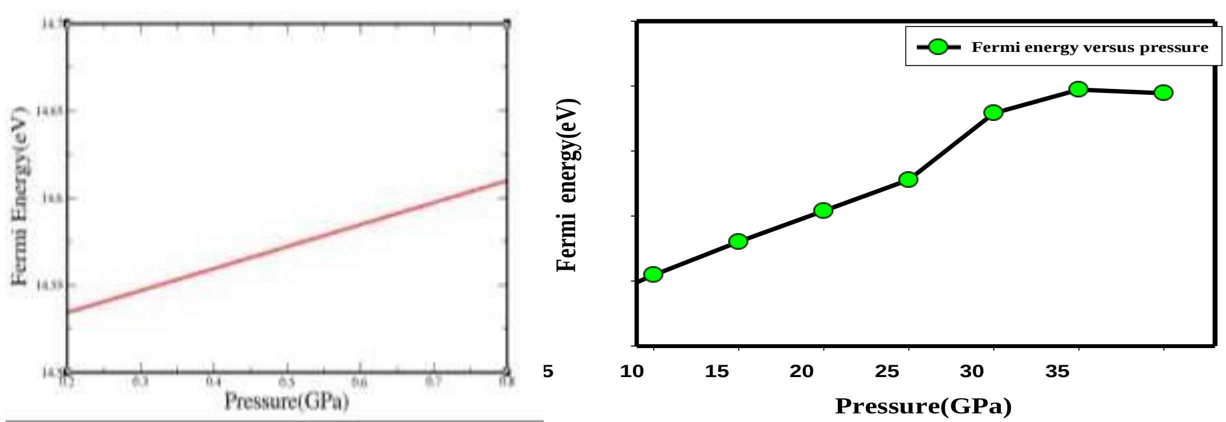

Fig. 4.7: Graphs of Fermi energy against pressure from 0.2-0.8Gpa and from 5-35GPa. The Fermi energy increases with an increase in pressure up to 0.8GPa. This indicates that the population of charge carries with respect to density of states increases hence more electrons are made available for electrical conductivity, hence enhancing electrical conductivity in the compound

A graph of total energy of the system against pressure was plotted and it took the shape shown in Fig. 4.8 below

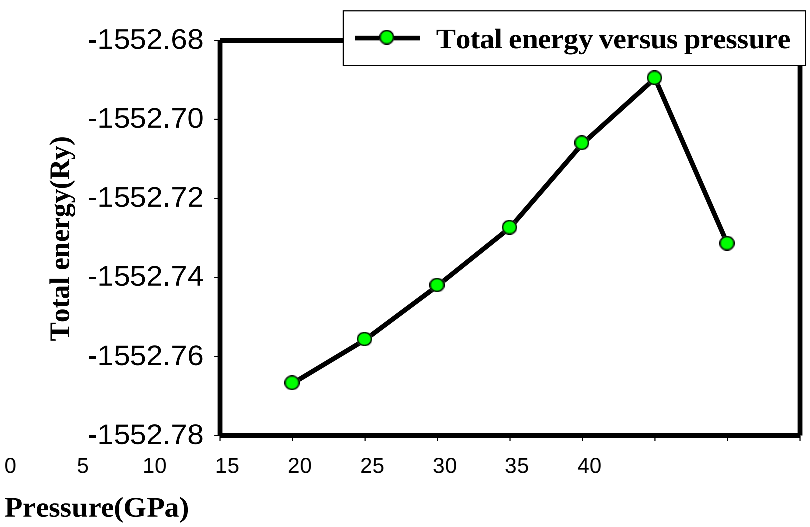

Fig. 4.8: A graph of total energy of the system against pressure. As the pressure is applied from 0.2GPa to 0.8GPa, the total energy of the system increases. A graph of pressure against the Fermi energy also shows a similar characteristic.

The final enthalpy of the system against pressure is also plotted: first, from a pressure of 0.2-1GPa and second from 5-30GPa. The graphs are as shown in Fig. 4.9 .

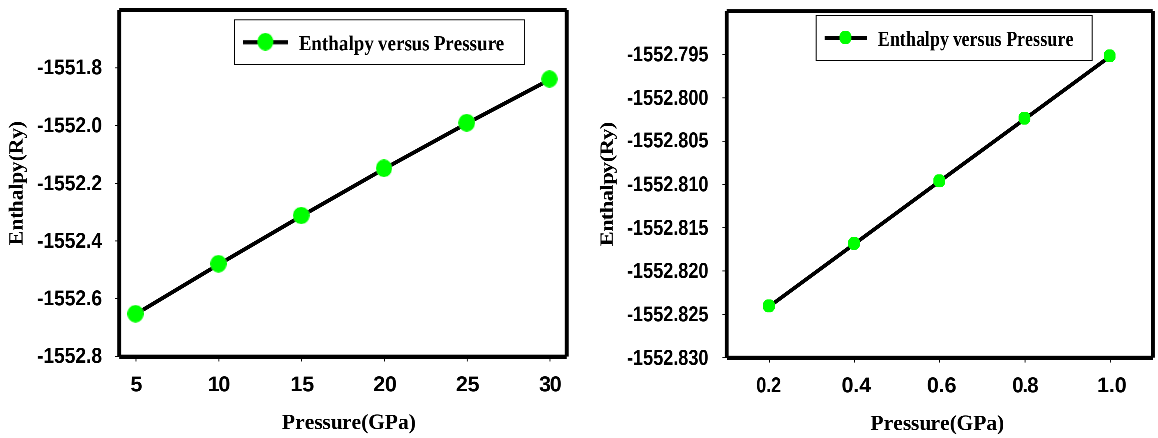

Fig. 4.9: Graphs of Enthalpy against pressure from 0.2-0.8Gpa and from 5-35GPa. At both pressures ranges, the enthalpy increases with a pressure increase, results which are in good agreement with previous studies on the material as seen from (Mahesh & Reddy, 2018)

Enthalpy is given as:

$$H = U + PV ,$$

Where, H is-Enthalpy, U is -Sum of internal energy, P is-Pressure on the system and V is-Volume of the system. Enthalpy is useful because it informs us on how much energy is in a given system.

As pressure increases, the enthalpy of this crystal system increases since as seen from the above equation, the two quantities are directly proportional. Graphs of volume against pressure were plotted and they are as shown in Fig. 4.10 :

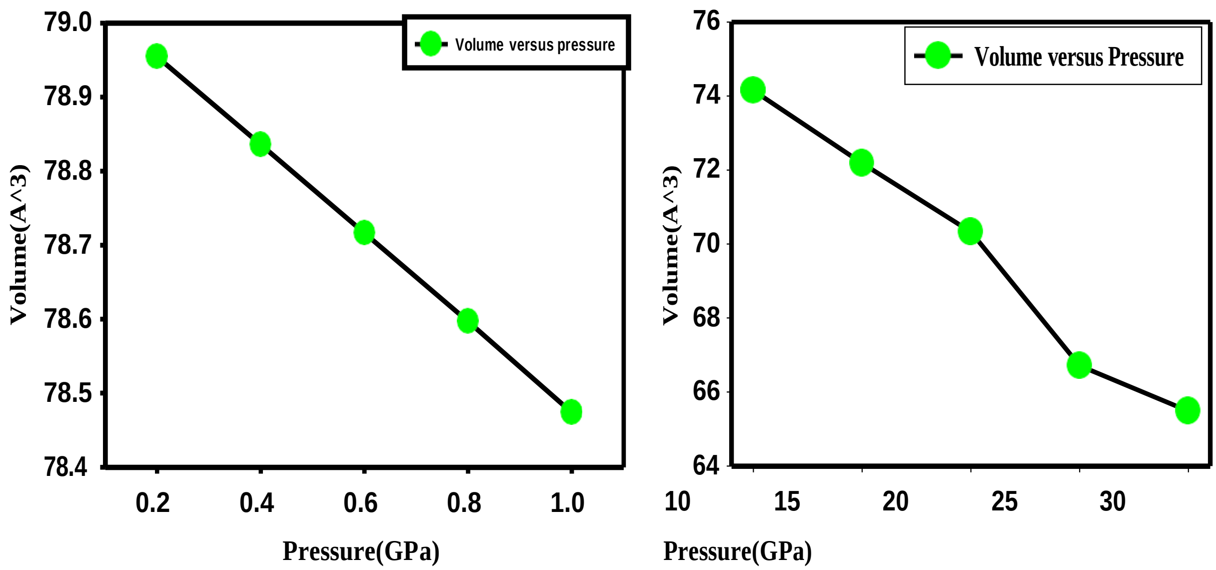

Fig. 4.10: Graphs of volume against pressure applied on the crystal system. Up to a pressure of 1GPa, application of pressure on the system leads to a decrease in the volume as expected from past experimental studies on the pnictide.(W. Uhoya *et al*., 2010)

4.5 Phonon dispersion

Below in Figure 4.11 is the phonon dispersion curve of the band structure (phonon bands)

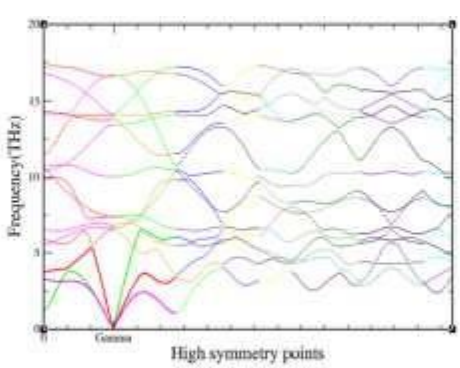

Fig. 4.11: The phonon dispersion curve. The optical (upper) mode and the acoustic (lower) mode are clearly differentiated.

Given that Europium diiron diarsenide has got five atoms; there are 15 modes of vibration. The acoustic modes converge at the gamma high symmetry point.

In the study of phonons, there exist three modes that are associated with each mode number n. For a primitive cell that has N atoms, there exist 3N degrees of freedom (Simon, 2013), taking into account the x, y, and z axes(Birman, 1984). The number of acoustic modes is usually three for crystals whose number of atoms is equal to or greater than two, and the optical modes are given by 3N-3(Mahan, 2011). Therefore, given that Europium diiron diarsenide has got five atoms; there are 15 modes of vibration expected. As seen in the Fig. 4.11 above, there are 15 vibration modes with twelve being optical modes and three being acoustic modes. The acoustic modes converge at the gamma high symmetry point. Acoustic modes vibrate at a slower frequency and are in the same phase with the unit cell. Optical modes of vibration have a higher frequency compared to acoustic modes and two neighboring atoms vibrate in a direction opposite to each other, that is to say, if one atom vibrates in the left direction, the adjacent atom will vibrate to the right. In the acoustic mode, the two adjacent atoms will vibrate together in the same direction. Phonon dispersions are computed along a given line of high symmetry points. The above information therefore confirms that the compound is dynamically stable.

The phonon density of states was also plotted and it is as shown in Fig. 4.12 below:

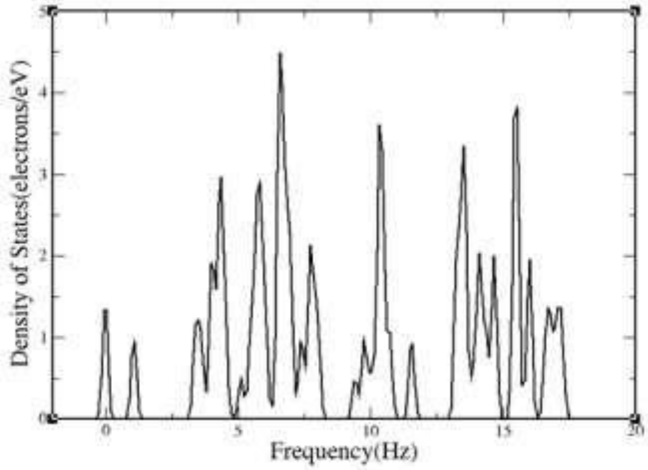

Fig. 4.12: The plotted phonon Density of States. The phonon Density of States is similar to the Density Functional Theory Density of States. As the wavelength becomes longer, the frequency of the acoustic modes of vibration goes to zero, while for longer wave lengths in optical phonons, the frequency does not go to zero as seen from the figure above.

A system is considered to be dynamically stable at equilibrium if the potential energy is always increasing for any combination of displacement of atoms, therefore, phonons should have non negative and real frequencies for stability (Togo & Tanaka, 2015). Negative frequencies imply that the potential energy reduces hence the system is unstable. Phonon frequencies arise as a result of the displacement of atoms in a given crystal from the rest position, which in turn makes the forces to rise (Togo & Tanaka, 2015). The phonon calculation of finite differences was done using Phonopy. A smearing of 0.2eV of the Methfessel-Paxton scheme was used. The finite displacement and super cell technique was used with a 2x2x2 super cell of the conventional unit cell. We used an energy cut off of 30Ry, which dictated the number of plane waves to be employed. It is important to establish the number of normal modes that are neighboring a certain phonon energy, these details are necessary when studying thermal and electrical conductivity and also establishing the critical temperature of superconducting materials(Giustino, 2014). The Debye temperature is a constant that is associated with the highest allowed mode of vibration (Hill, 1986). The Debye temperature in this study was 436.454K and the average Debye sound velocity was 3330.336 m/s. A Debye temperature of above 400K implies that the crystal's thermal conductivity is high (Low, 2012), and since the compound we were studying had a Debye temperature of above 400K, we concluded that the thermal conductivity is high. Note that, for temperatures that are below the Debye temperature, the heat capacity of the compound rises with the temperature cube and for temperatures above the Debye temperature, the heat capacity of the crystal remains constant, that is to say, it no longer depends on temperature. The Debye temperature and the heat capacity are directly proportional(Debye, 1912) A high Debye temperature implies that the material is hard for example, Diamond, while a low Debye temperature implies that the material is soft, for example, Lead has a low Debye temperature. The Debye temperature is the approximate limit below which the quantum effects in a system can be seen. It is defined by:

$$k\theta = h\nu ,$$

Where, k −Boltzmann constant, ν-Debye frequency, h- Planck's constant and θ is the Debye temperature. (Hill, 1986) The highest frequency of phonons and the Debye temperature are coupled with each other(Low, 2012).

CHAPTER FIVE

CONCLUSIONS AND RECCOMENDATIONS

The aim of this computational study was to provide additional information on the structural, mechanical and electronic structure properties of the iron pnictide compound Europium diiron diarsenide, and also provide more details on the behavior of the compound on subjection to external pressure. The thermodynamic property of Phonon vibration modes was also studied. There were guiding objectives in this study, which were achieved. The optimized lattice parameters in this computational study were in close agreement with available experimental values and values from other Density Functional Theory studies. The DFT technique mostly is suitable for ground state studies; hence the results obtained in this study were at the ground state of the compound.

The milestones below have been achieved in the study of the above mentioned iron pnictide compound:

1).The mechanical structure properties of Bulk, Shear and Young's modulus, and Poisson's ratio have also been studied. These have guided in classifying of the compound as a ductile material Poisson's ratio is in the range 0.25-0.5, implying that the forces present in the compound are central forces and that the compound is also hard due to its large bulk modulus and highly anisotropic.

The elastic constants have also been studied for the first time, which went on to further prove that the material is actually ductile. The elastic constants also show that the compound is of a stable tetragonal structure.

2). The electronic structure properties including the Density of States and Band Structure have been studied. It has been noted from the properties that there exists no band gap hence the compound is metallic, and the DOS graphs show properties similar to other compounds in the iron pnictide family.

3). The electronic and mechanical structure properties under application of increasing pressure ofup to 35Gpa were also studied. The study of the effect of pressure on volume of the material indicated that the volume decreases as the pressure increases, implying that the material shows normal compressional behavior. The study of the effect of pressure on the Fermi energy also showed that the Fermi energy increases with pressure, which implies that the population of charge carriers with respect to Density of States increases, hence more electrons are made available for electrical conductivity in the compound. The compound was quite expensive in terms of computational time and a bit challenging but we managed to make the above mentioned milestones.

4). The thermodynamic property of Phonon dispersion was also studied and the nature of optical and acoustic vibration modes confirmed that the compound is dynamically stable. There were no negative frequencies. The Debye temperature was also studied and it revealed that the compoundis a good thermal conductor

The findings in this study provided more information on the mechanical and electronic structure properties of the iron pnictide Europium diiron diarsenide. It also provided additional information on how the iron pnictide responds to pressure changes. This information can enhance future use of the iron pnictide as a superconductor in industry.

The challenges that were faced in this study included: Early on in the research, determination of the type of pseudo potentials to be used, whether hard or soft, PAW or USSP. Also, optimization of the crystal structure presented a challenge since it was a quite 'heavy' compound in terms of the number of electrons and the number of atoms. This increased the number of hours that were required to perform optimization of the energy, cell dimensions and k-points. Sometimes it made the computer to 'Hang', rendering it useless for the time period of the calculation. However, this challenge was later solved with the usage of the super computer in South Africa. Having a little background in usage of computers also presented a big challenge at the beginning, since the research was basically theoretical and needed us to use computer operating systems such as Ubuntu which was very new to me, also, installation and learning of the commands also presented a challenge at the beginning but with time, all that became a thing of the past.

The current research leaves gaps and questions which need to be addressed in future research, and include the following;

More study should be done on application of pressure on the material to explain more on the phase transition on the material. A phase transition study from one crystal structure to another and its effects on the structure and functioning of the iron pnictide should be done. In some crystals, pressure application leads to a change in the crystal structure. Also, more pressure should be applied on the compound so as to establish at what pressure the crystal structure get distorted, that is, to establish how much pressure the material can with stand. The partial density of states at various pressures should also be looked into so as to gain more understanding into the states available in the system. The phonon dispersion should also be closely looked into to understand more on the critical temperature of superconductivity of this particular iron Pnictide. Since the compound also shows some magnetism, more studies on the magnetic structure properties should be done to complement the available studies, and relate the magnetism to superconductivity. Optical properties should also be looked into. All the above properties studied, it will give scientists an in-depth understanding of the compound.

REFERENCES

Adhikary, G., Sahadev, N., Biswas, D., Bindu, R., Kumar, N., Thamizhavel, A., . . . Maiti, K. (2013). Electronic structure of EuFe2As2. *Journal of Physics: Condensed Matter, 25*(22), 225701.

Ali, M. S., Rahman, M. A., & Rahaman, M. Z. (2019). A theoretical investigation of ThCr2Si2-type Pd-based superconductors XPd2Ge2 (X= Ca, Sr, La, Nd). *Physica C: Superconductivity and its Applications, 561*, 35-44.

Alireza, P. L., Ko, Y. C., Gillett, J., Petrone, C. M., Cole, J. M., Lonzarich, G. G., & Sebastian, S. E. (2008). Superconductivity up to 29 K in SrFe2As2 and BaFe2As2 at high pressures. *Journal of Physics: Condensed Matter, 21*(1), 012208.

Ang, B., & Su, B. (2016). Carbon emission intensity in electricity production: A global analysis. *Energy Policy, 94*, 56-63.

Ashcroft, N. W., & Mermin, N. (2005). Solid state physics (holt, rinehart and winston, new york, 1976). *Google Scholar, 403*.

Bardeen, J., Cooper, L. N., & Schrieffer, J. R. (1957). Theory of superconductivity. *Physical review, 108*(5), 1175.

Becke, A. D. (1988). Density-functional exchange-energy approximation with correct asymptotic behavior. *Physical Review A, 38*(6), 3098.

Birman, J. (1984). Theory of Crystal Space Groups and Lattice Dynamic ed L Genzel: Berlin: Springer.

Ceder, G., & Persson, K. (2010). The Materials Project: A Materials Genome Approach. Ceperley, D. M., & Alder, B. J. (1980). Ground state of the electron gas by a stochastic method. *Physical Review Letters, 45*(7), 566.

Chen, W., Rylyakov, A., Patel, V., Lukens, J., & Likharev, K. (1999). Rapid single flux quantumT-flip flop operating up to 770 GHz. *IEEE Transactions on Applied Superconductivity, 9*(2), 3212-3215.

Colonna, N., Profeta, G., Continenza, A., & Massidda, S. (2011). Structural and magnetic properties of CaFe 2 As 2 and BaFe 2 As 2 from first-principles density functional theory. *Physical review B, 83*(9), 094529.

Dalgarno, A., Bottcher, C., & Victor, G. (1970). Pseudo-potential calculation of atomic interactions. *Chemical Physics Letters, 7*(2), 265-267.

Debye, P. (1912). Concerning the theory of specific heat. *Ann Physik, 39*, 789-839.

Deng, Z., Wang, X., Liu, Q., Zhang, S., Lv, Y., Zhu, J., . . . Jin, C. (2009). A new “111” type iron pnictide superconductor LiFeP. *Europhysics Letters, 87*(3), 37004.

Fiolhais, C., Nogueira, F., & Marques, M. A. (2003). *A primer in density functional theory* (Vol. 620): Springer Science & Business Media.

Frantsevich, I., Voronov, F., & Bokuta, S. (1983). In, Frantsevich, IN (Ed.), Elastic Constants and Elastic Moduli of Metals and Insulators. *Naukova Dumka, Kiev, 60*, 180.

Garrity, K. F., Bennett, J. W., Rabe, K. M., & Vanderbilt, D. (2014). Pseudopotentials for high-throughput DFT calculations. *Computational Materials Science, 81*, 446-452.

Gercek, H. (2007). Poisson's ratio values for rocks. *International Journal of Rock Mechanics and Mining Sciences, 44*(1), 1-13.

Giannozzi, P., Baroni, S., Bonini, N., Calandra, M., Car, R., Cavazzoni, C., . . . Dabo, I. (2009). QUANTUM ESPRESSO: a modular and open-source software project for quantum simulations of materials. *Journal of Physics: Condensed Matter, 21*(39), 395502.

Giustino, F. (2014). *Materials modelling using density functional theory: properties and predictions*: Oxford University Press.

Green, M. C. (2001). Radiotherapy machine including magnetic resonance imaging system: Google Patents.

Hamann, D. (1989). Generalized norm-conserving pseudopotentials. *Physical review B, 40*(5), 2980.

Hamann, D., Schlüter, M., & Chiang, C. (1979). Norm-conserving pseudopotentials. *Physical Review Letters, 43*(20), 1494.

Hao, S., Moran, B., Liu, W. K., & Olson, G. B. (2003). A hierarchical multi-physics model for design of high toughness steels. *Journal of Computer-Aided Materials Design, 10*(2), 99-142.

Hasnip, P. J., Refson, K., Probert, M. I., Yates, J. R., Clark, S. J., & Pickard, C. J. (2014). Density functional theory in the solid state. *Philosophical Transactions of the Royal Society A: Mathematical, Physical and Engineering Sciences, 372*(2011), 20130270.

Hill, T. L. (1986). *An introduction to statistical thermodynamics*: Courier Corporation. Ivanovskii, A. (2009). New superconductors based on (Ca, Sr, Ba) Fe 2 As 2 ternary arsenides: Synthesis, properties, and simulation. *Journal of Structural Chemistry, 50*(3), 539-551.

Jain, A., Ong, S. P., Hautier, G., Chen, W., Richards, W. D., Dacek, S., . . . Ceder, G. (2013). Commentary: The Materials Project: A materials genome approach to accelerating materials innovation. *Apl Materials, 1*(1), 011002.

Janesko, B. G. (2013). Rung 3.5 density functionals: Another step on Jacob's ladder. *International Journal of Quantum Chemistry, 113*(2), 83-88.

Kahn, L. R., Baybutt, P., & Truhlar, D. G. (1976). A binitio effective core potentials: Reduction of all-electron molecular structure calculations to calculations involving only valence electrons. *The Journal of chemical physics, 65*(10), 3826-3853.

Katase, T., Ishimaru, Y., Tsukamoto, A., Hiramatsu, H., Kamiya, T., Tanabe, K., & Hosono, H. (2011). Advantageous grain boundaries in iron pnictide superconductors. *Nature Communications, 2*(1), 409.

Kimber, S. A., Kreyssig, A., Zhang, Y.-Z., Jeschke, H. O., Valentí, R., Yokaichiya, F., . . . Chatterji, T. (2009). Similarities between structural distortions under pressure and chemical doping in superconducting BaFe 2 As 2. *Nature materials, 8*(6), 471.

Kresse, G., & Joubert, D. (1999). From ultrasoft pseudopotentials to the projector augmented-wave method. *Physical review B, 59*(3), 1758.

Lang, N. (1969). Self-consistent properties of the electron distribution at a metal surface. *Solid State Communications, 7*(15), 1047-1050.

Lang, N., & Kohn, W. (1971). Theory of metal surfaces: work function. *Physical review B, 3*(4), 1215.

Lang, N., & Kohn, W. (1973). Surface-dipole barriers in simple metals. *Physical review B, 8*(12), 6010.

Li, W., Zhu, J.-X., Chen, Y., & Ting, C. (2012). First-principles calculations of the electronic structure of iron-pnictide EuFe 2 (As, P) 2 superconductors: Evidence for antiferromagnetic spin order. *Physical review B, 86*(15), 155119.

Low, I.-M. (2012). *Advances in Science and Technology of Mn+ 1AXn phases*: Elsevier.

Lund, A. M., Orendt, A. M., Pagola, G. I., Ferraro, M. B., & Facelli, J. C. (2013). Optimizationof Crystal Structures of Archetypical Pharmaceutical Compounds: A Plane-Wave DFT-D Study Using Quantum Espresso. *Crystal Growth & Design, 13*(5), 2181-2189.

Mahan, G. D. (2011). *Condensed matter in a nutshell* (Vol. 8): Princeton University Press. Mahesh,

R., & Reddy, P. V. (2018). Formation of As–As Interlayer Bonding in the cT Phase of EuFe 2 As 2 and CeFeAsO Under Pressure from First Principle. *Journal of Superconductivity and Novel Magnetism, 31*(10), 3111-3117.

Maier, T., Graser, S., Scalapino, D., & Hirschfeld, P. (2009). Neutron scattering resonance and the iron-pnictide superconducting gap. *Physical review B*, *79*(13), 134520.

Maiti, K. (2015). Electronic structure of Fe-based superconductors. *Pramana, 84*(6), 947-956.

Meyers, H., & Myers, H. (1997). *Introductory solid state physics*: CRC press.

Miclea, C., Nicklas, M., Jeevan, H., Kasinathan, D., Hossain, Z., Rosner, H., . . . Steglich, F. (2009). Evidence for a reentrant superconducting state in EuFe 2 As 2 under pressure. *Physical review B*, *79*(21), 212509.

Misra, P. (2011). *Physics of condensed matter*: Academic Press.

Nandi, S., Jin, W., Xiao, Y., Su, Y., Price, S., Schmidt, W., . . . Gegenwart, P. (2014). Magnetic structure of the Eu 2+ moments in superconducting EuFe 2 (As 1− x P x) 2 with x= 0.19. *Physical review B, 90*(9), 094407.

Neyman, K., Pacchioni, G., & Rösch, N. (1996). Adsorption complexes on oxides: density functional model cluster studies *Theoretical and Computational Chemistry* (Vol. 4, pp. 569-619): Elsevier.

Ng, J. S. (1995). Automated wireless preventive maintenance monitoring system for magnetic levitation (MAGLEV) trains and other vehicles: Google Patents.

Ni, N., Nandi, S., Kreyssig, A., Goldman, A., Mun, E., Bud'Ko, S., & Canfield, P. (2008). First-order structural phase transition in CaFe 2 As 2. *Physical review B, 78*(1), 014523.

Nicolis, A., & Penco, R. (2018). Mutual interactions of phonons, rotons, and gravity. *Physical review B, 97*(13), 134516.

Norman, M. R. (2008). Trend: High-temperature superconductivity in the iron pnictides. *Physics,1*, 21.

Paramanik, U., Das, D., Prasad, R., & Hossain, Z. (2013). Reentrant superconductivity in Eu (Fe1−xIrx) 2As2. *Journal of Physics: Condensed Matter*, *25*(26), 265701.

Park, R. J. T. (1987). Seismic performance of steel-encased concrete piles. *Research Report*.

Parrinello, M., & Rahman, A. (1982). Strain fluctuations and elastic constants. *The Journal of chemical physics, 76*(5), 2662-2666.

Parvin, F., & Naqib, S. (2019). Structural, elastic, electronic, thermodynamic, and optical properties of layered BaPd2As2 pnictide superconductor: A first principles investigation. *Journal of Alloys and Compounds, 780*, 452-460.

Paulose, P., Jeevan, H., Geibel, C., & Hossain, Z. (2009). Superconductivity and magnetism in K-doped EuFe2As2. *Journal of Physics: Condensed Matter, 21*(26), 265701.

Perdew, J., McMullen, E., & Zunger, A. (1981). Density-functional theory of the correlation energy in atoms and ions: a simple analytic model and a challenge. *Physical Review A, 23*(6), 2785.

Pisana, S., Lazzeri, M., Casiraghi, C., Novoselov, K. S., Geim, A. K., Ferrari, A. C., & Mauri, F. (2007). Breakdown of the adiabatic Born–Oppenheimer approximation in graphene. *Nature materials, 6*(3), 198-201.

Piskunov, S., Heifets, E., Eglitis, R., & Borstel, G. (2004). Bulk properties and electronic structure of SrTiO3, BaTiO3, PbTiO3 perovskites: an ab initio HF/DFT study. *Computational Materials Science, 29*(2), 165-178.

Pugh, S. (1954). XCII. Relations between the elastic moduli and the plastic properties of polycrystalline pure metals. *The London, Edinburgh, and Dublin Philosophical Magazine and Journal of Science, 45*(367), 823-843.

Rychlewski, J. (1984). On Hooke's law. *Journal of Applied Mathematics and Mechanics, 48*(3), 303-314.

Shein, I., & Ivanovskii, A. (2008). Elastic properties of ternary arsenide SrFe2As2 and quaternary oxyarsenide LaOFeAs as basic phases for new 38-55K superconductors from first principles. *arXiv preprint arXiv:0807.0984*.

Sholl, D., & Steckel, J. A. (2011). *Density functional theory: a practical introduction*: John Wiley & Sons.

Si, Q., Yu, R., & Abrahams, E. (2016). High-temperature superconductivity in iron pnictides and chalcogenides. *Nature Reviews Materials, 1*(4), 1-15.

Simon, S. H. (2013). *The Oxford solid state basics*: OUP Oxford.

Tegel, M., Rotter, M., Weiss, V., Schappacher, F. M., Pöttgen, R., & Johrendt, D. (2008). Structural and magnetic phase transitions in the ternary iron arsenides SrFe2As2 and EuFe2As2. *Journal of Physics: Condensed Matter, 20*(45), 452201.

Terashima, T., Kimata, M., Satsukawa, H., Harada, A., Hazama, K., Uji, S., . . . Murata, K. (2009). EuFe2As2 under high pressure: an antiferromagnetic bulk superconductor. *Journal of the Physical Society of Japan, 78*(8), 083701.

Togo, A., & Tanaka, I. (2015). First principles phonon calculations in materials science. *Scripta Materialia, 108*, 1-5.

Troullier, N., & Martins, J. L. (1991). Efficient pseudopotentials for plane-wave calculations. *Physical review B, 43*(3), 1993.

Uhoya, W., Tsoi, G., Vohra, Y. K., McGuire, M. A., Sefat, A. S., Sales, B. C., . . . Weir, S. T. (2010). Anomalous compressibility effects and superconductivity of EuFe2As2 under high pressures. *Journal of Physics: Condensed Matter*, *22*(29), 292202.

Uhoya, W. O., Tsoi, G. M., Vohra, Y. K., McGuire, M. A., & Sefat, A. S. (2011). Structural phase transitions in EuFe2As2 superconductor at low temperatures and high pressures. *Journal of Physics: Condensed Matter, 23*(36), 365703.

Wales, D. J., & Scheraga, H. A. (1999). Global optimization of clusters, crystals, and biomolecules. *Science, 285*(5432), 1368-1372.

West, D., Sun, Y., & Zhang, S. (2012). Importance of the correct Fermi energy on the calculation of defect formation energies in semiconductors. *Applied Physics Letters, 101*(8), 082105.

Yang, W., Sorini, A., Chen, C., Moritz, B., Lee, W.-S., Vernay, F., . . . Chu, J.-H. (2009). Evidence for weak electronic correlations in iron pnictides. *Physical review B, 80*(1), 014508.

Yi, M., Lu, D., Analytis, J., Chu, J.-H., Mo, S.-K., He, R.-H., . . . Luo, J. (2009). Electronic structure of the BaFe 2 As 2 family of iron-pnictide superconductors. *Physical review B, 80*(2), 024515.

Yu, P. Y., & Cardona, M. (1996). *Fundamentals of semiconductors: physics and materials properties*: Springer.

APPENDICES

APPENDIX I: Input files

The input file of the iron pnictide Europium diiron diarsenide.

```
&control

   calculation = 'scf',
   restart_mode='from_scratch',
   prefix='EuFe2As2',
   pseudo_dir = './',
   outdir='./tempdir/',
/
 &system
   ibrav= 7,
   celldm(1) = 7.5419,
   celldm(3) = 5.1355,
   nat= 5,
   ntyp= 3,
   ecutwfc = 30,
   ecutrho = 240,
   occupations = 'smearing'
   smearing = 'gaussian'
   degauss = 0.01
 /
```

```
 &electrons
    mixing_beta = 0.2,
    conv_thr =  1.0d-8,
/
ATOMIC_SPECIES
 Eu 151.964  Eu.pbe-spdn-kjpaw_psl.1.0.0.UPF
 Fe 55.845  Fe.pbe-spn-kjpaw_psl.0.2.1.UPF
 As       74.922       As.pbe-n-kjpaw_psl.1.0.0.UPF
ATOMIC_POSITIONS (crystal)
Eu   0.000000000      0.000000000  0.000000000
Fe   0.817210010     0.272541202  0.455331192
Fe   0.182789990     0.727458798  0.544668808
As   0.633980657      0.649443121  0.015462464
As   0.366019343      0.350556879  0.015462464
K_POINTS (automatic)
 6 6 4 1 1 1
```

The nscf file

```
&control
    calculation         =         'nscf'
    restart_mode='from_scratch',
    prefix='EuFe2As2',
    pseudo_dir = './',
```

```
   outdir='./tempdir/'

/
&system
   ibrav= 7,
   celldm(1) = 7.5419,
   celldm(3) = 5.1355,
   nat=  5,
   ntyp= 3,
   ecutwfc = 45,
   ecutrho = 360,

/
&electrons
   mixing_beta    =    0.2
   conv_thr =  1.0d-8
/
ATOMIC_SPECIES
 Eu 151.964  Eu.pbe-spdn-kjpaw_psl.1.0.0.UPF
 Fe 55.845  Fe.pbe-spn-kjpaw_psl.1.0.0.UPF
 As       74.922        As.pbe-n-kjpaw_psl.1.0.0.UPF
ATOMIC_POSITIONS (crystal)
Eu      -0.000000000  0.000000000   0.000000000
```

```
Fe   0.977790038     0.242572369   0.264782331
Fe   0.022209962     0.757427631   0.735217669
As   0.713485486     0.632926667   -0.080558819
As   0.286514514     0.367073333   0.080558819
K_POINTS tpiba_b
 10
0.0000000000    0.0000000000   0.0000000000 30
0.0000000000    0.0000000000   0.5000000000 30
0.2500000000    0.2500000000   0.2500000000 30
0.0000000000    0.5000000000   0.0000000000 30
0.0000000000    0.0000000000   0.0000000000 30
0.5000000000    0.5000000000   -0.5000000000 30
 -1.000000000   2.5202352114   1.0000000000 30
0.0000000000    0.0000000000   0.0000000000 30
-0.1362877078   0.1362877078    7.3374188776 30
0.5000000000    0.5000000000   -0.5000000000 30
Variable cell relax calculation
&control
    calculation          =          'scf',
    restart_mode='from_scratch',
    prefix='EuFe2As2',
    pseudo_dir           =           './',
    outdir='./tempdir/',
```

```
 /
 &system
    ibrav= 7,
    celldm(1) = 7.5419,
    celldm(3) = 5.1355,
    nat= 5,
    ntyp= 3,
    ecutwfc = 30,
    ecutrho          =          240,
    occupations = 'smearing'
    smearing    =    'gaussian'
    degauss = 0.01
 /
 &electrons
    mixing_beta = 0.2,
    conv_thr =  1.0d-8,
/
&ion
Ion_dynamics = ‘bfgs’
&cell
Press= 0
/
ATOMIC_SPECIES
```

Eu 151.964 Eu.pbe-spdn-kjpaw_psl.1.0.0.UPF

Fe 55.845 Fe.pbe-spn-kjpaw_psl.0.2.1.UPF

As 74.922 As.pbe-n-kjpaw_psl.1.0.0.UPF

ATOMIC_POSITIONS (crystal)

Eu 0.000000000 0.000000000 0.000000000

Fe 0.817210010 0.272541202 0.455331192

Fe 0.182789990 0.727458798 0.544668808

As 0.633980657 0.649443121 0.015462464

As 0.366019343 0.350556879 0.015462464

K_POINTS (automatic)

6 6 4 1 1 1

Phonon Calculation

To compute phonons in Quantum Espresso, the following steps are followed:

1) A self-consistent field calculation
2) A non-self-consistent field calculation
3) Pseudo potential ph.x calculation
4) Pseudo potential q2r.x calculation
5) Pseudo potential matdyn.x calculation.

The scf computes the total energy of a crystal from its equilibrium position. Pseudo potential ph.x calculation computes the normal modes of a specific q-vector, beginning with files obtained from the pw.x calculation in the scf. Dynamical matrices are calculated at this level. The Pseudo potential q2r .x calculation code reads the dynamical matrices from the previous step and does a Fourier transform on them. The Pseudo potential matdyn.x calculation generates the modes of the phonons and their frequencies. The above procedure did not however yield results therefore a second method was used to calculate the phonons. This second method involves the creating of a super cell using a package known as Phonopy(Togo & Tanaka, 2015) and then generating force sets using Quantum ESSPRESSO for post processing. This second method proved to be successful. There were 9 super cells and a sample of the super cell information is as shown below:

Super cell 001

```
!    ibrav = 0, nat = 40, ntyp = 3
CELL_PARAMETERS bohr
  19.7213357861786740   -0.1907791352002044   0.0000000000000000
  11.1164888651131673    16.2905715232244397  0.0000000000000000
 -15.4189123256459197   -8.0498961940121188   9.2968100231471915
ATOMIC_SPECIES
 Eu  151.96400  Eu.pbe-spdn-kjpaw_psl.1.0.0.UPF
 Fe  55.84500   Fe.pbe-spn-kjpaw_psl.1.0.0.UPF
 As     74.92160      As.pbe-n-kjpaw_psl.1.0.0.UPF
ATOMIC_POSITIONS crystal
 Eu  0.0000000000000000   0.0000000000000000  0.0010140736703417
 Eu  0.5000000000000000   0.0000000000000000  0.0000000000000000
 Eu  0.0000000000000000   0.5000000000000000  0.0000000000000000
 Eu  0.5000000000000000   0.4999999999999999  0.0000000000000000
```

Eu	0.0000000000000000	0.0000000000000000	0.5000000000000000
Eu	0.5000000000000000	0.0000000000000000	0.5000000000000000
Eu	0.0000000000000001	0.4999999999999999	0.5000000000000000
Eu	0.5000000000000000	0.4999999999999999	0.5000000000000000
Fe	0.3749994735000000	0.1249994735000000	0.2499989475000000
Fe	0.8749994735000000	0.1249994735000000	0.2499989475000000
Fe	0.3749994735000001	0.6249994735000000	0.2499989475000000
Fe	0.8749994734999997	0.6249994735000000	0.2499989475000000
Fe	0.3749994735000001	0.1249994735000000	0.7499989475000001
Fe	0.8749994735000002	0.1249994735000001	0.7499989475000001
Fe	0.3749994735000002	0.6249994735000000	0.7499989475000001
Fe	0.8749994735000000	0.6249994735000000	0.7499989475000001
Fe	0.1250005265000000	0.3750005265000000	0.2500010525000000
Fe	0.6250005265000002	0.3750005265000000	0.2500010525000000
Fe	0.1250005265000000	0.8750005265000000	0.2500010525000000
Fe	0.6250005265000000	0.8750005264999999	0.2500010525000000
Fe	0.1250005265000000	0.3750005264999999	0.7500010525000000
Fe	0.6250005265000000	0.3750005265000000	0.7500010525000000
Fe	0.1250005265000000	0.8750005264999999	0.7500010525000000
Fe	0.6250005265000000	0.8750005264999999	0.7500010525000000
As	0.3105529344999999	0.3105533480000000	0.0000000000000000
As	0.8105529345000000	0.3105533480000000	0.0000000000000000
As	0.3105529345000000	0.8105533479999998	0.0000000000000000

```
 As  0.8105529345000000   0.8105533480000000  0.0000000000000000
 As  0.3105529345000000   0.3105533480000000  0.5000000000000000
 As  0.8105529345000000   0.3105533480000000  0.5000000000000000
 As  0.3105529345000001   0.8105533479999999  0.5000000000000000
 As  0.8105529345000000   0.8105533479999999  0.5000000000000000
 As  0.1894470655000000   0.1894466520000000  0.0000000000000000
 As  0.6894470655000000   0.1894466520000000  0.0000000000000000
 As  0.1894470655000000   0.6894466520000000  0.0000000000000000
 As  0.6894470655000000   0.6894466519999999  0.0000000000000000
 As  0.1894470655000000   0.1894466520000000  0.5000000000000000
 As  0.6894470655000000   0.1894466519999999  0.5000000000000000
 As  0.1894470655000001   0.6894466520000000  0.5000000000000000
 As  0.6894470655000000   0.6894466520000000  0.5000000000000000
```

Super cell 002

```
!    ibrav = 0, nat = 40, ntyp = 3
CELL_PARAMETERS bohr
  19.7213357861786740   -0.1907791352002044   0.0000000000000000
  11.1164888651131673    16.2905715232244397  0.0000000000000000
  -15.4189123256459197   -8.0498961940121188   9.2968100231471915
ATOMIC_SPECIES
 Eu  151.96400  Eu.pbe-spdn-kjpaw_psl.1.0.0.UPF
 Fe  55.84500   Fe.pbe-spn-kjpaw_psl.1.0.0.UPF
 As  74.92160   As.pbe-n-kjpaw_psl.1.0.0.UPF
```

ATOMIC_POSITIONS crystal

```
Eu   0.0010140826397086  0.0000000000000000   0.0000000000000000
Eu   0.5000000000000000  0.0000000000000000   0.0000000000000000
Eu   0.0000000000000000  0.5000000000000000   0.0000000000000000
Eu   0.5000000000000000  0.4999999999999999   0.0000000000000000
Eu   0.0000000000000000  0.0000000000000000   0.5000000000000000
Eu   0.5000000000000000  0.0000000000000000   0.5000000000000000
Eu   0.0000000000000001  0.4999999999999999   0.5000000000000000
Eu   0.5000000000000000  0.4999999999999999   0.5000000000000000
Fe   0.3749994735000000  0.1249994735000000   0.2499989475000000
Fe   0.8749994735000000  0.1249994735000000   0.2499989475000000
Fe   0.3749994735000001  0.6249994735000000   0.2499989475000000
Fe   0.8749994734999997  0.6249994735000000   0.2499989475000000
Fe   0.3749994735000001  0.1249994735000000   0.7499989475000001
Fe   0.8749994735000002  0.1249994735000001   0.7499989475000001
Fe   0.3749994735000002  0.6249994735000000   0.7499989475000001
Fe   0.8749994735000000  0.6249994735000000   0.7499989475000001
Fe   0.1250005265000000  0.3750005265000000   0.2500010525000000
Fe   0.6250005265000002  0.3750005265000000   0.2500010525000000
Fe   0.1250005265000000  0.8750005265000000   0.2500010525000000
Fe   0.6250005265000000  0.8750005264999999   0.2500010525000000
Fe   0.1250005265000000  0.3750005264999999   0.7500010525000000
Fe   0.6250005265000000  0.3750005265000000   0.7500010525000000
```

Fe 0.1250005265000000 0.8750005264999999 0.7500010525000000

Fe 0.6250005265000000 0.8750005264999999 0.7500010525000000

As 0.3105529344999999 0.3105533480000000 0.0000000000000000

As 0.8105529345000000 0.3105533480000000 0.0000000000000000

As 0.3105529345000000 0.8105533479999998 0.0000000000000000

As 0.8105529345000000 0.8105533480000000 0.0000000000000000

As 0.3105529345000000 0.3105533480000000 0.5000000000000000

As 0.8105529345000000 0.3105533480000000 0.5000000000000000

As 0.3105529345000001 0.8105533479999999 0.5000000000000000

As 0.8105529345000000 0.8105533479999999 0.5000000000000000

As 0.1894470655000000 0.1894466520000000 0.0000000000000000

As 0.6894470655000000 0.1894466520000000 0.0000000000000000

As 0.1894470655000000 0.6894466520000000 0.0000000000000000

As 0.6894470655000000 0.6894466519999999 0.0000000000000000

As 0.1894470655000000 0.1894466520000000 0.5000000000000000

As 0.6894470655000000 0.1894466519999999 0.5000000000000000

As 0.1894470655000001 0.6894466520000000 0.5000000000000000

As 0.6894470655000000 0.6894466520000000 0.5000000000000000

Super cell 003

! ibrav = 0, nat = 40, ntyp = 3

CELL_PARAMETERS bohr

19.7213357861786740 -0.1907791352002044 0.0000000000000000

11.1164888651131673 16.2905715232244397 0.0000000000000000

```
 -15.4189123256459197   -8.0498961940121188    9.2968100231471915
ATOMIC_SPECIES
 Eu  151.96400  Eu.pbe-spdn-kjpaw_psl.1.0.0.UPF
 Fe  55.84500   Fe.pbe-spn-kjpaw_psl.1.0.0.UPF
 As     74.92160     As.pbe-n-kjpaw_psl.1.0.0.UPF
ATOMIC_POSITIONS crystal
 Eu   0.0000000000000000  0.0000000000000000   0.0000000000000000
 Eu   0.5000000000000000  0.0000000000000000   0.0000000000000000
 Eu   0.0000000000000000  0.5000000000000000   0.0000000000000000
 Eu   0.5000000000000000  0.4999999999999999   0.0000000000000000
 Eu   0.0000000000000000  0.0000000000000000   0.5000000000000000
 Eu   0.5000000000000000  0.0000000000000000   0.5000000000000000
 Eu   0.0000000000000001  0.4999999999999999   0.5000000000000000
 Eu   0.5000000000000000  0.4999999999999999  0.5000000000000000
Fe   0.3749994735000000  0.1249994735000000   0.2510130211703417
Fe   0.8749994735000000  0.1249994735000000   0.2499989475000000
Fe   0.3749994735000001  0.6249994735000000   0.2499989475000000
Fe   0.8749994734999997  0.6249994735000000   0.2499989475000000
Fe   0.3749994735000001  0.1249994735000000   0.7499989475000001
Fe   0.8749994735000002  0.1249994735000001   0.7499989475000001
Fe   0.3749994735000002  0.6249994735000000   0.7499989475000001
Fe   0.8749994735000000  0.6249994735000000   0.7499989475000001
Fe   0.1250005265000000  0.3750005265000000   0.2500010525000000
```

Fe	0.6250005265000002	0.3750005265000000	0.2500010525000000
Fe	0.1250005265000000	0.8750005265000000	0.2500010525000000
Fe	0.6250005265000000	0.8750005264999999	0.2500010525000000
Fe	0.1250005265000000	0.3750005264999999	0.7500010525000000
Fe	0.6250005265000000	0.3750005265000000	0.7500010525000000
Fe	0.1250005265000000	0.8750005264999999	0.7500010525000000
Fe	0.6250005265000000	0.8750005264999999	0.7500010525000000
As	0.3105529344999999	0.3105533480000000	0.0000000000000000
As	0.8105529345000000	0.3105533480000000	0.0000000000000000
As	0.3105529345000000	0.8105533479999998	0.0000000000000000
As	0.8105529345000000	0.8105533480000000	0.0000000000000000
As	0.3105529345000000	0.3105533480000000	0.5000000000000000
As	0.8105529345000000	0.3105533480000000	0.5000000000000000
As	0.3105529345000001	0.8105533479999999	0.5000000000000000
As	0.8105529345000000	0.8105533479999999	0.5000000000000000
As	0.1894470655000000	0.1894466520000000	0.0000000000000000
As	0.6894470655000000	0.1894466520000000	0.0000000000000000
As	0.1894470655000000	0.6894466520000000	0.0000000000000000
As	0.6894470655000000	0.6894466519999999	0.0000000000000000
As	0.1894470655000000	0.1894466520000000	0.5000000000000000
As	0.6894470655000000	0.1894466519999999	0.5000000000000000
As	0.1894470655000001	0.6894466520000000	0.5000000000000000
As	0.6894470655000000	0.6894466520000000	0.5000000000000000

The output file for super cell 001 is as below

Program PWSCF v.6.4.1 starts on 28Apr2020 at 20:27:55

This program is part of the open-source Quantum ESPRESSO suite
for quantum simulation of materials; please cite
"P. Giannozzi et al., J. Phys.:Condens. Matter 21 395502 (2009);
"P. Giannozzi et al., J. Phys.:Condens. Matter 29 465901 (2017);
URL http://www.quantum-espresso.org",
in publications or presentations arising from this work. More details at
http://www.quantum-espresso.org/quote

Parallel version (MPI), running on 48 processors

MPI processes distributed on 2 nodes
R & G space division: proc/nbgrp/npool/nimage = 48
Reading input from supercell-001.in

Current dimensions of program PWSCF are:
Max number of different atomic species (ntypx) = 10
Max number of k-points (npk) = 40000
Max angular momentum in pseudopotentials (lmaxx) = 3
file Eu.pbe-spdn-kjpaw_psl.1.0.0.UPF: wavefunction(s) 5P renormalized
file Fe.pbe-spn-kjpaw_psl.1.0.0.UPF: wavefunction(s) 3P 3D renormalized

Subspace diagonalization in iterative solution of the eigenvalue problem:
one sub-group per band group will be used
scalapack distributed-memory algorithm (size of sub-group: 4* 4 procs)

Parallelization info

----

sticks:	dense	smooth	PW	G-vecs:	dense	smooth	PW
Min	171	85	26		6054	2140	365
Max	172	86	27		6057	2142	366
Sum	8227	4111	1263		290659	102771	17539

bravais-lattice index = 0

lattice parameter (alat) = 19.7223 a.u.

unit-cell volume = 3006.5198 (a.u.)^3

number of atoms/cell = 40

number of atomic types = 3

number of electrons = 424.00

number of Kohn-Sham states= 254

kinetic-energy cutoff = 40.0000 Ry

charge density cutoff = 320.0000 Ry

convergence threshold = 1.0E-09

mixing beta = 0.4000

number of iterations used = 8 plain mixing

Exchange-correlation = SLA PW PBX PBC (1 4 3 4 0 0)

celldm(1)= 19.722259 celldm(2)= 0.000000 celldm(3)= 0.000000

celldm(4)= 0.000000 celldm(5)= 0.000000 celldm(6)= 0.000000

crystal axes: (cart. coord. in units of alat)

a(1) = (0.999953 -0.009673 0.000000)

a(2) = (0.563652 0.825999 0.000000)

a(3) = (-0.781803 -0.408163 0.471387)

reciprocal axes: (cart. coord. in units 2 pi/alat) b(1) = (0.993489 -0.677945 1.060700)

b(2) = (0.011635 1.202715 1.060700)

b(3) = (0.000000 0.000000 2.121401)

PseudoPot. # 1 for Eu read from file:

./Eu.pbe-spdn-kjpaw_psl.1.0.0.UPF

MD5 check sum: 02c18b8c493c24051d280dd8a22a9cee

Pseudo is Projector augmented-wave + core cor, Zval = 11.0

Generated using "atomic" code by A. Dal Corso v.6.2.2

Shape of augmentation charge: PSQ

Using radial grid of 1261 points, 6 beta functions with:

l(1) = 0

l(2) = 0

l(3) = 1

l(4) = 1

l(5) = 2

l(6) = 2

Q(r) pseudized with 0 coefficients

PseudoPot. # 2 for Fe read from file:

./Fe.pbe-spn-kjpaw_psl.1.0.0.UPF

MD5 check sum: fc81f059e5c5069939230b1155715ae8

Pseudo is Projector augmented-wave + core cor, Zval = 16.0

Generated using "atomic" code by A. Dal Corso v.6.3

Shape of augmentation charge: PSQ

Using radial grid of 1191 points, 6 beta functions with:

l(1) = 0

l(2) = 0

l(3) = 1

l(4) = 1

l(5) = 2

l(6) = 2

Q(r) pseudized with 0 coefficients

PseudoPot. # 3 for As read from file:

./As.pbe-n-kjpaw_psl.1.0.0.UPF

MD5 check sum: 21b474db91924651be503153fb2dbf55

Pseudo is Projector augmented-wave + core cor, Zval = 5.0

Generated using "atomic" code by A. Dal Corso v.6.3

Shape of augmentation charge: PSQ

Using radial grid of 1209 points, 4 beta functions with:

l(1) = 0

l(2) = 0

l(3) = 1

l(4) = 1

Q(r) pseudized with 0 coefficients

atomic species	valence	mass	pseudopotential
Eu	11.00	151.96400	Eu(1.00)
Fe	16.00	55.84500	Fe(1.00)
As	5.00	74.92160	As(1.00)

No symmetry found

s frac. trans.

isym = 1 identity

cryst. s(1) = (1 0 0)
(0 1 0)
(0 0 1)

cart. s(1) = (1.0000000 0.0000000 0.0000000)
(-0.0000000 1.0000000 0.0000000)
(0.0000000 0.0000000 1.0000000)

Cartesian axes

site n.	atom	positions (alat units)
1	Eu tau(	1) = (-0.0007928 -0.0004139 0.0004780)
2	Eu tau(	2) = (0.4999766 -0.0048366 0.0000000)
3	Eu tau(	3) = (0.2818260 0.4129996 0.0000000)
4	Eu tau(	4) = (0.7818026 0.4081630 0.0000000)
5	Eu tau(	5) = (-0.3909013 -0.2040815 0.2356933)
6	Eu tau(	6) = (0.1090753 -0.2089181 0.2356933)
7	Eu tau(	7) = (-0.1090753 0.2089181 0.2356933)
8	Eu tau(	8) = (0.3909013 0.2040815 0.2356933)
9	Fe tau(	9) = (0.2499883 -0.0024183 0.1178462)
10	Fe tau(	10) = (0.7499649-0.0072550 0.1178462)
11	Fe tau(	11) = (0.53181430.4105813 0.1178462)
12	Fe tau(	12) = (1.03179090.4057447 0.1178462)
13	Fe tau(	13) = (-0.1409130 -0.2064998 0.3535395)
14	Fe tau(	14) = (0.3590636 -0.2113365 0.3535395)
15	Fe tau(	15) = (0.1409130 0.2064998 0.3535395)
16	Fe tau(	16) = (0.6408896 0.2016632 0.3535395)
17	Fe tau(	17) = (0.1409130 0.2064998 0.1178472)
18	Fe tau(	18) = (0.6408896 0.2016632 0.1178472)

19	Fe	tau(19) = (	0.4227389	0.6194995	0.1178472	)
20	Fe	tau(20) = (	0.9227155	0.6146628	0.1178472	)
21	Fe	tau(21) = (	-0.2499883	0.0024183	0.3535405	)
22	Fe	tau(22) = (	0.2499883	-0.0024183	0.3535405	)
23	Fe	tau(23) = (	0.0318377	0.4154180	0.3535405	)
24	Fe	tau(24) = (	0.5318143	0.4105813	0.3535405	)
25	As	tau(25) = (	0.4855824	0.2535128	0.0000000	)
26	As	tau(26) = (	0.9855590	0.2486761	0.0000000	)
27	As	tau(27) = (	0.7674084	0.6665124	0.0000000	)
28	As	tau(28) = (	1.2673850	0.6616758	0.0000000	)
29	As	tau(29) = (	0.0946811	0.0494313	0.2356933	)
30	As	tau(30) = (	0.5946577	0.0445946	0.2356933	)
31	As	tau(31) = (	0.3765071	0.4624309	0.2356933	)
32	As	tau(32) = (	0.8764837	0.4575943	0.2356933	)
33	As	tau(33) = (	0.2962202	0.1546502	0.0000000	)
34	As	tau(34) = (	0.7961968	0.1498136	0.0000000	)
35	As	tau(35) = (	0.5780461	0.5676499	0.0000000	)
36	As	tau(36) = (	1.0780227	0.5628132	0.0000000	)
37	As	tau(37) = (	-0.0946811	-0.0494313	0.2356933	)
38	As	tau(38) = (	0.4052955	-0.0542679	0.2356933	)
39	As	tau(39) = (	0.1871448	0.3635684	0.2356933	)
40	As	tau(40) = (	0.6871215	0.3587317	0.2356933	)

Crystallographic axes

site n.	atom	positions (cryst. coord.)				
1	Eu	tau(1) = (	0.0000000	0.0000000	0.0010141	)
2	Eu	tau(2) = (	0.5000000	0.0000000	0.0000000	)
3	Eu	tau(3) = (	0.0000000	0.5000000	0.0000000	)
4	Eu	tau(4) = (	0.5000000	0.5000000	0.0000000	)
5	Eu	tau(5) = (	0.0000000	0.0000000	0.5000000	)

6	Eu	tau(6) = (	0.5000000	0.0000000	0.5000000)
7	Eu	tau(7) = (	0.0000000	0.5000000	0.5000000)
8	Eu	tau(8) = (	0.5000000	0.5000000	0.5000000)
9	Fe	tau(9) = (	0.3749995	0.1249995	0.2499989)
10	Fe	tau(10) = (	0.8749995	0.1249995	0.2499989)
11	Fe	tau(11) = (	0.3749995	0.6249995	0.2499989)
12	Fe	tau(12) = (	0.8749995	0.6249995	0.2499989)
13	Fe	tau(13) = (	0.3749995	0.1249995	0.7499989)
14	Fe	tau(14) = (	0.8749995	0.1249995	0.7499989)
15	Fe	tau(15) = (	0.3749995	0.6249995	0.7499989)
16	Fe	tau(16) = (	0.8749995	0.6249995	0.7499989)
17	Fe	tau(17) = (	0.1250005	0.3750005	0.2500011)
18	Fe	tau(18) = (	0.6250005	0.3750005	0.2500011)
19	Fe	tau(19) = (	0.1250005	0.8750005	0.2500011)
20	Fe	tau(20) = (	0.6250005	0.8750005	0.2500011)
21	Fe	tau(21) = (	0.1250005	0.3750005	0.7500011)
22	Fe	tau(22) = (	0.6250005	0.3750005	0.7500011)
23	Fe	tau(23) = (	0.1250005	0.8750005	0.7500011)
24	Fe	tau(24) = (	0.6250005	0.8750005	0.7500011)
25	As	tau(25) = (	0.3105529	0.3105533	0.0000000)
26	As	tau(26) = (	0.8105529	0.3105533	0.0000000)
27	As	tau(27) = (	0.3105529	0.8105533	0.0000000)
28	As	tau(28) = (	0.8105529	0.8105533	0.0000000)
29	As	tau(29) = (	0.3105529	0.3105533	0.5000000)
30	As	tau(30) = (	0.8105529	0.3105533	0.5000000)
31	As	tau(31) = (	0.3105529	0.8105533	0.5000000)
32	As	tau(32) = (	0.8105529	0.8105533	0.5000000)
33	As	tau(33) = (	0.1894471	0.1894467	0.0000000)
34	As	tau(34) = (	0.6894471	0.1894467	0.0000000)
35	As	tau(35) = (	0.1894471	0.6894467	0.0000000)
36	As	tau(36) = (	0.6894471	0.6894467	0.0000000)

37 As tau(37) = (0.1894471 0.1894467 0.5000000)
38 As tau(38) = (0.6894471 0.1894467 0.5000000)
39 As tau(39) = (0.1894471 0.6894467 0.5000000)
40 As tau(40) = (0.6894471 0.6894467 0.5000000)

number of k points= 8 Marzari-Vanderbilt smearing, width (Ry)= 0.0147

cart. coord. in units 2pi/alat

k(1) = (0.0000000 0.0000000 0.0000000), wk = 0.2500000
k(2) = (0.0000000 0.0000000 -1.0607003), wk = 0.2500000
k(3) = (-0.0058174 -0.6013577 -0.5303502), wk = 0.2500000
k(4) = (-0.4967443 0.3389723 -0.5303502), wk = 0.2500000
k(5) = (-0.5025616 -0.2623854 -1.0607003), wk = 0.2500000
k(6) = (-0.5025616 -0.2623854 -2.1214006), wk = 0.2500000
k(7) = (0.0058174 0.6013577 -0.5303502), wk = 0.2500000
k(8) = (0.4967443 -0.3389723 -0.5303502), wk = 0.2500000

cryst. coord.

k(1) = (0.0000000 0.0000000 0.0000000), wk = 0.2500000
k(2) = (0.0000000 0.0000000 -0.5000000), wk = 0.2500000
k(3) = (0.0000000 -0.5000000 0.0000000), wk = 0.2500000
k(4) = (-0.5000000 0.0000000 0.0000000), wk = 0.2500000
k(5) = (-0.5000000 -0.5000000 0.0000000), wk = 0.2500000
k(6) = (-0.5000000 -0.5000000 -0.5000000), wk = 0.2500000
k(7) = (0.0000000 0.5000000 -0.5000000), wk = 0.2500000
k(8) = (0.5000000 0.0000000 -0.5000000), wk = 0.2500000

Dense grid: 290659 G-vectors FFT dimensions: (120, 120, 120)

Smooth grid: 102771 G-vectors FFT dimensions: (80, 80, 80)

Dynamical RAM for wfc: 1.03 MB

Dynamical RAM for wfc (w. buffer): 9.31 MB

Dynamical RAM for str. fact: 0.28 MB

Dynamical RAM for local pot: 0.00 MB

Dynamical RAM for nlocal pot: 2.28 MB

Dynamical RAM for qrad: 13.50 MB

Dynamical RAM for rho,v,vnew: 1.27 MB

Dynamical RAM for rhoin: 0.42 MB

Dynamical RAM for rho*nmix: 1.48 MB

Dynamical RAM for G-vectors: 0.36 MB

Dynamical RAM for h,s,v(r/c): 2.95 MB

Dynamical RAM for <psi|beta>: 2.17 MB

Dynamical RAM for psi: 4.14 MB

Dynamical RAM for hpsi: 4.14 MB

Dynamical RAM for spsi: 4.14 MB

Dynamical RAM for wfcinit/wfcrot: 5.14 MB

Dynamical RAM for addusdens: 18.66 MB

Dynamical RAM for addusforce: 28.29 MB

Dynamical RAM for addusstress: 18.57 MB

Estimated static dynamical RAM per process > 30.92 MB

Estimated max dynamical RAM per process > 59.21 MB

Estimated total dynamical RAM > 2.78 GB

Initial potential from superposition of free atoms

starting charge 423.81344, renormalised to 424.00000
Starting wfcs are 328 randomized atomic wfcs
Checking if some PAW data can be deallocated...
PAW data deallocated on 32 nodes for type: 1
PAW data deallocated on 32 nodes for type: 2
PAW data deallocated on 32 nodes for type: 3

total cpu time spent up to now is 5.7 secs

Self-consistent Calculation

iteration # 1 ecut= 40.00 Ry beta= 0.40
Davidson diagonalization with overlap
ethr = 1.00E-02, avg # of iterations = 2.9

Threshold (ethr) on eigenvalues was too large:
Diagonalizing with lowered threshold

Davidson diagonalization with overlap
ethr = 7.87E-04, avg # of iterations = 1.0

total cpu time spent up to now is 19.4 secs

total energy = -12415.35511877 Ry
Harris-Foulkes estimate = -12417.33672552 Ry
estimated scf accuracy < 3.34096610 Ry

iteration # 2 ecut= 40.00 Ry beta= 0.40
Davidson diagonalization with overlap
ethr = 7.88E-04, avg # of iterations = 6.2

total cpu time spent up to now is 34.7 secs

total energy = -12414.81195502 Ry
Harris-Foulkes estimate = -12418.20441481 Ry
estimated scf accuracy < 16.60428850 Ry

iteration # 3 ecut= 40.00 Ry beta= 0.40
Davidson diagonalization with overlap
ethr = 7.88E-04, avg # of iterations = 4.2

total cpu time spent up to now is 46.3 secs

total energy = -12416.08961670 Ry
Harris-Foulkes estimate = -12416.86371319 Ry
estimated scf accuracy < 6.33162685 Ry

iteration # 4 ecut= 40.00 Ry beta= 0.40

Davidson diagonalization with overlap
ethr = 7.88E-04, avg # of iterations = 2.0

total cpu time spent up to now is 52.5 secs

total energy = -12416.31335946 Ry
Harris-Foulkes estimate = -12416.74148722 Ry
estimated scf accuracy < 3.90944787 Ry

iteration # 5 ecut= 40.00 Ry beta= 0.40
Davidson diagonalization with overlap
ethr = 7.88E-04, avg # of iterations = 2.0

total cpu time spent up to now is 58.8 secs

total energy = -12416.01709394 Ry
Harris-Foulkes estimate = -12417.13761176 Ry
estimated scf accuracy < 19.84019358 Ry

iteration # 6 ecut= 40.00 Ry beta= 0.40
Davidson diagonalization with overlap
ethr = 7.88E-04, avg # of iterations = 1.2

total cpu time spent up to now is 64.5 secs

total energy = -12416.54200270 Ry
Harris-Foulkes estimate = -12416.60681356 Ry
estimated scf accuracy < 0.60731708 Ry

iteration # 7 ecut= 40.00 Ry beta= 0.40
Davidson diagonalization with overlap

ethr = 1.43E-04, avg # of iterations = 1.9

total cpu time spent up to now is 70.6 secs

total energy = -12416.57481256 Ry
Harris-Foulkes estimate = -12416.59654422 Ry
estimated scf accuracy < 0.22748752 Ry

iteration # 8 ecut= 40.00 Ry beta= 0.40
Davidson diagonalization with overlap
ethr = 5.37E-05, avg # of iterations = 2.0

total cpu time spent up to now is 77.0 secs

total energy = -12416.56968045 Ry
Harris-Foulkes estimate = -12416.60394832 Ry
estimated scf accuracy < 0.39044666 Ry

iteration # 9 ecut= 40.00 Ry beta= 0.40
Davidson diagonalization with overlap
ethr = 5.37E-05, avg # of iterations = 1.0

total cpu time spent up to now is 82.5 secs

total energy = -12416.58628903 Ry
Harris-Foulkes estimate = -12416.58851527 Ry
estimated scf accuracy < 0.01707445 Ry

iteration # 10 ecut= 40.00 Ry beta= 0.40
Davidson diagonalization with overlap
ethr = 4.03E-06, avg # of iterations = 4.9

total cpu time spent up to now is 92.7 secs

total energy = -12416.58426621 Ry

Harris-Foulkes estimate = -12416.59223848 Ry

estimated scf accuracy < 0.09471521 Ry

iteration # 11 ecut= 40.00 Ry beta= 0.40

Davidson diagonalization with overlap

ethr = 4.03E-06, avg # of iterations = 2.4

total cpu time spent up to now is 99.5 secs

total energy = -12416.58763214 Ry

Harris-Foulkes estimate = -12416.58865805 Ry

estimated scf accuracy < 0.00564409 Ry

iteration # 12 ecut= 40.00 Ry beta= 0.40

Davidson diagonalization with overlap

ethr = 1.33E-06, avg # of iterations = 2.6

total cpu time spent up to now is 106.7 secs

total energy = -12416.58794460 Ry

Harris-Foulkes estimate = -12416.58900155 Ry

estimated scf accuracy < 0.01227307 Ry

iteration # 13 ecut= 40.00 Ry beta= 0.40

Davidson diagonalization with overlap

ethr = 1.33E-06, avg # of iterations = 1.8

total cpu time spent up to now is 112.7 secs

total energy = -12416.58828668 Ry
Harris-Foulkes estimate = -12416.58869401 Ry
estimated scf accuracy < 0.00303896 Ry

iteration # 14 ecut= 40.00 Ry beta= 0.40
Davidson diagonalization with overlap
ethr = 7.17E-07, avg # of iterations = 1.9

total cpu time spent up to now is 118.8 secs

total energy = -12416.58843249 Ry
Harris-Foulkes estimate = -12416.58864477 Ry
estimated scf accuracy < 0.00157895 Ry

iteration # 15 ecut= 40.00 Ry beta= 0.40
Davidson diagonalization with overlap
ethr = 3.72E-07, avg # of iterations = 2.0

total cpu time spent up to now is 125.6 secs

total energy = -12416.58836997 Ry
Harris-Foulkes estimate = -12416.58875814 Ry
estimated scf accuracy < 0.00474805 Ry

iteration # 16 ecut= 40.00 Ry beta= 0.40
Davidson diagonalization with overlap
ethr = 3.72E-07, avg # of iterations = 1.5

total cpu time spent up to now is 131.6 secs

total energy = -12416.58853212 Ry
Harris-Foulkes estimate = -12416.58862197 Ry
estimated scf accuracy < 0.00099054 Ry

iteration # 17 ecut= 40.00 Ry beta= 0.40
Davidson diagonalization with overlap
ethr = 2.34E-07, avg # of iterations = 1.0

total cpu time spent up to now is 137.1 secs

total energy = -12416.58853623 Ry
Harris-Foulkes estimate = -12416.58860594 Ry
estimated scf accuracy < 0.00052268 Ry

iteration # 18 ecut= 40.00 Ry beta= 0.40
Davidson diagonalization with overlap
ethr = 1.23E-07, avg # of iterations = 2.0

total cpu time spent up to now is 143.6 secs

total energy = -12416.58848780 Ry
Harris-Foulkes estimate = -12416.58866341 Ry
estimated scf accuracy < 0.00199064 Ry

iteration # 19 ecut= 40.00 Ry beta= 0.40
Davidson diagonalization with overlap
ethr = 1.23E-07, avg # of iterations = 2.1

total cpu time spent up to now is 150.4 secs

total energy = -12416.58851646 Ry

Harris-Foulkes estimate = -12416.58864831 Ry

estimated scf accuracy < 0.00162978 Ry

iteration # 20 ecut= 40.00 Ry beta= 0.40

Davidson diagonalization with overlap

ethr = 1.23E-07, avg # of iterations = 1.9

total cpu time spent up to now is 156.5 secs

total energy = -12416.58855930 Ry

Harris-Foulkes estimate = -12416.58860279 Ry

estimated scf accuracy < 0.00043877 Ry

iteration # 21 ecut= 40.00 Ry beta= 0.40

Davidson diagonalization with overlap

ethr = 1.03E-07, avg # of iterations = 1.0

total cpu time spent up to now is 162.0 secs

total energy = -12416.58857044 Ry

Harris-Foulkes estimate = -12416.58859522 Ry

estimated scf accuracy < 0.00026970 Ry

iteration # 22 ecut= 40.00 Ry beta= 0.40

Davidson diagonalization with overlap

ethr = 6.36E-08, avg # of iterations = 1.0

total cpu time spent up to now is 167.5 secs

total energy = -12416.58857785 Ry

Harris-Foulkes estimate = -12416.58859042 Ry
estimated scf accuracy < 0.00013153 Ry

iteration # 23 ecut= 40.00 Ry beta= 0.40
Davidson diagonalization with overlap
ethr = 3.10E-08, avg # of iterations = 1.0

total cpu time spent up to now is 173.0 secs

total energy = -12416.58858349 Ry
Harris-Foulkes estimate = -12416.58858559 Ry
estimated scf accuracy < 0.00001235 Ry

iteration # 24 ecut= 40.00 Ry beta= 0.40
Davidson diagonalization with overlap
ethr = 2.91E-09, avg # of iterations = 2.5

total cpu time spent up to now is 180.2 secs

total energy = -12416.58858233 Ry
Harris-Foulkes estimate = -12416.58858750 Ry
estimated scf accuracy < 0.00005740 Ry

iteration # 25 ecut= 40.00 Ry beta= 0.40
Davidson diagonalization with overlap
ethr = 2.91E-09, avg # of iterations = 2.1

total cpu time spent up to now is 186.8 secs

total energy = -12416.58858429 Ry
Harris-Foulkes estimate = -12416.58858548 Ry

estimated scf accuracy < 0.00000874 Ry

iteration # 26 ecut= 40.00 Ry beta= 0.40

Davidson diagonalization with overlap

ethr = 2.06E-09, avg # of iterations = 2.0

total cpu time spent up to now is 193.1 secs

total energy = -12416.58858432 Ry

Harris-Foulkes estimate = -12416.58858577 Ry

estimated scf accuracy < 0.00001653 Ry

iteration # 27 ecut= 40.00 Ry beta= 0.40

Davidson diagonalization with overlap

ethr = 2.06E-09, avg # of iterations = 1.2

total cpu time spent up to now is 198.8 secs

total energy = -12416.58858479 Ry

Harris-Foulkes estimate = -12416.58858546 Ry

estimated scf accuracy < 0.00000742 Ry

iteration # 28 ecut= 40.00 Ry beta= 0.40

Davidson diagonalization with overlap

ethr = 1.75E-09, avg # of iterations = 1.0

total cpu time spent up to now is 204.4 secs

total energy = -12416.58858488 Ry

Harris-Foulkes estimate = -12416.58858539 Ry

estimated scf accuracy < 0.00000504 Ry

iteration # 29 ecut= 40.00 Ry beta= 0.40

Davidson diagonalization with overlap

ethr = 1.19E-09, avg # of iterations = 1.0

total cpu time spent up to now is 209.9 secs

total energy = -12416.58858503 Ry

Harris-Foulkes estimate = -12416.58858530 Ry

estimated scf accuracy < 0.00000225 Ry

iteration # 30 ecut= 40.00 Ry beta= 0.40

Davidson diagonalization with overlap

ethr = 5.31E-10, avg # of iterations = 1.9

total cpu time spent up to now is 216.0 secs

total energy = -12416.58858495 Ry

Harris-Foulkes estimate = -12416.58858541 Ry

estimated scf accuracy < 0.00000459 Ry

iteration # 31 ecut= 40.00 Ry beta= 0.40

Davidson diagonalization with overlap

ethr = 5.31E-10, avg # of iterations = 2.0

total cpu time spent up to now is 222.5 secs

total energy = -12416.58858486 Ry

Harris-Foulkes estimate = -12416.58858554 Ry

estimated scf accuracy < 0.00000874 Ry

iteration # 32   ecut=   40.00 Ry   beta= 0.40

Davidson diagonalization with overlap

ethr = 5.31E-10, avg # of iterations = 2.0

total cpu time spent up to now is   228.9 secs

total energy   =   -12416.58858507   Ry

Harris-Foulkes estimate = -12416.58858530 Ry

estimated scf accuracy   <   0.00000235 Ry

iteration # 33   ecut=   40.00 Ry   beta= 0.40

Davidson diagonalization with overlap

ethr =   5.31E-10,   avg # of iterations =   1.0

total cpu time spent up to now is   234.4 secs

total energy   =   -12416.58858514   Ry

Harris-Foulkes estimate = -12416.58858526 Ry

estimated scf accuracy   <   0.00000105 Ry

iteration # 34   ecut=   40.00 Ry   beta= 0.40

Davidson diagonalization with overlap

ethr = 2.47E-10, avg # of iterations = 1.0

total cpu time spent up to now is   239.9 secs

total energy   =   -12416.58858517   Ry

Harris-Foulkes estimate = -12416.58858525 Ry

estimated scf accuracy   <   0.00000090 Ry

iteration # 35   ecut=   40.00 Ry   beta= 0.40

Davidson diagonalization with overlap
ethr = 2.12E-10, avg # of iterations = 1.0

total cpu time spent up to now is 245.4 secs

total energy = -12416.58858519 Ry
Harris-Foulkes estimate = -12416.58858524 Ry
estimated scf accuracy < 0.00000051 Ry

iteration # 36 ecut= 40.00 Ry beta= 0.40
Davidson diagonalization with overlap
ethr = 1.21E-10, avg # of iterations = 1.0

total cpu time spent up to now is 250.9 secs

total energy = -12416.58858520 Ry
Harris-Foulkes estimate = -12416.58858523 Ry
estimated scf accuracy < 0.00000035 Ry

iteration # 37 ecut= 40.00 Ry beta= 0.40
Davidson diagonalization with overlap
ethr = 8.33E-11, avg # of iterations = 1.0

total cpu time spent up to now is 256.5 secs

total energy = -12416.58858521 Ry
Harris-Foulkes estimate = -12416.58858522 Ry
estimated scf accuracy < 0.00000015 Ry

iteration # 38 ecut= 40.00 Ry beta= 0.40
Davidson diagonalization with overlap

ethr = 3.44E-11, avg # of iterations = 1.0

total cpu time spent up to now is 262.1 secs

total energy = -12416.58858521 Ry
Harris-Foulkes estimate = -12416.58858522 Ry
estimated scf accuracy < 0.00000007 Ry

iteration # 39 ecut= 40.00 Ry beta= 0.40
Davidson diagonalization with overlap
ethr = 1.54E-11, avg # of iterations = 1.0

total cpu time spent up to now is 267.6 secs

total energy = -12416.58858522 Ry
Harris-Foulkes estimate = -12416.58858522 Ry
estimated scf accuracy < 0.00000007 Ry

iteration # 40 ecut= 40.00 Ry beta= 0.40
Davidson diagonalization with overlap
ethr = 1.54E-11, avg # of iterations = 1.0

total cpu time spent up to now is 273.1 secs

total energy = -12416.58858522 Ry
Harris-Foulkes estimate = -12416.58858522 Ry
estimated scf accuracy < 0.00000004 Ry

iteration # 41 ecut= 40.00 Ry beta= 0.40
Davidson diagonalization with overlap
ethr = 9.72E-12, avg # of iterations = 1.0

total cpu time spent up to now is 278.6 secs

total energy = -12416.58858522 Ry

Harris-Foulkes estimate = -12416.58858522 Ry

estimated scf accuracy < 0.00000005 Ry

iteration # 42 ecut= 40.00 Ry beta= 0.40

Davidson diagonalization with overlap

ethr = 9.72E-12, avg # of iterations = 1.0

total cpu time spent up to now is 284.2 secs

total energy = -12416.58858522 Ry

Harris-Foulkes estimate = -12416.58858522 Ry

estimated scf accuracy < 0.00000005 Ry

iteration # 43 ecut= 40.00 Ry beta= 0.40

Davidson diagonalization with overlap

ethr = 9.72E-12, avg # of iterations = 1.4

total cpu time spent up to now is 290.0 secs

total energy = -12416.58858522 Ry

Harris-Foulkes estimate = -12416.58858522 Ry

estimated scf accuracy < 0.00000007 Ry

iteration # 44 ecut= 40.00 Ry beta= 0.40

Davidson diagonalization with overlap

ethr = 9.72E-12, avg # of iterations = 1.2

total cpu time spent up to now is 295.7 secs

total energy = -12416.58858522 Ry
Harris-Foulkes estimate = -12416.58858522 Ry
estimated scf accuracy < 0.00000004 Ry

iteration # 45 ecut= 40.00 Ry beta= 0.40
Davidson diagonalization with overlap
ethr = 9.63E-12, avg # of iterations = 1.0

total cpu time spent up to now is 301.2 secs

total energy = -12416.58858522 Ry
Harris-Foulkes estimate = -12416.58858522 Ry
estimated scf accuracy < 0.00000002 Ry

iteration # 46 ecut= 40.00 Ry beta= 0.40
Davidson diagonalization with overlap
ethr = 3.74E-12, avg # of iterations = 1.0

total cpu time spent up to now is 306.7 secs

total energy = -12416.58858522 Ry
Harris-Foulkes estimate = -12416.58858522 Ry
estimated scf accuracy < 0.00000001 Ry

iteration # 47 ecut= 40.00 Ry beta= 0.40
Davidson diagonalization with overlap
ethr = 2.52E-12, avg # of iterations = 1.0

total cpu time spent up to now is 312.2 secs

total energy = -12416.58858522 Ry

Harris-Foulkes estimate = -12416.58858522 Ry

estimated scf accuracy < 0.00000001 Ry

iteration # 48 ecut= 40.00 Ry beta= 0.40

Davidson diagonalization with overlap

ethr = 2.52E-12, avg # of iterations = 1.0

total cpu time spent up to now is 317.7 secs

total energy = -12416.58858522 Ry

Harris-Foulkes estimate = -12416.58858522 Ry

estimated scf accuracy < 2.7E-09 Ry

iteration # 49 ecut= 40.00 Ry beta= 0.40

Davidson diagonalization with overlap

ethr = 6.32E-13, avg # of iterations = 1.0

total cpu time spent up to now is 323.3 secs

total energy = -12416.58858522 Ry

Harris-Foulkes estimate = -12416.58858522 Ry

estimated scf accuracy < 2.0E-09 Ry

iteration # 50 ecut= 40.00 Ry beta= 0.40

Davidson diagonalization with overlap

ethr = 4.81E-13, avg # of iterations = 1.0

total cpu time spent up to now is 328.8 secs

End of self-consistent calculation

k = 0.0000 0.0000 0.0000 (12843 PWs) bands (ev):

-65.6686	-65.6672	-65.6270	-65.6270	-65.6269	-65.6269	-65.6268	-65.6268
-65.6266	-65.6266	-65.6266	-65.6266	-65.6255	-65.6245	-65.5883	-65.5872
-31.8741	-31.8735	-31.8597	-31.8286	-31.8258	-31.8251	-31.8057	-31.8050
-31.7229	-31.6959	-31.6959	-31.6958	-31.6958	-31.6888	-31.6888	-31.6887
-31.6887	-31.6852	-31.6823	-31.6823	-31.6822	-31.6822	-31.6820	-31.6819
-31.6818	-31.6818	-31.6725	-31.6724	-31.6582	-31.6582	-31.6582	-31.6581
-31.6571	-31.6509	-31.6508	-31.6508	-31.6507	-31.6507	-31.6190	-31.6178
-31.5778	-31.5773	-31.5613	-31.5609	-31.5053	-31.5048	-31.4952	-31.4929
-20.0084	-20.0017	-19.9364	-19.9364	-19.9364	-19.9364	-19.8750	-19.8749
-0.3241	-0.3240	-0.3240	-0.3240	0.2770	0.2772	0.3262	0.3264
0.6132	0.8698	1.0262	1.0262	1.0262	1.0262	1.1184	1.1188
1.1292	1.1296	1.2024	1.2025	1.2997	1.2997	1.2997	1.2997
5.3604	6.2782	6.5207	6.5215	8.1974	8.1974	8.1974	8.1974
8.5672	9.0157	9.0157	9.0158	9.0158	10.1629	10.1635	10.2527
12.1320	13.7794	13.7794	13.7794	13.7794	13.8377	13.8407	14.2162
14.6074	14.6074	14.6075	14.6075	14.9865	14.9869	15.2605	15.2633
15.6839	15.6839	15.6839	15.6839	16.1338	16.1339	16.5245	16.5251
16.5973	16.5981	17.0921	17.0926	17.0926	17.0926	17.2252	17.2253
17.2253	17.2255	17.3112	17.3903	17.3904	17.3904	17.3904	17.5208
17.5217	17.6244	17.6526	17.6848	17.8144	17.8271	17.8477	17.8522
17.8527	17.9686	17.9691	18.7404	18.7463	18.8371	18.8379	19.0104
19.0104	19.0104	19.0104	19.0689	19.2356	19.2365	19.4351	19.5843
19.5843	19.5843	19.5843	19.6245	19.6245	19.6246	19.6246	19.6925
19.7769	19.7769	19.7769	19.7770	20.0253	20.0253	20.0253	20.0253
20.0731	20.1179	20.1179	20.1179	20.1179	20.2239	20.2391	20.7821
20.7828	20.8409	20.8410	21.0058	21.0090	21.0324	21.0325	21.0726
21.0726	21.0727	21.0727	21.5663	21.6129	21.6130	21.6507	22.8055

22.8327	22.8823	22.9714	22.9716	23.0669	23.0673	23.0673	23.0674
23.1308	23.1541	23.1541	23.1542	23.1546	23.2228	23.4767	23.4771
23.5185	23.5194	24.5499	24.8364	24.8966	25.0251	25.0262	25.0264
25.0265	25.0477	25.0478	25.0479	25.0494	25.1543	25.1550	26.4893
26.4894	26.4895	26.4895	26.6011	27.1803	27.1819		

occupation numbers

1.0000	1.0000	1.0000	1.0000	1.0000	1.0000	1.0000	1.0000
1.0000	1.0000	1.0000	1.0000	1.0000	1.0000	1.0000	1.0000
1.0000	1.0000	1.0000	1.0000	1.0000	1.0000	1.0000	1.0000
1.0000	1.0000	1.0000	1.0000	1.0000	1.0000	1.0000	1.0000
1.0000	1.0000	1.0000	1.0000	1.0000	1.0000	1.0000	1.0000
1.0000	1.0000	1.0000	1.0000	1.0000	1.0000	1.0000	1.0000
1.0000	1.0000	1.0000	1.0000	1.0000	1.0000	1.0000	1.0000
1.0000	1.0000	1.0000	1.0000	1.0000	1.0000	1.0000	1.0000
1.0000	1.0000	1.0000	1.0000	1.0000	1.0000	1.0000	1.0000
1.0000	1.0000	1.0000	1.0000	1.0000	1.0000	1.0000	1.0000
1.0000	1.0000	1.0000	1.0000	1.0000	1.0000	1.0000	1.0000
1.0000	1.0000	1.0000	1.0000	1.0000	1.0000	1.0000	1.0000
1.0000	1.0000	1.0000	1.0000	1.0000	1.0000	1.0000	1.0000
1.0000	1.0000	1.0000	1.0000	1.0000	1.0000	1.0000	1.0000
1.0000	1.0000	1.0000	1.0000	1.0000	1.0000	1.0000	1.0000
1.0000	1.0000	1.0000	1.0000	1.0000	1.0000	1.0000	1.0000
1.0000	1.0000	1.0000	1.0000	1.0000	1.0000	1.0000	1.0000
1.0000	1.0000	1.0000	1.0000	1.0000	1.0000	1.0000	1.0000
1.0000	1.0000	1.0000	1.0000	1.0000	1.0000	1.0000	1.0000
1.0000	1.0000	1.0000	1.0000	1.0000	1.0000	1.0000	1.0000
1.0000	1.0000	1.0000	1.0000	1.0000	1.0000	1.0000	1.0000
1.0000	1.0000	1.0000	1.0000	1.0000	1.0000	1.0000	1.0000
1.0000	1.0000	1.0000	1.0000	1.0000	1.0000	1.0000	1.0000
1.0000	1.0000	1.0000	1.0000	1.0000	1.0000	1.0000	1.0000

1.0000	1.0000	1.0000	1.0000	1.0000	1.0000	1.0000	1.0006
1.0007	1.0024	1.0024	1.0360	1.0373	1.0477	1.0477	1.0663
1.0663	1.0664	1.0664	0.0693	0.0323	0.0323	0.0162	0.0000
0.0000	0.0000	0.0000	0.0000	0.0000	0.0000	0.0000	0.0000
0.0000	0.0000	0.0000	0.0000	0.0000	0.0000	0.0000	0.0000
0.0000	0.0000	0.0000	0.0000	0.0000	0.0000	0.0000	0.0000
0.0000	0.0000	0.0000	0.0000	0.0000	0.0000	0.0000	0.0000
0.0000	0.0000	0.0000	0.0000	0.0000	0.0000		

k = 0.0000 0.0000-1.0607 (12866 PWs) bands (ev):

-65.6472	-65.6469	-65.6468	-65.6466	-65.6464	-65.6464	-65.6463	-65.6462
-65.6082	-65.6080	-65.6074	-65.6072	-65.6072	-65.6070	-65.6070	-65.6070
-31.8472	-31.8471	-31.8471	-31.8470	-31.8465	-31.8463	-31.8453	-31.8451
-31.7046	-31.7045	-31.7045	-31.7044	-31.6992	-31.6992	-31.6991	-31.6990
-31.6884	-31.6880	-31.6843	-31.6842	-31.6816	-31.6811	-31.6754	-31.6754
-31.6750	-31.6750	-31.6674	-31.6673	-31.6673	-31.6672	-31.6647	-31.6645
-31.6603	-31.6598	-31.6424	-31.6420	-31.6342	-31.6342	-31.6338	-31.6338
-31.5420	-31.5418	-31.5332	-31.5331	-31.5330	-31.5330	-31.5330	-31.5328
-19.9404	-19.9400	-19.9386	-19.9386	-19.9386	-19.9385	-19.9371	-19.9367
0.3373	0.3379	0.3643	0.3646	0.3647	0.3650	0.3979	0.3984
0.6852	0.6873	0.6966	0.6967	0.6967	0.6968	0.7055	0.7076
0.9356	0.9367	0.9952	0.9956	0.9958	0.9961	1.0493	1.0500
7.0442	7.0447	7.2492	7.2498	7.2499	7.2505	7.5079	7.5082
8.9025	8.9042	9.3814	9.3821	9.3837	9.3843	9.9628	9.9636
13.0786	13.0787	14.1229	14.1236	14.1238	14.1245	14.8434	14.8438
14.8839	14.8854	14.9682	14.9686	14.9692	14.9696	15.3954	15.3972
15.5906	15.5907	15.5929	15.5930	15.7251	15.7281	15.8749	15.8771
16.0486	16.0491	16.3955	16.3963	16.6894	16.6904	16.6915	16.6925
16.8568	16.8590	17.2598	17.2617	17.2625	17.2644	17.6406	17.6434
17.6436	17.6462	17.6735	17.6753	18.0912	18.0927	18.2812	18.2813

18.3959	18.3962	18.4473	18.4481	18.5253	18.5257	18.5447	18.5449
18.5457	18.5460	19.0489	19.0490	19.0504	19.0505	19.0652	19.0677
19.2940	19.2951	19.4622	19.4630	19.4637	19.4645	19.7652	19.7663
20.3275	20.3279	20.3401	20.3406	20.7708	20.7710	20.7728	20.7738
20.7743	20.7752	20.8021	20.8029	20.8052	20.8052	20.8060	20.8061
20.8330	20.8335	20.9289	20.9299	20.9314	20.9324	21.0168	21.0170
21.3400	21.3413	21.3445	21.3458	21.4256	21.4262	21.9015	21.9045
22.1160	22.1187	22.2131	22.2148	22.2164	22.2183	22.8817	22.8823
22.9924	22.9931	22.9935	22.9942	23.0130	23.0131	23.5808	23.5843
23.7134	23.7138	24.4404	24.4428	24.5520	24.5587	24.8337	24.8346
24.8361	24.8370	25.4528	25.4545	25.4555	25.4571	25.8853	25.8928
26.2296	26.2326	26.2327	26.2358	26.5067	26.5108		

occupation numbers

1.0000	1.0000	1.0000	1.0000	1.0000	1.0000	1.0000	1.0000
1.0000	1.0000	1.0000	1.0000	1.0000	1.0000	1.0000	1.0000
1.0000	1.0000	1.0000	1.0000	1.0000	1.0000	1.0000	1.0000
1.0000	1.0000	1.0000	1.0000	1.0000	1.0000	1.0000	1.0000
1.0000	1.0000	1.0000	1.0000	1.0000	1.0000	1.0000	1.0000
1.0000	1.0000	1.0000	1.0000	1.0000	1.0000	1.0000	1.0000
1.0000	1.0000	1.0000	1.0000	1.0000	1.0000	1.0000	1.0000
1.0000	1.0000	1.0000	1.0000	1.0000	1.0000	1.0000	1.0000
1.0000	1.0000	1.0000	1.0000	1.0000	1.0000	1.0000	1.0000
1.0000	1.0000	1.0000	1.0000	1.0000	1.0000	1.0000	1.0000
1.0000	1.0000	1.0000	1.0000	1.0000	1.0000	1.0000	1.0000
1.0000	1.0000	1.0000	1.0000	1.0000	1.0000	1.0000	1.0000
1.0000	1.0000	1.0000	1.0000	1.0000	1.0000	1.0000	1.0000
1.0000	1.0000	1.0000	1.0000	1.0000	1.0000	1.0000	1.0000
1.0000	1.0000	1.0000	1.0000	1.0000	1.0000	1.0000	1.0000
1.0000	1.0000	1.0000	1.0000	1.0000	1.0000	1.0000	1.0000
1.0000	1.0000	1.0000	1.0000	1.0000	1.0000	1.0000	1.0000

1.0000 1.0000 1.0000 1.0000 1.0000 1.0000 1.0000 1.0000
1.0000 1.0000 1.0000 1.0000 1.0000 1.0000 1.0000 1.0000
1.0000 1.0000 1.0000 1.0000 1.0000 1.0000 1.0000 1.0000
1.0000 1.0000 1.0000 1.0000 1.0000 1.0000 1.0000 1.0000
1.0000 1.0000 1.0000 1.0000 1.0000 1.0000 1.0000 1.0000
1.0000 1.0000 1.0000 1.0000 1.0000 1.0000 1.0000 1.0000
1.0000 1.0000 1.0000 1.0000 1.0005 1.0005 1.0005 1.0005
1.0005 1.0005 1.0010 1.0011 1.0011 1.0011 1.0011 1.0011
1.0021 1.0021 1.0124 1.0126 1.0129 1.0131 1.0407 1.0407
0.6882 0.6834 0.6715 0.6666 0.3752 0.3735 0.0000 0.0000
0.0000 0.0000 0.0000 0.0000 0.0000 0.0000 0.0000 0.0000
0.0000 0.0000 0.0000 0.0000 0.0000 0.0000 0.0000 0.0000
0.0000 0.0000 0.0000 0.0000 0.0000 0.0000 0.0000 0.0000
0.0000 0.0000 0.0000 0.0000 0.0000 0.0000 0.0000 0.0000
0.0000 0.0000 0.0000 0.0000 0.0000 0.0000

k =-0.0058-0.6014-0.5304 (12838 PWs) bands (ev):

-65.6558 -65.6556 -65.6555 -65.6553 -65.6264 -65.6264 -65.6263 -65.6262
-65.6262 -65.6262 -65.6261 -65.6260 -65.5994 -65.5992 -65.5990 -65.5989
-31.8065 -31.8064 -31.8059 -31.8057 -31.8009 -31.8008 -31.8003 -31.8001
-31.7853 -31.7850 -31.7838 -31.7835 -31.7772 -31.7772 -31.7761 -31.7760
-31.6963 -31.6962 -31.6877 -31.6876 -31.6594 -31.6593 -31.6592 -31.6591
-31.6566 -31.6565 -31.6565 -31.6564 -31.6389 -31.6388 -31.6270 -31.6269
-31.6061 -31.6061 -31.5989 -31.5989 -31.5942 -31.5940 -31.5939 -31.5936
-31.5633 -31.5632 -31.5628 -31.5627 -31.5544 -31.5543 -31.5539 -31.5537
-19.9727 -19.9725 -19.9694 -19.9692 -19.9060 -19.9058 -19.9058 -19.9056
-0.0383 -0.0371 -0.0371 -0.0359 0.2892 0.2917 0.3137 0.3158
0.7691 0.7710 0.7710 0.7729 0.8197 0.8198 0.9403 0.9412
1.1121 1.1125 1.1126 1.1129 1.2076 1.2080 1.2128 1.2132
6.6834 6.6840 7.2124 7.2127 7.3647 7.3654 7.3655 7.3662

8.8402	8.8417	9.5225	9.5235	9.5237	9.5248	9.6867	9.6887
13.2938	13.2949	13.9837	13.9845	13.9847	13.9854	14.1793	14.1795
14.8827	14.8838	14.8846	14.8856	15.2434	15.2446	15.5810	15.5816
15.7232	15.7234	15.7255	15.7257	16.0195	16.0211	16.3144	16.3179
16.3245	16.3262	16.6005	16.6026	16.6028	16.6051	16.8665	16.8687
17.0006	17.0030	17.0199	17.0229	17.0238	17.0267	17.7166	17.7208
17.7536	17.7567	17.9053	17.9071	17.9071	17.9089	17.9682	17.9705
18.0637	18.0641	18.2276	18.2277	18.6672	18.6677	18.6679	18.6684
18.9901	18.9901	18.9912	18.9914	19.1099	19.1110	19.2072	19.2075
19.2078	19.2079	19.4527	19.4543	19.5483	19.5503	19.9194	19.9204
20.2274	20.2298	20.2298	20.2302	20.2309	20.2324	20.3897	20.3913
20.5502	20.5507	20.5512	20.5514	20.7629	20.7633	20.7634	20.7637
20.8494	20.8507	20.9706	20.9710	21.0181	21.0185	21.2725	21.2737
21.3312	21.3315	21.3325	21.3328	21.5159	21.5189	21.6655	21.6678
21.9601	21.9611	22.2820	22.2856	22.5504	22.5511	22.5526	22.5535
23.0600	23.0614	23.1889	23.1903	23.1908	23.1921	23.4700	23.4732
23.8273	23.8305	24.0252	24.0267	24.0291	24.0305	24.1582	24.1637
24.5349	24.5395	26.0152	26.0196	26.2616	26.2645	26.3507	26.3546
26.3552	26.3591	26.5737	26.5802	26.5814	26.5824		

occupation numbers

1.0000	1.0000	1.0000	1.0000	1.0000	1.0000	1.0000	1.0000
1.0000	1.0000	1.0000	1.0000	1.0000	1.0000	1.0000	1.0000
1.0000	1.0000	1.0000	1.0000	1.0000	1.0000	1.0000	1.0000
1.0000	1.0000	1.0000	1.0000	1.0000	1.0000	1.0000	1.0000
1.0000	1.0000	1.0000	1.0000	1.0000	1.0000	1.0000	1.0000
1.0000	1.0000	1.0000	1.0000	1.0000	1.0000	1.0000	1.0000
1.0000	1.0000	1.0000	1.0000	1.0000	1.0000	1.0000	1.0000
1.0000	1.0000	1.0000	1.0000	1.0000	1.0000	1.0000	1.0000
1.0000	1.0000	1.0000	1.0000	1.0000	1.0000	1.0000	1.0000
1.0000	1.0000	1.0000	1.0000	1.0000	1.0000	1.0000	1.0000

1.0000	1.0000	1.0000	1.0000	1.0000	1.0000	1.0000	1.0000
1.0000	1.0000	1.0000	1.0000	1.0000	1.0000	1.0000	1.0000
1.0000	1.0000	1.0000	1.0000	1.0000	1.0000	1.0000	1.0000
1.0000	1.0000	1.0000	1.0000	1.0000	1.0000	1.0000	1.0000
1.0000	1.0000	1.0000	1.0000	1.0000	1.0000	1.0000	1.0000
1.0000	1.0000	1.0000	1.0000	1.0000	1.0000	1.0000	1.0000
1.0000	1.0000	1.0000	1.0000	1.0000	1.0000	1.0000	1.0000
1.0000	1.0000	1.0000	1.0000	1.0000	1.0000	1.0000	1.0000
1.0000	1.0000	1.0000	1.0000	1.0000	1.0000	1.0000	1.0000
1.0000	1.0000	1.0000	1.0000	1.0000	1.0000	1.0000	1.0000
1.0000	1.0000	1.0000	1.0000	1.0000	1.0000	1.0000	1.0000
1.0000	1.0000	1.0000	1.0000	1.0000	1.0000	1.0000	1.0000
1.0000	1.0000	1.0000	1.0000	1.0000	1.0000	1.0000	1.0000
1.0000	1.0000	1.0000	1.0000	1.0000	1.0000	1.0000	1.0000
1.0000	1.0000	1.0000	1.0000	1.0004	1.0004	1.0004	1.0004
1.0029	1.0030	1.0231	1.0232	1.0412	1.0414	0.9107	0.9072
0.7203	0.7192	0.7155	0.7145	0.1409	0.1354	0.0121	0.0115
0.0000	0.0000	0.0000	0.0000	0.0000	0.0000	0.0000	0.0000
0.0000	0.0000	0.0000	0.0000	0.0000	0.0000	0.0000	0.0000
0.0000	0.0000	0.0000	0.0000	0.0000	0.0000	0.0000	0.0000
0.0000	0.0000	0.0000	0.0000	0.0000	0.0000	0.0000	0.0000
0.0000	0.0000	0.0000	0.0000	0.0000	0.0000		

k =-0.4967 0.3390-0.5304 (12836 PWs) bands (ev):

-65.6557	-65.6556	-65.6554	-65.6552	-65.6264	-65.6264	-65.6263	-65.6262
-65.6262	-65.6262	-65.6261	-65.6260	-65.5994	-65.5992	-65.5990	-65.5989
-31.8065	-31.8064	-31.8059	-31.8057	-31.8009	-31.8008	-31.8003	-31.8001
-31.7853	-31.7850	-31.7838	-31.7835	-31.7772	-31.7772	-31.7761	-31.7760
-31.6963	-31.6962	-31.6873	-31.6872	-31.6594	-31.6593	-31.6592	-31.6591
-31.6566	-31.6565	-31.6565	-31.6564	-31.6389	-31.6388	-31.6270	-31.6269

-31.6061	-31.6061	-31.5961	-31.5960	-31.5940	-31.5940	-31.5938	-31.5936
-31.5633	-31.5632	-31.5628	-31.5627	-31.5544	-31.5543	-31.5539	-31.5537
-19.9727	-19.9725	-19.9694	-19.9692	-19.9060	-19.9058	-19.9058	-19.9056
-0.0383	-0.0371	-0.0371	-0.0359	0.2892	0.2917	0.3137	0.3158
0.7691	0.7710	0.7710	0.7729	0.8197	0.8198	0.9403	0.9413
1.1121	1.1125	1.1126	1.1129	1.2076	1.2080	1.2128	1.2132
6.6834	6.6840	7.2124	7.2127	7.3647	7.3654	7.3655	7.3662
8.8402	8.8417	9.5225	9.5236	9.5237	9.5248	9.6868	9.6887
13.2941	13.2953	13.9837	13.9845	13.9847	13.9854	14.1793	14.1795
14.8827	14.8838	14.8846	14.8856	15.2435	15.2446	15.5810	15.5816
15.7232	15.7234	15.7255	15.7257	16.0195	16.0211	16.3145	16.3179
16.3245	16.3262	16.6005	16.6026	16.6028	16.6051	16.8664	16.8687
17.0006	17.0030	17.0199	17.0229	17.0238	17.0267	17.7166	17.7208
17.7539	17.7570	17.9053	17.9071	17.9071	17.9088	17.9684	17.9706
18.0637	18.0642	18.2297	18.2297	18.6672	18.6677	18.6679	18.6684
18.9901	18.9902	18.9912	18.9914	19.1098	19.1110	19.2072	19.2074
19.2079	19.2079	19.4532	19.4548	19.5482	19.5503	19.9200	19.9209
20.2274	20.2298	20.2298	20.2303	20.2309	20.2324	20.3917	20.3933
20.5502	20.5507	20.5512	20.5514	20.7629	20.7633	20.7634	20.7637
20.8494	20.8507	20.9730	20.9733	21.0181	21.0185	21.2749	21.2761
21.3313	21.3315	21.3326	21.3328	21.5158	21.5188	21.6656	21.6679
21.9601	21.9610	22.2820	22.2856	22.5504	22.5511	22.5526	22.5535
23.0600	23.0615	23.1890	23.1903	23.1909	23.1921	23.4704	23.4736
23.8273	23.8306	24.0251	24.0267	24.0291	24.0305	24.1584	24.1639
24.5349	24.5396	26.0152	26.0195	26.2613	26.2643	26.3507	26.3546
26.3552	26.3590	26.5738	26.5807	26.5834	26.5892		

occupation numbers

1.0000	1.0000	1.0000	1.0000	1.0000	1.0000	1.0000	1.0000
1.0000	1.0000	1.0000	1.0000	1.0000	1.0000	1.0000	1.0000
1.0000	1.0000	1.0000	1.0000	1.0000	1.0000	1.0000	1.0000

1.0000	1.0000	1.0000	1.0000	1.0000	1.0000	1.0000	1.0000
1.0000	1.0000	1.0000	1.0000	1.0000	1.0000	1.0000	1.0000
1.0000	1.0000	1.0000	1.0000	1.0000	1.0000	1.0000	1.0000
1.0000	1.0000	1.0000	1.0000	1.0000	1.0000	1.0000	1.0000
1.0000	1.0000	1.0000	1.0000	1.0000	1.0000	1.0000	1.0000
1.0000	1.0000	1.0000	1.0000	1.0000	1.0000	1.0000	1.0000
1.0000	1.0000	1.0000	1.0000	1.0000	1.0000	1.0000	1.0000
1.0000	1.0000	1.0000	1.0000	1.0000	1.0000	1.0000	1.0000
1.0000	1.0000	1.0000	1.0000	1.0000	1.0000	1.0000	1.0000
1.0000	1.0000	1.0000	1.0000	1.0000	1.0000	1.0000	1.0000
1.0000	1.0000	1.0000	1.0000	1.0000	1.0000	1.0000	1.0000
1.0000	1.0000	1.0000	1.0000	1.0000	1.0000	1.0000	1.0000
1.0000	1.0000	1.0000	1.0000	1.0000	1.0000	1.0000	1.0000
1.0000	1.0000	1.0000	1.0000	1.0000	1.0000	1.0000	1.0000
1.0000	1.0000	1.0000	1.0000	1.0000	1.0000	1.0000	1.0000
1.0000	1.0000	1.0000	1.0000	1.0000	1.0000	1.0000	1.0000
1.0000	1.0000	1.0000	1.0000	1.0000	1.0000	1.0000	1.0000
1.0000	1.0000	1.0000	1.0000	1.0000	1.0000	1.0000	1.0000
1.0000	1.0000	1.0000	1.0000	1.0000	1.0000	1.0000	1.0000
1.0000	1.0000	1.0000	1.0000	1.0000	1.0000	1.0000	1.0000
1.0000	1.0000	1.0000	1.0000	1.0000	1.0000	1.0000	1.0000
1.0000	1.0000	1.0000	1.0000	1.0004	1.0004	1.0004	1.0004
1.0029	1.0030	1.0239	1.0240	1.0412	1.0414	0.9039	0.9005
0.7201	0.7191	0.7154	0.7143	0.1410	0.1356	0.0121	0.0115
0.0000	0.0000	0.0000	0.0000	0.0000	0.0000	0.0000	0.0000
0.0000	0.0000	0.0000	0.0000	0.0000	0.0000	0.0000	0.0000
0.0000	0.0000	0.0000	0.0000	0.0000	0.0000	0.0000	0.0000
0.0000	0.0000	0.0000	0.0000	0.0000	0.0000	0.0000	0.0000
0.0000	0.0000	0.0000	0.0000	0.0000	0.0000		

k =-0.5026-0.2624-1.0607 (12866 PWs) bands (ev):

-65.6470	-65.6470	-65.6467	-65.6467	-65.6465	-65.6464	-65.6463	-65.6462
-65.6081	-65.6081	-65.6073	-65.6073	-65.6072	-65.6071	-65.6070	-65.6069
-31.8479	-31.8478	-31.8477	-31.8476	-31.8458	-31.8458	-31.8446	-31.8446
-31.7051	-31.7051	-31.7050	-31.7050	-31.6987	-31.6986	-31.6986	-31.6985
-31.6882	-31.6882	-31.6848	-31.6848	-31.6813	-31.6813	-31.6756	-31.6752
-31.6752	-31.6748	-31.6669	-31.6668	-31.6667	-31.6666	-31.6652	-31.6651
-31.6601	-31.6600	-31.6422	-31.6422	-31.6344	-31.6340	-31.6339	-31.6335
-31.5415	-31.5414	-31.5336	-31.5335	-31.5334	-31.5333	-31.5326	-31.5325
-19.9402	-19.9402	-19.9389	-19.9386	-19.9386	-19.9382	-19.9370	-19.9369
0.3370	0.3373	0.3645	0.3651	0.3652	0.3657	0.3976	0.3978
0.6865	0.6867	0.6944	0.6964	0.6965	0.6984	0.7067	0.7069
0.9361	0.9362	0.9947	0.9956	0.9957	0.9967	1.0497	1.0497
7.0450	7.0450	7.2486	7.2493	7.2494	7.2501	7.5086	7.5086
8.9032	8.9032	9.3811	9.3825	9.3836	9.3850	9.9629	9.9630
13.0788	13.0789	14.1227	14.1235	14.1236	14.1244	14.8435	14.8435
14.8849	14.8849	14.9672	14.9688	14.9689	14.9705	15.3964	15.3965
15.5898	15.5915	15.5921	15.5938	15.7268	15.7268	15.8755	15.8755
16.0492	16.0492	16.3959	16.3959	16.6892	16.6912	16.6918	16.6938
16.8571	16.8571	17.2591	17.2617	17.2619	17.2643	17.6405	17.6433
17.6436	17.6463	17.6744	17.6745	18.0921	18.0921	18.2817	18.2817
18.3959	18.3963	18.4479	18.4481	18.5261	18.5261	18.5441	18.5443
18.5451	18.5454	19.0485	19.0491	19.0503	19.0508	19.0668	19.0668
19.2942	19.2942	19.4624	19.4637	19.4639	19.4652	19.7652	19.7652
20.3273	20.3273	20.3402	20.3402	20.7704	20.7704	20.7730	20.7741
20.7745	20.7755	20.8023	20.8023	20.8054	20.8057	20.8063	20.8065
20.8331	20.8331	20.9282	20.9300	20.9314	20.9331	21.0165	21.0165
21.3400	21.3416	21.3446	21.3462	21.4255	21.4256	21.9031	21.9031
22.1174	22.1174	22.2132	22.2150	22.2167	22.2187	22.8819	22.8819
22.9924	22.9931	22.9934	22.9942	23.0132	23.0132	23.5824	23.5826
23.7144	23.7144	24.4413	24.4414	24.5557	24.5557	24.8327	24.8340

24.8353	24.8366	25.4469	25.4540	25.4548	25.4620	25.8895	25.8896
26.2297	26.2328	26.2332	26.2364	26.5096	26.5096		

occupation numbers

1.0000	1.0000	1.0000	1.0000	1.0000	1.0000	1.0000	1.0000
1.0000	1.0000	1.0000	1.0000	1.0000	1.0000	1.0000	1.0000
1.0000	1.0000	1.0000	1.0000	1.0000	1.0000	1.0000	1.0000
1.0000	1.0000	1.0000	1.0000	1.0000	1.0000	1.0000	1.0000
1.0000	1.0000	1.0000	1.0000	1.0000	1.0000	1.0000	1.0000
1.0000	1.0000	1.0000	1.0000	1.0000	1.0000	1.0000	1.0000
1.0000	1.0000	1.0000	1.0000	1.0000	1.0000	1.0000	1.0000
1.0000	1.0000	1.0000	1.0000	1.0000	1.0000	1.0000	1.0000
1.0000	1.0000	1.0000	1.0000	1.0000	1.0000	1.0000	1.0000
1.0000	1.0000	1.0000	1.0000	1.0000	1.0000	1.0000	1.0000
1.0000	1.0000	1.0000	1.0000	1.0000	1.0000	1.0000	1.0000
1.0000	1.0000	1.0000	1.0000	1.0000	1.0000	1.0000	1.0000
1.0000	1.0000	1.0000	1.0000	1.0000	1.0000	1.0000	1.0000
1.0000	1.0000	1.0000	1.0000	1.0000	1.0000	1.0000	1.0000
1.0000	1.0000	1.0000	1.0000	1.0000	1.0000	1.0000	1.0000
1.0000	1.0000	1.0000	1.0000	1.0000	1.0000	1.0000	1.0000
1.0000	1.0000	1.0000	1.0000	1.0000	1.0000	1.0000	1.0000
1.0000	1.0000	1.0000	1.0000	1.0000	1.0000	1.0000	1.0000
1.0000	1.0000	1.0000	1.0000	1.0000	1.0000	1.0000	1.0000
1.0000	1.0000	1.0000	1.0000	1.0000	1.0000	1.0000	1.0000
1.0000	1.0000	1.0000	1.0000	1.0000	1.0000	1.0000	1.0000
1.0000	1.0000	1.0000	1.0000	1.0000	1.0000	1.0000	1.0000
1.0000	1.0000	1.0000	1.0000	1.0000	1.0000	1.0000	1.0000
1.0000	1.0000	1.0000	1.0000	1.0005	1.0005	1.0005	1.0005
1.0005	1.0006	1.0010	1.0010	1.0011	1.0011	1.0011	1.0011
1.0021	1.0021	1.0123	1.0126	1.0129	1.0133	1.0405	1.0405
0.6883	0.6823	0.6711	0.6652	0.3756	0.3755	0.0000	0.0000

0.0000	0.0000	0.0000	0.0000	0.0000	0.0000	0.0000	0.0000
0.0000	0.0000	0.0000	0.0000	0.0000	0.0000	0.0000	0.0000
0.0000	0.0000	0.0000	0.0000	0.0000	0.0000	0.0000	0.0000
0.0000	0.0000	0.0000	0.0000	0.0000	0.0000	0.0000	0.0000
0.0000	0.0000	0.0000	0.0000	0.0000	0.0000		

k =-0.5026-0.2624-2.1214 (12848 PWs) bands (ev):

-65.6669	-65.6668	-65.6276	-65.6276	-65.6273	-65.6273	-65.6270	-65.6270
-65.6267	-65.6267	-65.6264	-65.6263	-65.6262	-65.6262	-65.5869	-65.5868
-31.8730	-31.8729	-31.8723	-31.8722	-31.8080	-31.8079	-31.8073	-31.8072
-31.6981	-31.6981	-31.6981	-31.6981	-31.6963	-31.6959	-31.6929	-31.6929
-31.6929	-31.6929	-31.6914	-31.6914	-31.6913	-31.6913	-31.6819	-31.6819
-31.6818	-31.6818	-31.6623	-31.6623	-31.6619	-31.6619	-31.6618	-31.6618
-31.6615	-31.6614	-31.6586	-31.6585	-31.6581	-31.6581	-31.6044	-31.6040
-31.5520	-31.5519	-31.5516	-31.5515	-31.5047	-31.5046	-31.5040	-31.5040
-20.0051	-20.0051	-19.9364	-19.9364	-19.9364	-19.9364	-19.8750	-19.8750
-0.3229	-0.3229	-0.3229	-0.3228	0.3014	0.3016	0.3016	0.3018
0.7352	0.7360	1.0240	1.0241	1.0241	1.0243	1.1239	1.1239
1.1242	1.1243	1.2026	1.2026	1.2996	1.2997	1.2997	1.2997
5.7818	5.7818	6.5207	6.5207	8.1695	8.1697	8.1697	8.1698
9.0868	9.0872	9.0874	9.0878	9.2522	9.2552	10.1548	10.1548
13.3732	13.3734	13.3743	13.3745	13.4556	13.4568	14.2968	14.2970
14.2973	14.2975	15.0006	15.0011	15.0013	15.0018	15.3242	15.3242
15.6748	15.6749	15.6750	15.6751	16.3184	16.3186	16.3192	16.3195
16.8900	16.8900	16.8901	16.8902	17.1900	17.1905	17.1928	17.1934
17.2860	17.2912	17.3876	17.3877	17.3877	17.3878	17.6849	17.6863
17.7085	17.7085	17.7481	17.7485	17.7496	17.7502	17.9316	17.9317
17.9321	17.9322	18.1243	18.1280	18.7792	18.7799	18.7801	18.7809
18.7869	18.7873	18.7878	18.7881	19.0230	19.0231	19.0231	19.0231
19.2633	19.2633	19.4948	19.4950	19.4951	19.4953	19.6351	19.6354

20.0230	20.0231	20.0232	20.0233	20.0968	20.0969	20.0969	20.0970
20.4663	20.4664	20.4670	20.4671	21.0042	21.0043	21.0224	21.0224
21.0808	21.0823	21.0825	21.0839	21.1931	21.1938	21.1939	21.1946
21.2100	21.2101	21.2118	21.2118	21.2639	21.2646	21.2655	21.2662
21.5447	21.5472	21.7301	21.7324	22.9015	22.9017	23.0683	23.0685
23.0693	23.0695	23.3300	23.3300	23.9912	23.9936	23.9937	23.9961
24.2563	24.2567	24.2590	24.2594	24.5717	24.5735	24.5736	24.5753
24.7200	24.7214	26.2287	26.2288	26.2308	26.2310	26.4816	26.4852
26.4852	26.4887	26.5727	26.5830	27.0005	27.0015		

occupation numbers

1.0000	1.0000	1.0000	1.0000	1.0000	1.0000	1.0000	1.0000
1.0000	1.0000	1.0000	1.0000	1.0000	1.0000	1.0000	1.0000
1.0000	1.0000	1.0000	1.0000	1.0000	1.0000	1.0000	1.0000
1.0000	1.0000	1.0000	1.0000	1.0000	1.0000	1.0000	1.0000
1.0000	1.0000	1.0000	1.0000	1.0000	1.0000	1.0000	1.0000
1.0000	1.0000	1.0000	1.0000	1.0000	1.0000	1.0000	1.0000
1.0000	1.0000	1.0000	1.0000	1.0000	1.0000	1.0000	1.0000
1.0000	1.0000	1.0000	1.0000	1.0000	1.0000	1.0000	1.0000
1.0000	1.0000	1.0000	1.0000	1.0000	1.0000	1.0000	1.0000
1.0000	1.0000	1.0000	1.0000	1.0000	1.0000	1.0000	1.0000
1.0000	1.0000	1.0000	1.0000	1.0000	1.0000	1.0000	1.0000
1.0000	1.0000	1.0000	1.0000	1.0000	1.0000	1.0000	1.0000
1.0000	1.0000	1.0000	1.0000	1.0000	1.0000	1.0000	1.0000
1.0000	1.0000	1.0000	1.0000	1.0000	1.0000	1.0000	1.0000
1.0000	1.0000	1.0000	1.0000	1.0000	1.0000	1.0000	1.0000
1.0000	1.0000	1.0000	1.0000	1.0000	1.0000	1.0000	1.0000
1.0000	1.0000	1.0000	1.0000	1.0000	1.0000	1.0000	1.0000
1.0000	1.0000	1.0000	1.0000	1.0000	1.0000	1.0000	1.0000
1.0000	1.0000	1.0000	1.0000	1.0000	1.0000	1.0000	1.0000
1.0000	1.0000	1.0000	1.0000	1.0000	1.0000	1.0000	1.0000

1.0000	1.0000	1.0000	1.0000	1.0000	1.0000	1.0000	1.0000
1.0000	1.0000	1.0000	1.0000	1.0000	1.0000	1.0000	1.0000
1.0000	1.0000	1.0000	1.0000	1.0000	1.0000	1.0000	1.0000
1.0000	1.0000	1.0000	1.0000	1.0000	1.0000	1.0000	1.0000
1.0000	1.0000	1.0000	1.0000	1.0353	1.0354	1.0431	1.0431
1.0698	1.0705	1.0706	1.0711	1.0577	1.0571	1.0570	1.0562
1.0383	1.0383	1.0359	1.0358	0.9332	0.9315	0.9292	0.9274
0.0953	0.0919	0.0030	0.0029	0.0000	0.0000	0.0000	0.0000
0.0000	0.0000	0.0000	0.0000	0.0000	0.0000	0.0000	0.0000
0.0000	0.0000	0.0000	0.0000	0.0000	0.0000	0.0000	0.0000
0.0000	0.0000	0.0000	0.0000	0.0000	0.0000	0.0000	0.0000
0.0000	0.0000	0.0000	0.0000	0.0000	0.0000		

k = 0.0058 0.6014-0.5304 (12838 PWs) bands (ev):

-65.6557	-65.6557	-65.6554	-65.6554	-65.6264	-65.6264	-65.6263	-65.6262
-65.6262	-65.6262	-65.6261	-65.6260	-65.5993	-65.5993	-65.5990	-65.5989
-31.8065	-31.8064	-31.8058	-31.8058	-31.8009	-31.8008	-31.8002	-31.8002
-31.7852	-31.7851	-31.7837	-31.7836	-31.7772	-31.7772	-31.7761	-31.7760
-31.6964	-31.6962	-31.6878	-31.6876	-31.6594	-31.6593	-31.6592	-31.6591
-31.6566	-31.6565	-31.6565	-31.6564	-31.6390	-31.6388	-31.6271	-31.6269
-31.6061	-31.6061	-31.5989	-31.5989	-31.5942	-31.5941	-31.5938	-31.5937
-31.5633	-31.5632	-31.5627	-31.5627	-31.5543	-31.5543	-31.5538	-31.5538
-19.9727	-19.9725	-19.9694	-19.9692	-19.9060	-19.9058	-19.9058	-19.9056
-0.0383	-0.0371	-0.0371	-0.0359	0.2894	0.2915	0.3135	0.3160
0.7691	0.7710	0.7710	0.7729	0.8192	0.8203	0.9407	0.9408
1.1121	1.1125	1.1126	1.1129	1.2076	1.2080	1.2128	1.2132
6.6836	6.6838	7.2120	7.2131	7.3647	7.3654	7.3655	7.3662
8.8398	8.8421	9.5224	9.5235	9.5237	9.5249	9.6864	9.6889
13.2932	13.2955	13.9834	13.9844	13.9849	13.9857	14.1793	14.1795
14.8834	14.8839	14.8845	14.8849	15.2435	15.2445	15.5801	15.5824

15.7222	15.7239	15.7250	15.7268	16.0202	16.0204	16.3154	16.3169
16.3243	16.3264	16.5987	16.6023	16.6032	16.6067	16.8657	16.8695
17.0005	17.0030	17.0215	17.0232	17.0234	17.0252	17.7165	17.7209
17.7551	17.7552	17.9061	17.9066	17.9076	17.9080	17.9682	17.9706
18.0637	18.0641	18.2276	18.2277	18.6674	18.6675	18.6680	18.6681
18.9895	18.9904	18.9911	18.9918	19.1093	19.1116	19.2073	19.2074
19.2076	19.2081	19.4526	19.4544	19.5485	19.5501	19.9193	19.9205
20.2287	20.2295	20.2300	20.2304	20.2306	20.2312	20.3898	20.3912
20.5505	20.5508	20.5509	20.5513	20.7626	20.7634	20.7634	20.7641
20.8494	20.8507	20.9708	20.9708	21.0182	21.0184	21.2722	21.2739
21.3308	21.3318	21.3322	21.3332	21.5148	21.5199	21.6655	21.6679
21.9601	21.9611	22.2821	22.2855	22.5505	22.5516	22.5522	22.5533
23.0594	23.0619	23.1900	23.1904	23.1906	23.1911	23.4699	23.4733
23.8282	23.8295	24.0246	24.0278	24.0279	24.0312	24.1588	24.1632
24.5354	24.5391	26.0159	26.0189	26.2606	26.2654	26.3519	26.3541
26.3558	26.3579	26.5763	26.5802	26.5835	26.5846		

occupation numbers

1.0000	1.0000	1.0000	1.0000	1.0000	1.0000	1.0000	1.0000
1.0000	1.0000	1.0000	1.0000	1.0000	1.0000	1.0000	1.0000
1.0000	1.0000	1.0000	1.0000	1.0000	1.0000	1.0000	1.0000
1.0000	1.0000	1.0000	1.0000	1.0000	1.0000	1.0000	1.0000
1.0000	1.0000	1.0000	1.0000	1.0000	1.0000	1.0000	1.0000
1.0000	1.0000	1.0000	1.0000	1.0000	1.0000	1.0000	1.0000
1.0000	1.0000	1.0000	1.0000	1.0000	1.0000	1.0000	1.0000
1.0000	1.0000	1.0000	1.0000	1.0000	1.0000	1.0000	1.0000
1.0000	1.0000	1.0000	1.0000	1.0000	1.0000	1.0000	1.0000
1.0000	1.0000	1.0000	1.0000	1.0000	1.0000	1.0000	1.0000
1.0000	1.0000	1.0000	1.0000	1.0000	1.0000	1.0000	1.0000
1.0000	1.0000	1.0000	1.0000	1.0000	1.0000	1.0000	1.0000
1.0000	1.0000	1.0000	1.0000	1.0000	1.0000	1.0000	1.0000

1.0000 1.0000 1.0000 1.0000 1.0000 1.0000 1.0000 1.0000
1.0000 1.0000 1.0000 1.0000 1.0000 1.0000 1.0000 1.0000
1.0000 1.0000 1.0000 1.0000 1.0000 1.0000 1.0000 1.0000
1.0000 1.0000 1.0000 1.0000 1.0000 1.0000 1.0000 1.0000
1.0000 1.0000 1.0000 1.0000 1.0000 1.0000 1.0000 1.0000
1.0000 1.0000 1.0000 1.0000 1.0000 1.0000 1.0000 1.0000
1.0000 1.0000 1.0000 1.0000 1.0000 1.0000 1.0000 1.0000
1.0000 1.0000 1.0000 1.0000 1.0000 1.0000 1.0000 1.0000
1.0000 1.0000 1.0000 1.0000 1.0000 1.0000 1.0000 1.0000
1.0000 1.0000 1.0000 1.0000 1.0000 1.0000 1.0000 1.0000
1.0000 1.0000 1.0000 1.0000 1.0000 1.0000 1.0000 1.0000
1.0000 1.0000 1.0000 1.0000 1.0004 1.0004 1.0004 1.0004
1.0029 1.0030 1.0232 1.0232 1.0413 1.0414 0.9113 0.9066
0.7219 0.7180 0.7166 0.7130 0.1427 0.1336 0.0121 0.0115
0.0000 0.0000 0.0000 0.0000 0.0000 0.0000 0.0000 0.0000
0.0000 0.0000 0.0000 0.0000 0.0000 0.0000 0.0000 0.0000
0.0000 0.0000 0.0000 0.0000 0.0000 0.0000 0.0000 0.0000
0.0000 0.0000 0.0000 0.0000 0.0000 0.0000 0.0000 0.0000
0.0000 0.0000 0.0000 0.0000 0.0000 0.0000

k = 0.4967-0.3390-0.5304 (12836 PWs) bands (ev):

-65.6557 -65.6557 -65.6553 -65.6553 -65.6264 -65.6264 -65.6263 -65.6262
-65.6262 -65.6262 -65.6261 -65.6260 -65.5993 -65.5993 -65.5990 -65.5989
-31.8065 -31.8064 -31.8058 -31.8058 -31.8009 -31.8008 -31.8002 -31.8002
-31.7852 -31.7851 -31.7836 -31.7836 -31.7772 -31.7772 -31.7761 -31.7760
-31.6964 -31.6962 -31.6873 -31.6872 -31.6594 -31.6593 -31.6592 -31.6591
-31.6566 -31.6565 -31.6565 -31.6563 -31.6389 -31.6388 -31.6271 -31.6269
-31.6061 -31.6061 -31.5961 -31.5960 -31.5940 -31.5940 -31.5938 -31.5937
-31.5633 -31.5632 -31.5628 -31.5627 -31.5544 -31.5543 -31.5538 -31.5538
-19.9727 -19.9725 -19.9694 -19.9692 -19.9060 -19.9058 -19.9058 -19.9056

-0.0383	-0.0371	-0.0371	-0.0359	0.2894	0.2915	0.3135	0.3160
0.7691	0.7710	0.7710	0.7729	0.8191	0.8203	0.9408	0.9408
1.1121	1.1125	1.1126	1.1129	1.2076	1.2080	1.2128	1.2132
6.6836	6.6838	7.2120	7.2131	7.3647	7.3654	7.3655	7.3662
8.8398	8.8421	9.5224	9.5235	9.5237	9.5249	9.6865	9.6890
13.2935	13.2959	13.9834	13.9844	13.9849	13.9857	14.1793	14.1795
14.8834	14.8839	14.8845	14.8849	15.2435	15.2445	15.5801	15.5824
15.7222	15.7239	15.7250	15.7267	16.0202	16.0204	16.3155	16.3170
16.3243	16.3263	16.5987	16.6023	16.6032	16.6067	16.8657	16.8695
17.0005	17.0030	17.0215	17.0233	17.0234	17.0252	17.7165	17.7209
17.7554	17.7555	17.9061	17.9065	17.9076	17.9080	17.9683	17.9707
18.0638	18.0641	18.2297	18.2298	18.6675	18.6675	18.6680	18.6681
18.9895	18.9904	18.9912	18.9918	19.1092	19.1115	19.2073	19.2074
19.2077	19.2081	19.4531	19.4549	19.5485	19.5501	19.9199	19.9210
20.2287	20.2296	20.2300	20.2304	20.2307	20.2312	20.3918	20.3932
20.5505	20.5507	20.5508	20.5513	20.7626	20.7633	20.7633	20.7641
20.8494	20.8507	20.9731	20.9731	21.0182	21.0184	21.2747	21.2764
21.3308	21.3319	21.3323	21.3333	21.5148	21.5199	21.6655	21.6680
21.9601	21.9611	22.2821	22.2855	22.5505	22.5515	22.5522	22.5533
23.0595	23.0620	23.1900	23.1904	23.1906	23.1911	23.4703	23.4737
23.8283	23.8296	24.0246	24.0277	24.0279	24.0312	24.1589	24.1633
24.5354	24.5391	26.0158	26.0189	26.2604	26.2652	26.3518	26.3542
26.3559	26.3578	26.5775	26.5803	26.5811	26.5864		

occupation numbers

1.0000	1.0000	1.0000	1.0000	1.0000	1.0000	1.0000	1.0000
1.0000	1.0000	1.0000	1.0000	1.0000	1.0000	1.0000	1.0000
1.0000	1.0000	1.0000	1.0000	1.0000	1.0000	1.0000	1.0000
1.0000	1.0000	1.0000	1.0000	1.0000	1.0000	1.0000	1.0000
1.0000	1.0000	1.0000	1.0000	1.0000	1.0000	1.0000	1.0000
1.0000	1.0000	1.0000	1.0000	1.0000	1.0000	1.0000	1.0000

1.0000	1.0000	1.0000	1.0000	1.0000	1.0000	1.0000	1.0000
1.0000	1.0000	1.0000	1.0000	1.0000	1.0000	1.0000	1.0000
1.0000	1.0000	1.0000	1.0000	1.0000	1.0000	1.0000	1.0000
1.0000	1.0000	1.0000	1.0000	1.0000	1.0000	1.0000	1.0000
1.0000	1.0000	1.0000	1.0000	1.0000	1.0000	1.0000	1.0000
1.0000	1.0000	1.0000	1.0000	1.0000	1.0000	1.0000	1.0000
1.0000	1.0000	1.0000	1.0000	1.0000	1.0000	1.0000	1.0000
1.0000	1.0000	1.0000	1.0000	1.0000	1.0000	1.0000	1.0000
1.0000	1.0000	1.0000	1.0000	1.0000	1.0000	1.0000	1.0000
1.0000	1.0000	1.0000	1.0000	1.0000	1.0000	1.0000	1.0000
1.0000	1.0000	1.0000	1.0000	1.0000	1.0000	1.0000	1.0000
1.0000	1.0000	1.0000	1.0000	1.0000	1.0000	1.0000	1.0000
1.0000	1.0000	1.0000	1.0000	1.0000	1.0000	1.0000	1.0000
1.0000	1.0000	1.0000	1.0000	1.0000	1.0000	1.0000	1.0000
1.0000	1.0000	1.0000	1.0000	1.0000	1.0000	1.0000	1.0000
1.0000	1.0000	1.0000	1.0000	1.0000	1.0000	1.0000	1.0000
1.0000	1.0000	1.0000	1.0000	1.0000	1.0000	1.0000	1.0000
1.0000	1.0000	1.0000	1.0000	1.0000	1.0000	1.0000	1.0000
1.0000	1.0000	1.0000	1.0000	1.0004	1.0004	1.0004	1.0004
1.0029	1.0030	1.0239	1.0239	1.0413	1.0414	0.9046	0.8999
0.7217	0.7179	0.7165	0.7128	0.1429	0.1337	0.0121	0.0115
0.0000	0.0000	0.0000	0.0000	0.0000	0.0000	0.0000	0.0000
0.0000	0.0000	0.0000	0.0000	0.0000	0.0000	0.0000	0.0000
0.0000	0.0000	0.0000	0.0000	0.0000	0.0000	0.0000	0.0000
0.0000	0.0000	0.0000	0.0000	0.0000	0.0000	0.0000	0.0000
0.0000	0.0000	0.0000	0.0000	0.0000	0.0000		

the Fermi energy is 21.4181 ev

! total energy = -12416.58858522 Ry

Harris-Foulkes estimate = -12416.58858522 Ry estimated scf accuracy < 8.2E-10 Ry

total all-electron energy = -286580.605066 Ry

The total energy is the sum of the following terms:

one-electron contribution = -2345.90180039 Ry
hartree contribution = 1525.02901527 Ry
xc contribution = -1156.46991273 Ry
ewald contribution = -3259.17105260 Ry
one-center paw contrib. = -7180.07686909 Ry
-> PAW hartree energy AE = 46.38132384 Ry
-> PAW hartree energy PS = -46.31023689 Ry
-> PAW xc energy AE = -483.05709339 Ry
-> PAW xc energy PS = 63.16021088 Ry
-> total E_H with PAW = 1525.10010221 Ry
-> total E_XC with PAW = -1576.36679523 Ry
smearing contrib. (-TS) = 0.00203433 Ry

convergence has been achieved in 50 iterations

Forces acting on atoms (cartesian axes, Ry/au):

atom 1 type 1 force = 0.00561713 0.00293390 -0.00509014
atom 2 type 1 force = 0.00011904 -0.00003720 -0.00002775
atom 3 type 1 force = 0.00003822 0.00011738 -0.00003084
atom 4 type 1 force = -0.00019394 -0.00010005 0.00033869
atom 5 type 1 force = 0.00011621 0.00006377 -0.00003894
atom 6 type 1 force = 0.00022485 -0.00016069 0.00018784
atom 7 type 1 force = -0.00000642 0.00027250 0.00018777
atom 8 type 1 force = 0.00003820 0.00001949 0.00013537

atom	9 type	2	force =	-0.00045996	0.00016075	-0.00036639
atom	10 type	2	force =	-0.00074551	0.00028266	0.00058733
atom	11 type	2	force =	-0.00009640	-0.00000656	0.00005108
atom	12 type	2	force =	-0.00008104	0.00003130	-0.00005408
atom	13 type	2	force =	-0.00001605	-0.00008853	-0.00005695
atom	14 type	2	force =	-0.00018591	-0.00075441	0.00057281
atom	15 type	2	force =	-0.00005611	-0.00007123	0.00005126
atom	16 type	2	force =	-0.00012873	-0.00047367	-0.00036933
atom	17 type	2	force =	-0.00013140	-0.00046639	-0.00039050
atom	18 type	2	force =	-0.00005883	-0.00007442	0.00002927
atom	19 type	2	force =	-0.00019207	-0.00077454	0.00056710
atom	20 type	2	force =	-0.00001838	-0.00008440	-0.00007483
atom	21 type	2	force =	-0.00008248	0.00003483	-0.00007648
atom	22 type	2	force =	-0.00009323	-0.00000605	0.00002891
atom	23 type	2	force =	-0.00072379	0.00028218	0.00054768
atom	24 type	2	force =	-0.00045936	0.00016387	-0.00039268
atom	25 type	3	force =	0.00006548	0.00002004	-0.00000714
atom	26 type	3	force =	0.00024475	-0.00096148	-0.00006940
atom	27 type	3	force =	-0.00063575	0.00072787	-0.00006644
atom	28 type	3	force =	-0.00005395	-0.00004075	0.00001595
atom	29 type	3	force =	0.00028143	0.00013068	0.00000295
atom	30 type	3	force =	-0.00009885	-0.00004060	0.00002075
atom	31 type	3	force =	-0.00007659	-0.00008345	0.00002219
atom	32 type	3	force =	-0.00066179	-0.00035850	0.00188929
atom	33 type	3	force =	-0.00011812	-0.00004772	0.00001829
atom	34 type	3	force =	-0.00070573	0.00073135	-0.00007341
atom	35 type	3	force =	0.00018680	-0.00097530	-0.00007355
atom	36 type	3	force =	-0.00000416	0.00001359	-0.00000676
atom	37 type	3	force =	-0.00074581	-0.00037295	0.00195618
atom	38 type	3	force =	-0.00014782	-0.00008881	0.00001990
atom	39 type	3	force =	-0.00016754	-0.00004633	0.00002144

atom 40 type 3 force = 0.00021358 0.00012787 0.00001360

The non-local contrib. to forces

atom 1 type 1 force = 0.00381747 0.00199422 -0.00201584

atom 2 type 1 force = 0.00006207 -0.00005769 0.00003585

atom 3 type 1 force = -0.00001106 0.00008281 0.00003304

atom 4 type 1 force = -0.00001219 -0.00000560 0.00010174

atom 5 type 1 force = 0.00002566 0.00001577 -0.00012227

atom 6 type 1 force = -0.00008778 -0.00009074 0.00008717

atom 7 type 1 force = -0.00012691 -0.00002311 0.00008694

atom 8 type 1 force = 0.00002431 0.00001197 0.00003632

atom 9 type 2 force = 0.00067706 -0.00013069 0.00065977

atom 10 type 2 force = 0.00135003 -0.00025563 -0.00061869

atom 11 type 2 force = 0.00015202 -0.00007367 0.00002098

atom 12 type 2 force = 0.00013602 -0.00002848 0.00024182

atom 13 type 2 force = 0.00005673 0.00012404 0.00024046

atom 14 type 2 force = 0.00054085 0.00120951 -0.00059687

atom 15 type 2 force = 0.00002134 0.00016927 0.00001523

atom 16 type 2 force = 0.00028537 0.00064248 0.00067262

atom 17 type 2 force = 0.00027901 0.00063180 0.00063431

atom 18 type 2 force = 0.00002595 0.00016811 -0.00000545

atom 19 type 2 force = 0.00056220 0.00125309 -0.00064595

atom 20 type 2 force = 0.00005517 0.00012618 0.00021514

atom 21 type 2 force = 0.00013411 -0.00002407 0.00021394

atom 22 type 2 force = 0.00015037 -0.00007855 -0.00000921

atom 23 type 2 force = 0.00130156 -0.00024883 -0.00062422

atom 24 type 2 force = 0.00069048 -0.00013276 0.00064521

atom 25 type 3 force = -0.08667313 -0.04526362 0.00001207

atom 26 type 3 force = -0.08669552 -0.04578959 0.00002848

atom 27 type 3 force = -0.08711625 -0.04498164 0.00003061

atom 28 type 3 force = -0.08650628 -0.04517524 0.00003893

atom 29 type 3 force = -0.08664979 -0.04525286 0.00007803

atom 30 type 3 force = -0.08667528 -0.04525854 0.00003269

atom 31 type 3 force = -0.08666899 -0.04527043 0.00003377

atom 32 type 3 force = -0.08715577 -0.04551458 0.00097734

atom 33 type 3 force = 0.08678052 0.04531950 0.00003779

atom 34 type 3 force = 0.08616953 0.04551979 0.00002750

atom 35 type 3 force = 0.08659682 0.04470333 0.00002744

atom 36 type 3 force = 0.08661378 0.04523376 0.00001227

atom 37 type 3 force = 0.08611761 0.04497499 0.00101636

atom 38 type 3 force = 0.08661519 0.04522717 0.00003209

atom 39 type 3 force = 0.08661130 0.04523799 0.00003333

atom 40 type 3 force = 0.08664073 0.04524804 0.00008388

The ionic contribution to forces

atom 1 type 1 force = 0.34125760 0.17816868 -0.07613463

atom 2 type 1 force = -0.01857216 -0.00237680 -0.00055253

atom 3 type 1 force = -0.01256656 -0.01388080 -0.00055272

atom 4 type 1 force = 0.01155184 0.00603140 0.00824885

atom 5 type 1 force = -0.01864304 -0.00973328 0.00718930

atom 6 type 1 force = 0.03341203 -0.00772887 0.01172786

atom 7 type 1 force = 0.01275646 0.03183390 0.01172897

atom 8 type 1 force = -0.01249461 -0.00652342 -0.00578698

atom 9 type 2 force = -0.03047389 0.01094674 -0.03958320

atom 10 type 2 force = -0.07628440 0.01519472 0.03269252

atom 11 type 2 force = 0.00363563 -0.01056684 0.00031358

atom 12 type 2 force = -0.00679536 -0.00429859 0.01187954

atom 13 type 2 force = -0.00727755 -0.00313463 0.01198312

atom 14 type 2 force = -0.03110001 -0.07053710 0.03244318

atom 15 type 2 force = -0.00668329 0.00890771 0.00026347

atom 16 type 2 force = -0.00810129 -0.03112432 -0.03984527

atom 17 type 2 force = -0.00843675 -0.03126183 -0.04052472

atom 18 type 2 force = -0.00659169 0.00902303 -0.00062673

atom 19 type 2 force = -0.03113847 -0.07127954 0.03175338

atom 20 type 2 force = -0.00741143 -0.00311873 0.01093960

atom 21 type 2 force = -0.00673154 -0.00417946 0.01104225

atom 22 type 2 force = 0.00348900 -0.01057591 -0.00067701

atom 23 type 2 force = -0.07565290 0.01480208 0.03150154

atom 24 type 2 force = -0.03016898 0.01114356 -0.04078455

atom 25 type 3 force = -10.44666878 -5.45436944 0.00071033

atom 26 type 3 force = -10.42834038 -5.46244710 -0.00462258

atom 27 type 3 force = -10.44282055 -5.43471334 -0.00462235

atom 28 type 3 force = -10.45660145 -5.45955505 -0.00230439

atom 29 type 3 force = -10.42814557 -5.44469872 -0.00291098

atom 30 type 3 force = -10.44797348 -5.45361008 0.00049312

atom 31 type 3 force = -10.44679153 -5.45587414 0.00049323

atom 32 type 3 force = -10.44295190 -5.45242879 0.02827738

atom 33 type 3 force = 10.42711787 5.44416217 -0.00224985

atom 34 type 3 force = 10.44099173 5.46898600 -0.00467857

atom 35 type 3 force = 10.45541741 5.44135663 -0.00467880

atom 36 type 3 force = 10.43694947 5.44929501 0.00069378

atom 37 type 3 force = 10.44078353 5.45129684 0.02852350

atom 38 type 3 force = 10.43682534 5.44781977 0.00048442

atom 39 type 3 force = 10.43566815 5.45003639 0.00048431

atom 40 type 3 force = 10.45556152 5.45901212 -0.00273137

The local contribution to forces

atom 1 type 1 force = -0.33900676 -0.17698927 0.07269618

atom 2 type 1 force = 0.01864842 0.00237377 0.00050453

atom 3 type 1 force = 0.01261117 0.01393843 0.00049095

atom 4 type 1 force = -0.01172385 -0.00611675 -0.00800494

atom 5 type 1 force = 0.01873207 0.00979198 -0.00714286

atom 6 type 1 force = -0.03309401 0.00764501 -0.01160938

atom 7 type 1 force = -0.01265522 -0.03153998 -0.01161035

atom 8 type 1 force = 0.01251804 0.00653224 0.00590145

atom 9 type 2 force = 0.02932022 -0.01068189 0.03855586 atom 10 type 2 force = 0.07414192 -0.01463843 -0.03147111

atom 11 type 2 force = -0.00385567 0.01062782 -0.00027419

atom 12 type 2 force = 0.00655897 0.00438055 -0.01217552

atom 13 type 2 force = 0.00721812 0.00292709 -0.01225516

atom 14 type 2 force = 0.03033325 0.06853636 -0.03128210

atom 15 type 2 force = 0.00659918 -0.00915777 -0.00019641

atom 16 type 2 force = 0.00768157 0.02999766 0.03877661

atom 17 type 2 force = 0.00801056 0.03013120 0.03947906

atom 18 type 2 force = 0.00651829 -0.00925526 0.00065383

atom 19 type 2 force = 0.03036762 0.06922051 -0.03052972

atom 20 type 2 force = 0.00732734 0.00291079 -0.01122896

atom 21 type 2 force = 0.00652741 0.00424194 -0.01133510

atom 22 type 2 force = -0.00373909 0.01063660 0.00070250

atom 23 type 2 force = 0.07356955 -0.01427483 -0.03030960

atom 24 type 2 force = 0.02900469 -0.01083606 0.03972675

atom 25 type 3 force = 10.50291626 5.48373174 -0.00072683

atom 26 type 3 force = 10.48480792 5.49118455 0.00450001

atom 27 type 3 force = 10.49868909 5.46461197 0.00451455

atom 28 type 3 force = 10.51255619 5.48877294 0.00228187

atom 29 type 3 force = 10.48461817 5.47416891 0.00285663

atom 30 type 3 force = 10.50407246 5.48290610 -0.00050532

atom 31 type 3 force = 10.50290753 5.48513962 -0.00049784

atom 32 type 3 force = 10.49881992 5.48159989 -0.02703493

atom 33 type 3 force = -10.48353349 -5.47361405 0.00223082

atom 34 type 3 force = -10.49750570 -5.49774170 0.00455896

atom 35 type 3 force = -10.51131045 -5.47128802 0.00455897

atom 36 type 3 force = -10.49309336 -5.47859601 -0.00070944

atom 37 type 3 force = -10.49729524 -5.48078854 -0.02723862

atom 38 type 3 force = -10.49310103 -5.47721570 -0.00049740

atom 39 type 3 force = -10.49195208 -5.47939614 -0.00048946

atom 40 type 3 force = -10.51147320 -5.48819067 0.00267853

The core correction contribution to forces

atom 1 type	1	force =	-0.00044451	-0.00023221	0.00035690
atom 2 type	1	force =	-0.00002601	0.00001446	-0.00001138
atom 3 type	1	force =	-0.00000301	-0.00002967	-0.00001133
atom 4 type	1	force =	-0.00000082	-0.00000041	-0.00000475
atom 5 type	1	force =	-0.00001715	-0.00000896	0.00003775
atom 6 type	1	force =	0.00001517	0.00001513	-0.00001566
atom 7 type	1	force =	0.00002109	0.00000380	-0.00001560
atom 8 type	1	force =	-0.00001196	-0.00000621	-0.00001197
atom 9 type	2	force =	0.00002427	-0.00000216	0.00001068
atom 10 type	2	force =	0.00004458	0.00000135	-0.00002158
atom 11 type	2	force =	-0.00000406	-0.00000010	-0.00000342
atom 12 type	2	force =	-0.00000158	-0.00000078	-0.00000521
atom 13 type	2	force =	-0.00000164	-0.00000078	-0.00000520
atom 14 type	2	force =	0.00002658	0.00003534	-0.00002145
atom 15 type	2	force =	-0.00000250	-0.00000340	-0.00000337
atom 16 type	2	force =	0.00001186	0.00002117	0.00001092
atom 17 type	2	force =	0.00001209	0.00002112	0.00001948
atom 18 type	2	force =	-0.00000244	-0.00000329	0.00000531
atom 19 type	2	force =	0.00002653	0.00003586	-0.00001292
atom 20 type	2	force =	-0.00000158	-0.00000085	0.00000346
atom 21 type	2	force =	-0.00000158	-0.00000085	0.00000348
atom 22 type	2	force =	-0.00000416	-0.00000010	0.00000537
atom 23 type	2	force =	0.00004416	0.00000156	-0.00001264
atom 24 type	2	force =	0.00002409	-0.00000234	0.00001963
atom 25 type	3	force =	0.03049131	0.01592324	-0.00000265
atom 26 type	3	force =	0.03047065	0.01609273	0.00001591
atom 27 type	3	force =	0.03061855	0.01580941	0.00001589
atom 28 type	3	force =	0.03049084	0.01592295	-0.00000514
atom 29 type	3	force =	0.03046239	0.01590815	-0.00001566
atom 30 type	3	force =	0.03047744	0.01591865	-0.00000138

atom 31 type 3 force = 0.03047958 0.01591456 -0.00000140
atom 32 type 3 force = 0.03062542 0.01599324 -0.00033263
atom 33 type 3 force = -0.03048482 -0.01591986 -0.00000494
atom 34 type 3 force = -0.03035698 -0.01603362 0.00001646
atom 35 type 3 force = -0.03050514 -0.01574988 0.00001650
atom 36 type 3 force = -0.03048380 -0.01591935 -0.00000266
atom 37 type 3 force = -0.03034713 -0.01584803 -0.00034061
atom 38 type 3 force = -0.03049517 -0.01592790 -0.00000139
atom 39 type 3 force = -0.03049736 -0.01592376 -0.00000142
atom 40 type 3 force = -0.03051360 -0.01593489 -0.00001799
The Hubbard contrib. to forces
atom 1 type 1 force = 0.00000000 0.00000000 0.00000000
atom 2 type 1 force = 0.00000000 0.00000000 0.00000000
atom 3 type 1 force = 0.00000000 0.00000000 0.00000000
atom 4 type 1 force = 0.00000000 0.00000000 0.00000000
atom 5 type 1 force = 0.00000000 0.00000000 0.00000000
atom 6 type 1 force = 0.00000000 0.00000000 0.00000000
atom 7 type 1 force = 0.00000000 0.00000000 0.00000000
atom 8 type 1 force = 0.00000000 0.00000000 0.00000000
atom 9 type 2 force = 0.00000000 0.00000000 0.00000000
atom 10 type 2 force = 0.00000000 0.00000000 0.00000000
atom 11 type 2 force = 0.00000000 0.00000000 0.00000000
atom 12 type 2 force = 0.00000000 0.00000000 0.00000000
atom 13 type 2 force = 0.00000000 0.00000000 0.00000000
atom 14 type 2 force = 0.00000000 0.00000000 0.00000000
atom 15 type 2 force = 0.00000000 0.00000000 0.00000000
atom 16 type 2 force = 0.00000000 0.00000000 0.00000000
atom 17 type 2 force = 0.00000000 0.00000000 0.00000000
atom 18 type 2 force = 0.00000000 0.00000000 0.00000000
atom 19 type 2 force = 0.00000000 0.00000000 0.00000000
atom 20 type 2 force = 0.00000000 0.00000000 0.00000000

atom 21 type 2 force = 0.00000000 0.00000000 0.00000000

atom 22 type 2 force = 0.00000000 0.00000000 0.00000000

atom 23 type 2 force = 0.00000000 0.00000000 0.00000000

atom 24 type 2 force = 0.00000000 0.00000000 0.00000000

atom 25 type 3 force = 0.00000000 0.00000000 0.00000000

atom 26 type 3 force = 0.00000000 0.00000000 0.00000000

atom 27 type 3 force = 0.00000000 0.00000000 0.00000000

atom 28 type 3 force = 0.00000000 0.00000000 0.00000000

atom 29 type 3 force = 0.00000000 0.00000000 0.00000000

atom 30 type 3 force = 0.00000000 0.00000000 0.00000000

atom 31 type 3 force = 0.00000000 0.00000000 0.00000000

atom 32 type 3 force = 0.00000000 0.00000000 0.00000000

atom 33 type 3 force = 0.00000000 0.00000000 0.00000000

atom 34 type 3 force = 0.00000000 0.00000000 0.00000000

atom 35 type 3 force = 0.00000000 0.00000000 0.00000000

atom 36 type 3 force = 0.00000000 0.00000000 0.00000000

atom 37 type 3 force = 0.00000000 0.00000000 0.00000000

atom 38 type 3 force = 0.00000000 0.00000000 0.00000000

atom 39 type 3 force = 0.00000000 0.00000000 0.00000000

atom 40 type 3 force = 0.00000000 0.00000000 0.00000000

The SCF correction term to forces

atom 1 type 1 force = -0.00000635 -0.00000742 0.00000707

atom 2 type 1 force = 0.00000705 0.00000916 -0.00000441

atom 3 type 1 force = 0.00000801 0.00000670 0.00000905

atom 4 type 1 force = -0.00000859 -0.00000861 -0.00000238

atom 5 type 1 force = 0.00001899 -0.00000165 -0.00000103

atom 6 type 1 force = -0.00002024 -0.00000114 -0.00000232

atom 7 type 1 force = -0.00000152 -0.00000202 -0.00000236

atom 8 type 1 force = 0.00000274 0.00000501 -0.00000362

atom 9 type 2 force = -0.00000730 0.00002883 -0.00000967

atom 10 type 2 force = 0.00000268 -0.00001928 0.00000601

atom 11 type 2 force = -0.00002400 0.00000632 -0.00000604
atom 12 type 2 force = 0.00002124 -0.00002131 0.00000513
atom 13 type 2 force = -0.00001138 -0.00000416 -0.00002035
atom 14 type 2 force = 0.00001375 0.00000158 0.00002987
atom 15 type 2 force = 0.00000949 0.00001304 -0.00002784
atom 16 type 2 force = -0.00000591 -0.00001057 0.00001561
atom 17 type 2 force = 0.00000400 0.00001142 0.00000119
atom 18 type 2 force = -0.00000861 -0.00000692 0.00000215
atom 19 type 2 force = -0.00000963 -0.00000437 0.00000214
atom 20 type 2 force = 0.00001244 -0.00000169 -0.00000425
atom 21 type 2 force = -0.00001055 -0.00000264 -0.00000123
atom 22 type 2 force = 0.00001097 0.00001200 0.00000710
atom 23 type 2 force = 0.00001417 0.00000229 -0.00000757
atom 24 type 2 force = -0.00000931 -0.00000845 0.00000010
atom 25 type 3 force = 0.00000014 -0.00000180 -0.00000024
atom 26 type 3 force = 0.00000240 -0.00000199 0.00000862
atom 27 type 3 force = -0.00000626 0.00000155 -0.00000531
atom 28 type 3 force = 0.00000707 -0.00000628 0.00000451
atom 29 type 3 force = -0.00000345 0.00000530 -0.00000525
atom 30 type 3 force = 0.00000035 0.00000337 0.00000146
atom 31 type 3 force = -0.00000286 0.00000703 -0.00000574
atom 32 type 3 force = 0.00000087 -0.00000818 0.00000195
atom 33 type 3 force = 0.00000213 0.00000461 0.00000430
atom 34 type 3 force = -0.00000399 0.00000097 0.00000207
atom 35 type 3 force = -0.00001152 0.00000273 0.00000217
atom 36 type 3 force = 0.00001007 0.00000027 -0.00000088
atom 37 type 3 force = -0.00000425 -0.00000813 -0.00000461
atom 38 type 3 force = 0.00000818 0.00000793 0.00000201
atom 39 type 3 force = 0.00000276 -0.00000072 -0.00000549
atom 40 type 3 force = -0.00000155 -0.00000665 0.00000038

Total force = 0.009209 Total SCF correction = 0.000100

Computing stress (Cartesian axis) and pressure

total stress (Ry/bohr**3) (kbar) P= 61.42

-0.00002314 -0.00038944 -0.00000004 -3.40 -57.29 -0.01

-0.00038944 0.00051353 -0.00000002 -57.29 75.54 -0.00

-0.00000004 -0.00000002 0.00076217 -0.01 -0.00 112.12

kinetic stress (kbar) 52416.59 -45.06 -0.01

-45.06 52479.68 -0.00

-0.01 -0.00 52505.87

local stress (kbar) 30493.19 31310.00 0.02

31310.00 -13131.72 0.01

0.02 0.01 -29470.87

nonloc. stress (kbar) -9459.98 -51.58 0.00

-51.58 -9388.92 0.00

0.00 0.00 -9357.10

hartree stress (kbar) 8486.11 -14858.62 0.00

-14858.62 29188.51 0.00

0.00 0.00 36943.04

exc-cor stress (kbar) 17993.88 -1.69 -0.00

-1.69 17996.23 -0.00

-0.00 -0.00 17997.12

corecor stress (kbar) -28674.67 4.95 0.00

4.95 -28681.57 0.00

0.00 0.00 -28684.18

ewald stress (kbar) -71258.52 -16415.28 -0.02

-16415.28 -48386.67 -0.01

-0.02 -0.01 -39821.76

hubbard stress (kbar) 0.00 0.00 0.00

0.00 0.00 0.00

0.00 0.00 0.00

london stress (kbar) 0.00 0.00 0.00

0.00 0.00 0.00

0.00 0.00 0.00

DFT-D3 stress (kbar) 0.00 0.00 0.00

0.00 0.00 0.00

0.00 0.00 0.00

XDM stress (kbar) 0.00 0.00 0.00

0.00 0.00 0.00

0.00 0.00 0.00

dft-nl stress (kbar) 0.00 0.00 0.00

0.00 0.00 0.00

0.00 0.00 0.00

TS-vdW stress (kbar) 0.00 0.00 0.00

0.00 0.00 0.00

0.00 0.00 0.00

Writing output data file EuFe2As2.save/

```
init_run     :      3.38s CPU      3.49s WALL (       1 calls)
electrons    :    317.17s CPU    323.12s WALL (       1 calls)
forces       :      1.15s CPU      1.16s WALL (       1 calls)
stress       :      3.60s CPU      3.60s WALL (       1 calls)

Called by init_run:
wfcinit      :      2.59s CPU      2.64s WALL (       1 calls)
wfcinit:atom :      0.01s CPU      0.01s WALL (       8 calls)
wfcinit:wfcr :      2.54s CPU      2.58s WALL (       8 calls)
potinit      :      0.31s CPU      0.32s WALL (       1 calls)
hinit0       :      0.35s CPU      0.38s WALL (       1 calls)

Called by electrons:
c_bands      :    265.39s CPU    270.53s WALL (      51 calls)
sum_band     :     40.45s CPU     41.09s WALL (      51 calls)
v_of_rho     :      1.77s CPU      1.78s WALL (      51 calls)
v_h          :      0.13s CPU      0.13s WALL (      51 calls)
v_xc         :      1.70s CPU      1.71s WALL (      53 calls)
newd         :      2.23s CPU      2.25s WALL (      51 calls)
PAW_pot      :      6.98s CPU      7.05s WALL (      51 calls)
mix_rho      :      0.35s CPU      0.35s WALL (      51 calls)

Called by c_bands:
init_us_2    :      0.95s CPU      0.98s WALL (     840 calls)
cegterg      :    260.24s CPU    265.27s WALL (     408 calls)

Called by sum_band:
```

sum_band:bec : 0.60s CPU 0.60s WALL (408 calls)

addusdens : 2.60s CPU 2.62s WALL (51 calls)

Called by *egterg:

h_psi : 147.41s CPU 149.67s WALL (1103 calls)

s_psi : 9.22s CPU 9.24s WALL (1103 calls)

g_psi : 0.22s CPU 0.22s WALL (687 calls)

cdiaghg : 78.35s CPU 80.84s WALL (1087 calls)

cegterg:over : 10.88s CPU 11.10s WALL (687 calls)

cegterg:upda : 5.96s CPU 5.98s WALL (687 calls)

cegterg:last : 4.47s CPU 4.48s WALL (408 calls)

cdiaghg:chol : 5.30s CPU 5.69s WALL (1087 calls)

cdiaghg:inve : 4.68s CPU 4.70s WALL (1087 calls)

cdiaghg:para : 8.51s CPU 9.34s WALL (2174 calls)

Called by h_psi:

h_psi:pot : 147.18s CPU 149.43s WALL (1103 calls)

h_psi:calbec : 10.77s CPU 10.80s WALL (1103 calls)

vloc_psi : 127.03s CPU 129.25s WALL (1103 calls)

add_vuspsi : 9.38s CPU 9.39s WALL (1103 calls)

General routines

calbec : 16.50s CPU 16.54s WALL (1551 calls)

fft : 1.65s CPU 1.69s WALL (687 calls)

ffts : 0.08s CPU 0.08s WALL (102 calls)

fftw : 150.53s CPU 153.01s WALL (536030 calls)

interpolate : 0.17s CPU 0.17s WALL (51 calls)

Parallel routines

fft_scatt_xy : 7.49s CPU 8.62s WALL (536819 calls)

fft_scatt_yz : 102.55s CPU 102.73s WALL (536819 calls)

PAW routines

PAW_pot : 6.98s CPU 7.05s WALL (51 calls)

PWSCF : 5m30.45s CPU 5m39.24s WALL

This run was terminated on: 20:33:34 28Apr2020

JOB DONE.

Et cetera

APPENDIX II

Structural and electronic properties of the iron pnictide compound EuFe2As2 from first principles.We report results of the electronic and mechanical structure properties of the iron pnictide compound $EuFe_2As_2$, at zero pressure. The open source computer code Quantum Espresso, which incorporates the Density Functional Theory (DFT), Pseudo Potentials (PP) and the Plane Wave (PW) were used to perform calculations from first principles. Projector-Augmented Wave (PAW) Pseudo Potentials were used in these calculations. The Density of States exhibits a sizeable superconducting gap and the band structure has no band gap. Calculations were performed from scratch.

APPENDIX III: First principle study of the Mechanical properties and phonon dispersion of the iron pnictide compound EuFe2As2

We present results on the first principle study of the elastic constants and the phonon dispersion of $EuFe_2As_2$ at zero pressure. The ground-state energy calculations were performed within Density Functional Theory (DFT) and the generalized gradient approximation using the pseudo potential method with plane-wave basis sets. The projector augmented-wave (PAW) pseudo potentials were used in our calculation. The open source code QUANTUM ESPRESSSO was used with its pseudo potential database. The study on the elastic constants at zero pressure was a clear indication that the compound is mechanically stable, and the phonon dispersion study also indicated that the compound is dynamically stable. The elastic constants and mechanical properties also led to the conclusion that the compound is ductile and anisotropic.

APPENDIX IV: Letter of Introduction

FONS SCIENTIAE

KISII UNIVERSITY

DEPARTMENT OF PHYSICS

Telephone : +254797145872
Facsimile : 020 2491131
Email: cotieno@kisiiuniversity.ac.ke

P. O. Box 408-40200
KISII, KENYA
www.kisiiuniversity.ac.ke

SCHOOL OF PURE AND APPLIED SCIENCES

27[TH] November 2019

To: whom it may concern,

Re: NAOMY KERUBO OMBOGA

This is to inform you that Ms. **Naomy Kerubo Omboga** Reg. No. **MPS21/00001/19** is a Bonafide student of **Kisii University** Department of Physics. Ms.Kerubo is currently pursuing her **MSc. Degree in Physics**. Ms. Kerubo has successfully defended her proposal entitled "**AB-INITIO STUDY OF ELECTRONIC PROPERTIES, MECHANICAL STRUCTURE AND PHASE CHANGES OF THE SUPERCONDUCTING IRON PNICTIDE COMPOUND $EuFe_2As_2$**

This Letter is to request your office to facilitate the processing of **her research permit**. Kindly contact the undersigned in case you have questions.

Thanks in advance.

Sincerely,

KISII UNIVERSITY
School Of Pure And Applied Sciences
27 NOV 2019
P. O. BOX 408 - 40200, KISII KENYA
www.kisiiuniversity.ac.ke

Dr. Calford Otieno, PhD.
CHAIR, DEPARTMENT OF PHYSICS

APPENDIX V: Research Permit

REPUBLIC OF KENYA

NATIONAL COMMISSION FOR SCIENCE,TECHNOLOGY & INNOVATION

Ref No: **751887**

Date of Issue: **07/January/2020**

RESEARCH LICENSE

This is to Certify that Miss.. NAOMY OMBOGA of Kisii University, has been licensed to conduct research in Kisii on the topic: AB-INITIO STUDY OF ELECTRONIC PROPERTIES, MECHANICAL STRUCTURE AND PHASE CHANGES OF THE SUPERCONDUCTING IRON PNICTIDE EuFe2As2 for the period ending : 07/January/2021.

License No: **NACOSTI/P/20/3291**

751887

Applicant Identification Number

Director General
NATIONAL COMMISSION FOR SCIENCE,TECHNOLOGY & INNOVATION

Verification QR Code

NOTE: This is a computer generated License. To verify the authenticity of this document, Scan the QR Code using QR scanner application.

APPENDIX VI: Plagiarism Report

AB-INITIO STUDY OF ELECTRONIC AND MECHANICAL STRUCTURE PROPERTIES OF THE SUPERCONDUCTING IRON PNICTIDE □□□□□□□�

ORIGINALITY REPORT

17%	13%	3%	7%
SIMILARITY INDEX	INTERNET SOURCES	PUBLICATIONS	STUDENT PAPERS

PRIMARY SOURCES

1	lists.quantum-espresso.org Internet Source	6%
2	www.crystallography.net Internet Source	5%
3	Submitted to University of Nairobi Student Paper	2%
4	"Handbook of Computational Chemistry", Springer Science and Business Media LLC, 2017 Publication	1%
5	"Encyclopedia of Nanotechnology", Springer Nature, 2016 Publication	1%
6	www.phys.ufl.edu Internet Source	1%
7	Eugene S. Kryachko, Eduardo V. Ludeña. "Energy Density Functional Theory of Many-Electron Systems", Springer Science and Business Media LLC, 1990 Publication	<1%
8	Atodiresei, N.. "First Principles Theory of Organic Molecules on Metal surfaces", Forschungszentrum Jülich, Zentralbibliothek, Verlag, 2005. Publication	<1%
9	Local Density Approximations in Quantum Chemistry and Solid State Physics, 1984.	<1%